AD NUMBER
AD814879
LIMITATION CHANGES
TO: **Approved for public release; distribution is unlimited.**
FROM: **Distribution authorized to DoD only; Test and Evaluation; MAR 1967. Other requests shall be referred to Army Chemical Research Laboratory, Attn: SMUEA-TSTI-T, Edgewood Arsenal, MD 21010.**
AUTHORITY
usaea notice, 4 oct 1967

5

Report No. IITRI-U6017-6

THE CATALYTIC ACTIVITY OF METAL OXIDES ON THERMAL DECOMPOSITION REACTIONS

Final Technical Report

by

E. S. Freeman and W. Rudloff

March 3, 1967

U.S. ARMY MUNITIONS COMMAND

Chemical Research Laboratory
RESEARCH LABORATORIES

Contract DA-18-035-AMC-341(A)

IIT RESEARCH INSTITUTE
10 West 35th Street
Chicago, Illinois 60616

Each transmittal of this document outside the Department of Defense must have prior approval of CO, ATTN: SMUEA-TSTI-T, US Army Edgewood Arsenal, Edgewood Arsenal, Maryland 21010

Report No. IITRI-U6017- 6

THE CATALYTIC ACTIVITY OF METAL OXIDES ON THERMAL DECOMPOSITION REACTIONS

Final Technical Report

by

E. S. Freeman and W. Rudloff

March 3, 1967

Chemical Research Laboratory
RESEARCH LABORATORIES

Contract DA-18-035-AMC-341(A)
Project 1C522301A060

IIT RESEARCH INSTITUTE
10 West 35th Street
Chicago, Illinois 60616

Each transmittal of this document outside the Department of Defense must have prior approval of CO, ATTN: SMUEA-TSTI-T, US Army Edgewood Arsenal, Edgewood Arsenal, Maryland 21010

FOREWORD

The work described in this report was authorized under project 1C522301A060, Chemical Agents (U). This report covers the period from 22 March, 1965 through 30 September, 1966

ACKNOWLEDGMENTS

The authors wish to acknowledge the experimental work of Mr. Brent Boldt. They would like to acknowledge Miss Anne O'Donnell for the x-ray studies

NOTICES

Reproduction of this document in whole or in part is prohibited except with permission of CO, US Army Edgewood Arsenal, ATTN: SMUEA-RCRP(3) Edgewood Arsenal, Maryland 21010; however, DDC is authorized to reproduce for United States Government purposes.

The information in this report has not been cleared for release to the general public.

DISCLAIMER

DISPOSITION

When this report has served its purpose, DESTROY it.

DIGEST

The effects of a selected series of solid metal oxides on the catalysis of the thermal decomposition of potassium chlorate and potassium perchlorate have been investigated. The initial phases of this investigation included establishing experimental reproducibility, and considering the effects of sample purity as well as the effects of gaseous environment on reaction rate. The kinetics and rate parameters of the decomposition reactions have been studied and compared to the rate parameters of $KClO_3$ in the absence of the solid oxides. The decomposition of potassium perchlorate was also studied since the initial reaction of potassium chlorate is disproportionation to perchlorate and chloride. Two oxides were selected for more precisely correlating the relationships between the electronic defect structure of the oxides and their catalytic behavior. The oxides investigated from this point of view were: Fe_2O_3 and MgO. These oxides have been doped with selected altervalent cation impurities, and subjected to heat treatment at temperatures ranging from 700°C to 1000°C in oxygen and inert gas environment. The purpose of these experiments was to introduce electronic defects. In addition, changes in catalytic activity in relationship to electronic changes as a result of exposure to Co^{60} gamma rays were investigated. The changes in semiconducting properties were studied by conductivity and magnetic susceptibility techniques and the results correlated to the

changes in catalytic activity. A mechanism of decomposition of $KClO_3$ is discussed as well as a proposed mechanism for the interaction of sulfur and $KClO_3$. The results of this program are summarized as follows:

Summary

1. The decomposition of potassium chlorate appears to be non-reversing with respect to molecular oxygen.

2. Potassium chloride appears to inhibit the disproportionation of potassium chlorate below 550°C. Above 550°C the chloride appears to accelerate the decomposition of $KClO_3$.

3. The activation energy for the decomposition of potassium chlorate was determined to be 51 kcal/mole.

4. The effects of creating electronic defect structure by doping with altervalent cationic impurities, by exposure to gamma ray radiation and heat treatment was investigated in relationship to catalytic activity. The results are consistent with a rate controlling electron transfer mechanism.

5. The higher the "p" or "n" semiconducting character of the metal oxides the higher appears to be the catalytic activity.

TABLE OF CONTENTS

TABLE OF CONTENTS (Cont.)

TABLE OF CONTENTS (Cont.)

LIST OF ILLUSTRATIONS

LIST OF ILLUSTRATIONS (Cont.)

LIST OF ILLUSTRATIONS (Cont.)

LIST OF TABLES

THE CATALYTIC ACTIVITY OF METAL OXIDES ON THERMAL DECOMPOSITION REACTIONS

INTRODUCTION

The objective of this program was to investigate the relationships between the electronic defect structure of solid oxide catalysts and their catalytic activity with respect to the thermal decomposition of potassium chlorate. The thermal decomposition of potassium perchlorate was also considered since it is one of the decomposition products in addition to potassium chloride and oxygen. Another consideration was the effect of chloride on the kinetics of decomposition.

Although this is a basic investigation on the mechanisms of the heterogeneous catalysis of the thermal decomposition of potassium chlorate, the long range goal is to provide information which could establish the basis for new and improved pyrotechnic compositions. This is especially true for the possible development of compositions with improved storage stability as well as compositions having more reproducible performance, and with greater control over their burning rates.

Metal oxides have been known to catalyze many kinds of reactions[1] including the thermal decomposition of chlorates and perchlorates.[2-14] The oxides were also of particular interest, because of past work on the thermal decomposition of N_2O[1] in which there appeared to be a relationship between the "p" semiconducting character of the oxides and catalytic activity. The catalytic activity appeared to increase with an increase in the "p" character. Based on this work the rate controlling mechanism appeared to involve the transfer of an electron from the adsorbed species to positive holes in the valence band of the solid.

In this present program a series of oxides was initially selected corresponding to the order of "p" character reported in the N_2O investigation[1] which also served as a basis for comparison. It should be born in mind, however, that the methods of preparation, impurities and defect structure can significantly influence the semiconducting character of the oxide.[1,15] It was, indeed, found that the order of catalytic activity of the metal oxides on the decomposition of potassium chlorate did differ somewhat from the order reported for N_2O decomposition. Following the initial phase a more detailed investigation of MgO, Cr_2O_3, and Fe_2O_3 was conducted to more firmly establish correlations between the type of electronic defects and catalytic activity. To do this "n" and "p" type character was induced by heat treatment in oxygen and in argon, by doping with impurity ions and by exposure to Co^{60} gamma rays.

Another aspect of this study was the rather complex decomposition mechanism of pure $KClO_3$ which decomposes via $KClO_4$ as intermediate going to KCl and O_2.[10,16] Conflicting interpretations[16,17] and the need to more readily understand its decomposition mechanism in contact with metal oxides made this phase of our study advisable. Finally, exploratory investigations on the mechanism of the sulfur-potassium chlorate reaction and on the influence of several catalysts on this reaction were initiated.

EXPERIMENTAL

A. Preparation and Standardization of Samples

1. Preparation and Standardization of Potassium Chlorate Samples

Since the purity of the samples is of the utmost importance for the reproducibility of DTA and TGA data, special attention was focused on the influence of purification on the differential thermal analysis and thermogravimetric analysis curves. Reagent grade potassium chlorate (B and A Reagent Grade A.C.S. Code 2103) of 99.5% minimum $KClO_3$ assay was recrystallized and before and after recrystallization tested with DTA and TGA. As will be seen from Figure 7, recrystallization does not make any significant difference in the DTA curves, if compared with the original material as received. Consequently, the original material was used without recrystallization for all experiments involving the catalysts.

To standardize the samples, they were crushed in a mortar, sieved, and the sieve fractions between 230 and 270 mesh (standard mesh) used for the experiments. The influence of crushing on the DTA/TGA curves was also tested. As was expected, the crushing in case of $KClO_3$ did not influence the curve shape, since reaction occurs in the molten state, and possible lattice faults are no longer present.

Prior to the DTA and TGA experiments the samples were dried at 110°C and stored in a desiccator.

2. Preparation and Standardization of Potassium Perchlorate Samples

Potassium perchlorate (B & A, reagent grade) was three times recrystallized from water, crushed in a mortar and sieved. The fraction between 230-270 mesh was taken, dried, mixed in various ratios with the metal oxides and stored in a desiccator for use in the experimental runs.

3. Preparation and Standardization of Reagent Grade Catalysts

Reagent grade metal oxides were sieved thoroughly, and again the sieve fraction between 230 and 270 mesh used for the DTA and TGA experiments. The oxides had the following purity specifications:

(a) Nickel oxide, B and A reagent grade, Code 2012, assay as Ni minimum 77.0%.

(b) Cuprous oxide, B and A reagent grade, Code 1661, assay (Cu_2O) min. 97.0%.

(c) Cupric oxide, B and A reagent grade, Code 1645, assay (CuO) min. 99.0%.

(d) Manganese dioxide, B and A reagent grade, Code 1948, assay (MnO_2) min. 99.5%.

(e) Ferric oxide, B and A reagent grade, Code 1741, assay (Fe_2O_3) min. 99.0%.

(f) Aluminum oxide, B and A reagent grade, Code 1236

(g) Titanic oxide, Fisher reagent grade, less than 0.013 impurities.

(h) Cobalt (II, III) oxide, B and A reagent grade, Code 1590, assay (as CO) minimum 70%.

(i) Magnesium oxide, B and A reagent grade, Code 1917, assay (MgO) after ignition) minimum 99.0%.

(j) Zinc oxide, U.S.P., Code 2451, no purity specifications listed.

(k) Silver oxide, Goldsmith Bros. Div. of National Lead Co., no purity specifications listed.

(l) Chrom (III) oxide, B and A purified, Code 1581.

(m) Chrom (VI) oxide, Baker analyzed reagent, assay CrO_3 99.4%

4. Preparation and Standardization of Iron (III) Oxides of Different Defect Structures

(a) Fe_2O_3 was precipitated as hydroxide with NaOH, the precipitation washed thoroughly, and ignited in a muffle furnace at 700°C.

(b) Fe_2O_3 was again precipitated as hydroxide, this time, however, with ammonia buffered by NH_4Cl, washed with hot 2% NH_4NO_3-solution, dried, and ignited at 700°C.

(c) One part of the oxide under b was heated to 800°C.

(d) Another part of the same oxide was heated to 900°C.

In order to investigate the influence of defect structure of iron oxide on its catalytic activity in a systematic way, a series of iron oxides was prepared under identical conditions by the following procedure. Reagent grade iron chloride was dissolved in a slightly acidic medium, and the solution standardized.

Equal parts of the solution were then pippeted and mixed with 1/2 mole % of various cations in solution. All the mixtures were then precipitated with ammonia buffered by NH_4Cl. The precipitates were filtered directly and then ignited in a muffle furnace at 700°C. The following oxides were prepared:

(e) Iron (III) oxide, pure, ignition 700°C.
(f) Iron (III) oxide, + Li_2O (1/2 mole %).
(g) Iron (III) oxide, + BeO (1/2 mole %). Ignition 700°C
(h) Iron (III) oxide, + Cr_2O_3 (1/2 mole %).
(i) Iron (III) oxide, +ZrO_2 (1/2 mole %).

Parts of the original Fe_2O_3 (e) were taken and heated in different atmospheres to create defects.

(j) Iron (III) oxide, heated in oxygen at 800°C.
(k) Iron (III) oxide, heated in oxygen at 900°C.
(l) Iron (III) oxide, heated in oxygen at 1000°C.
(m) Iron (III) oxide, heated in argon at 800°C.
(n) Iron (III) oxide, heated in argon at 900°C.
(o) Iron (III) oxide, heated in argon at 1000°C.

It is expected that heating in argon at very high temperature creates a slight oxygen deficiency on the surface of the oxide only. No appreciable weight loss could be observed after the heat treatment.

In another series of oxides the influence of γ-irradiation defects on the catalytic activity of oxides was investigated. To this end, reagent grade Iron (III) oxide (3e), was irradiated for 65 hrs;

(p) Iron (III) oxide, B and A reagent grade, Code 1741, assay (Fe_2O_3) min. 99.0%, γ-irradiated, 5 x 10^6 rads.

All chlorate-catalyst mixtures were weighed in the proper ratios and then mixed for several hours on a shaker, dried and stored in a desiccator.

5. Preparation and Standardization of p-type Magnesium Oxides of Varying Defect Structure

A magnesium oxide single crystal was cut in half, and heated to about 800°C in different atmospheres:

(a) Magnesium oxide, single crystal, Semi-Elements, Inc., 99.99% purity, heated at 800°C in argon,

(b) Same, heated at 800°C in oxygen,

(c) Magnesium oxide, B and A reagent grade, Code 1917, assay (MgO after ignition) minimum 99.0%, irradiated with γ-rays of a cobalt^{60} source for 17 hours, total dose 2.5 x 10^5 rads of γ-rays.

Samples (a) and (b) were crushed, all three samples dried, sieved, and mixed in the proper mole ratios with $KClO_3$, and stored in a desiccator before using in the experiments.

B. Differential Thermal Analysis, (DTA), Thermogravimetric Analysis, (TGA), and Differential Thermogravimetric Analysis, (DTGA)

1. Differential Thermal Analysis

Differential thermal analysis is a convenient method to investigate and compare the energetics of reacting systems under dynamic conditions. The sample under investigation is placed into a sample holder which is then heated at a constant, predetermined heating rate. The temperature difference, ΔT, between the sample and an inert reference (e.g., ignited Al_2O_3), within the heating block is plotted as a function of reference temperature or time. Initially, bare chromel-alumel thermocouples were used for temperature measurements. It was, however, found that after a few runs these thermocouples apparently oxidize and subsequently catalyze the decomposition reaction. To avoid this, Pt versus Pt 10% Rh thermocouples were used. The DTA apparatus contains gas inlets into both the sample and the reference tube connected via a flowmeter to a gas cylinder which provides for standardized gas flow. A West controller controls the heating rate in the sample holder. Most initial experiments were done under a constant flow of argon. The Stone DTA/EGA apparatus was used in a few experiments, where proper atmospheric flow had to be provided. This equipment provides for highly sensitive and completely automatic DTA/EGA measurements.

2. Thermogravimetric Analysis (TGA)

The Chevenard thermobalance was modified to simultaneously record weight changes and temperature during reaction as a function of time. In thermogravimetric analysis (TGA) the sample is weighed into a crucible which is mounted on top of the Chevenard balance rod. The sample temperature is measured with a thermocouple and recorded simultaneously with the weight changes on a two-pen recorder. Weight changes are electronically recorded by way of an induction coil, the electrical field of which changes, if a small metal rod-as counterweight-moves up or down according to weight changes on the other end of the balance beam. In cases where a different atmosphere is desired, argon or other gases can be admitted via a flowmeter over the sample.

Both the DTA apparatus constructed in our laboratory and the simple Chevenard thermobalance were used for preliminary comparison of various oxide catalyst-potassium chlorate reactions. For the major comparative study the combined DTA/TGA apparatus described in the following subsection was used.

3. The Combined DTA/TGA Apparatus

The Chevenard thermobalance was modified to permit the simultaneous recording of the DTA/TGA curves and sample temperature. (See Figure 1) The sample vessel which is a quartz crucible is divided into two compartments. The first contains the sample and the second the Al_2O_3 reference material. The thermocouple wires are led through a four hole ceramic rod which is connected to the Chevenard balance beam. The crucible is held by the thermocouples on top of the rod. A brief description of the Chevenard thermobalance was given in the previous subsection.

Fig. 1. SCHEMATICS OF THE COMBINED DTA/TGA APPARATUS

1a Crucible for the Combined DTA/TGA

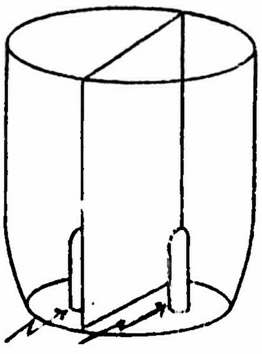

1b Electrical Wiring for the 2nd Recorder Pen of the Combined DTA/TGA Apparatus for Recording ΔT and T

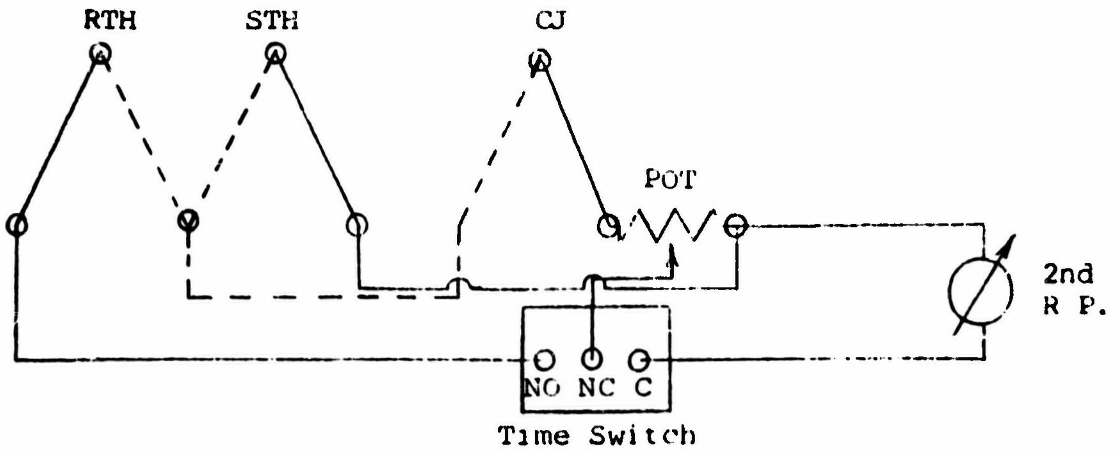

RTH = Reference Thermocouple
STH = Sample Thermocouple
CJ = Cold Junction
POT = 10,000 Ω Potentiometer

R.P. = Recorder Pen
N.O. = Normally Open
N.C. = Normally Closed
C = Common

A Bristol two-pen recorder in combination with a time switch is connected to the induction coil of the Chevenard balance. This permits weight changes to be recorded with one pen, and differential temperature and sample temperature to be recorded via the time switch by the second pen. Figure 2 shows a typical DTA/TGA temperature curve. The uppermost curve gives the weight change during the heating. The y-axis of the second curve, which is the upper boundary of the second pen-trace, represents sample temperature. One inch = 100°C. The third curve, the lower boundary of the second pen-trace shows the differential temperature, ΔT. The melting endotherm of the chlorate is seen at approximately 360°C. The reactions are exothermal and occur in three steps as indicated by the DTA bands.

4. <u>Stone-Cahn TGA/DTGA Thermobalance.</u>

For quantitative thermogravimetric analysis the Stone-Cahn microbalance was used. A time derivative computer was specifically designed to produce derivative thermogravimetric analysis curves in addition to its integrated TGA curves.

The TGA/DTGA is particularly valuable if rate parameters such as reaction order and/or activation energies are to be evaluated using the Freeman-Carroll equation.[18]

Fig. 2. TRACE OF THE SIMULTANEOUS RECORDING OF TGA, DTA AND SAMPLE TEMPERATURE

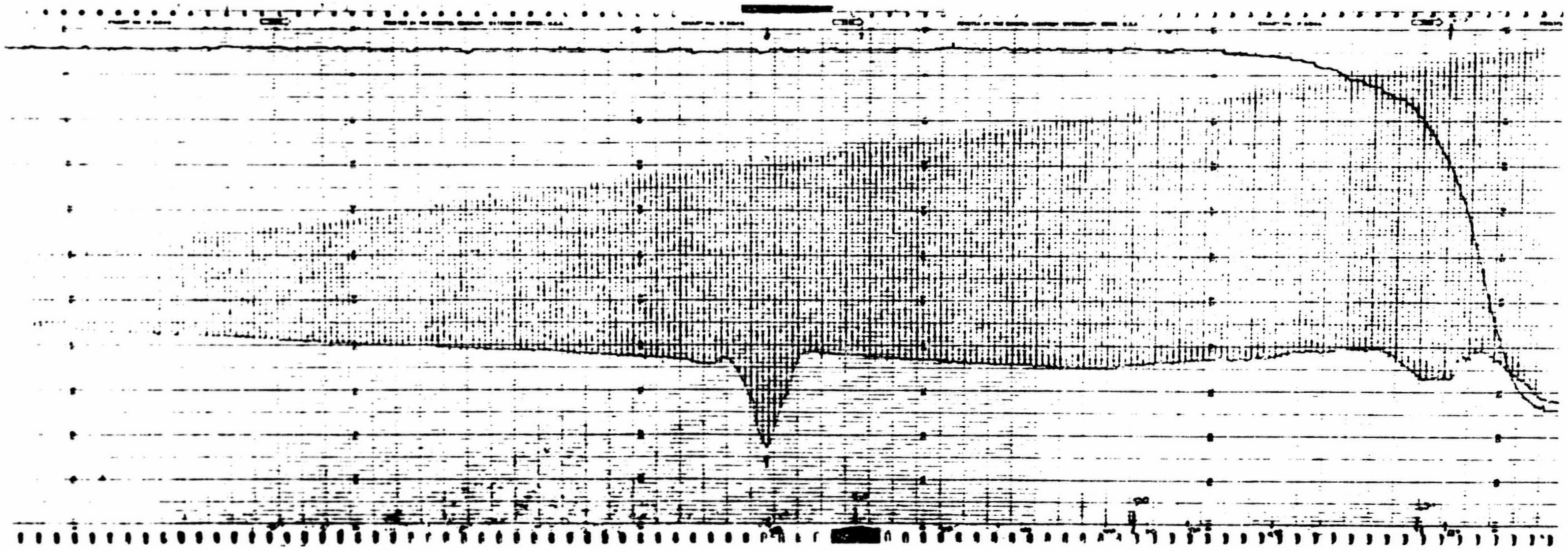

C. Isothermal Experiments

Isothermal experiments were performed on the Chevenard thermobalance. The method of measurements was as follows:

The sample under investigation was weighed into the crucible which was fixed on top of the thermocouples leading out of the balance rod. The furnace was brought to the desired temperature, and then suddenly pulled over the sample holder-balance rod assembly. Weightloss and temperature were simultaneously recorded as in the TGA Experiments.

D. Electrical Conductivity Measurements and the Determination of Contact Potentials

Electrical conductivity of the oxides was measured in an apparatus pictured in Figure 3. Single crystal material such as MgO was platinum-coated in vacuum on two opposite sides in order to obtain intimate electrical contact between the oxide and platinum electrodes. Powders were pressed at 30,000 psi into cylindrical pellets, cut to similar size and pressed between electrodes E1 and E2.

One electrode (E1) within a flow tube of vycor glass is mounted on a glass disc which in turn is fused on to a sturdy glass capillary fixed at one side of the flow tube. The other electrode (E2) is fixed on a similar disc, glass capillary combination. The glass capillary is led through a special Teflon stopper, in order to provide for adjustable distances between the electrode. In addition, a spring provides adequate pressure of the electrodes to the single crystal or powder pellets for good electrical contact. The flow tube is placed in a tube

Fig. 3. ELECTRICAL CONDUCTIVITY APPARATUS

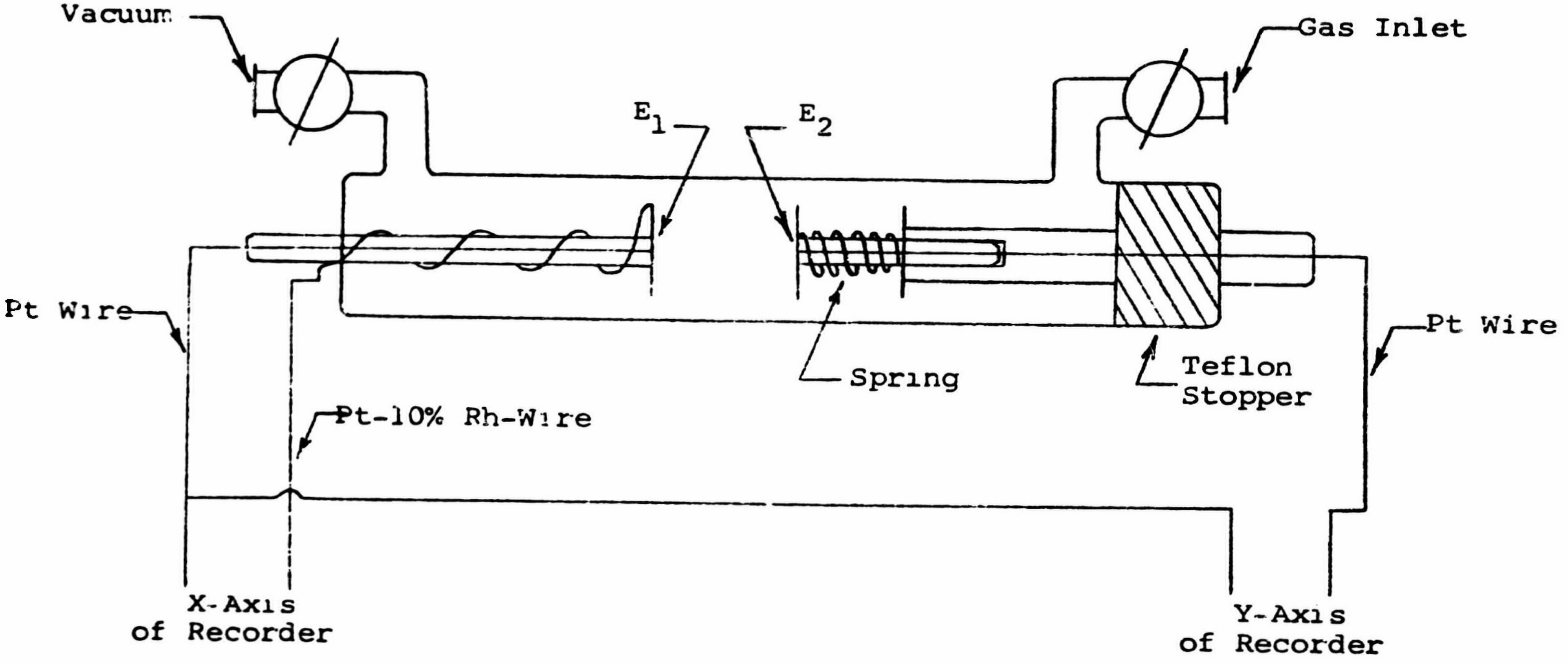

furnace which is heated at a nominally constant rate. A wire of Pt-10% Rh is fused to one Pt-electrode, and this junction serves as a thermocouple junction. Thus, simultaneously with the recording of electrical conductivity (as the y-axis on a Mosley x-y recorder), the temperature can be recorded (as x-axis on the x-y recorder). Gas inlets and outlets provide for a proper flow or non-flow atmosphere. The conductance (or rather resistance) is measured with a General Radio electrometer which in turn is connected to the y-axis of the recorder. During operation the whole system had to be shielded very carefully because of noise pickup from the surroundings. This occurs mainly, if high-resistances are involved.

Quite recently, attempts were made to measure comparative contact potentials of the metal oxides under investigation, in order to deduce and correlate workfunctions, which are a direct measure of the energy necessary for an electron transfer through the surface barrier, to catalytic activity of the oxides. To this end a contact potential apparatus was used which is described as follows:[19]

An inert reference electrode (Teflon coated gold) R, is moved with respect to the sensor electrode, S. the reference electrode is vibrated electromechanically by an AC current. The material under investigation is placed on the sensor electrode which is grounded through an adjustable potentiometer (Figure 4) The value of ΔE used to bring the AC detector signal to a minimum is equal to the contact potential.

Fig. 4. SCHEMATICS OF THE CONTACT POTENTIAL APPARATUS

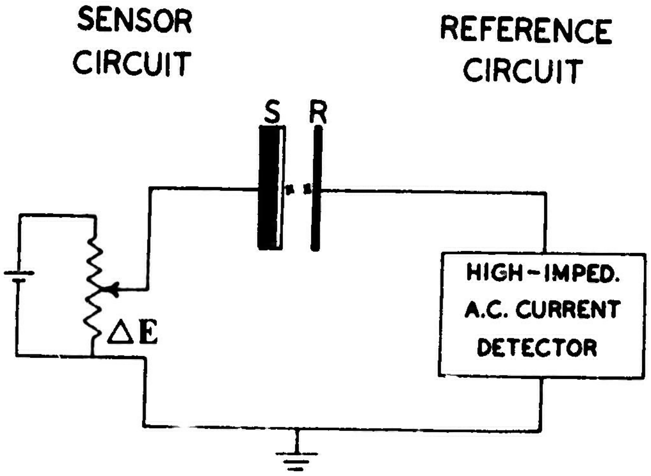

The change in ΔE caused by the interaction of the investigated material (say Fe_2O_3 powder) with the sensor is the detection signal. The difference in ΔE between the clean sensor and the sensor in contact with the material under investigation is a relative measure of the workfunction of the material.

E. Magnetic Susceptibility Measurements

Magnetic susceptibilities were measured on a variety of oxides at room temperatures with a view to elucidating the catalytic role played by the unpaired d-electrons in the thermal decomposition of $KClO_3$.

The magnetic susceptibility apparatus utilizes the standard technique of measuring the force exerted on a sample by a non-uniform magnetic field and is shown in Figure 5.

For a sample of mass m in grams, in a magnetic field of H or with a vertical field gradient of dH/dZ [oe/cm] at the sample, the vertical force, F, in dynes on the sample is given by

$$F = m \chi H \frac{dH}{dZ} \qquad (1)$$

where χ is the mass susceptibility. In our apparatus, a 4 inch electromagnet with shaped pole faces was used. This resulted in a $(H \frac{dH}{dZ})$ of up to 3×10^7 [oe^2/cm], calibration being carried out using high purity platinum metal of known susceptibility.

Vertical forces (showing up as weight changes in the sample) were measured using a Cahn electrobalance capable of weighing to parts of a microgram and having a graphic output.

All magnetic susceptibility measurements were done at ambient temperatures. To avoid misreading due to static electricity, the balance was kept in an atmosphere of constant moisture content.

Fig. 5. SCHEMATIC REPRESENTATION OF THE MAGNETIC SUSCEPTIBILITY APPARATUS

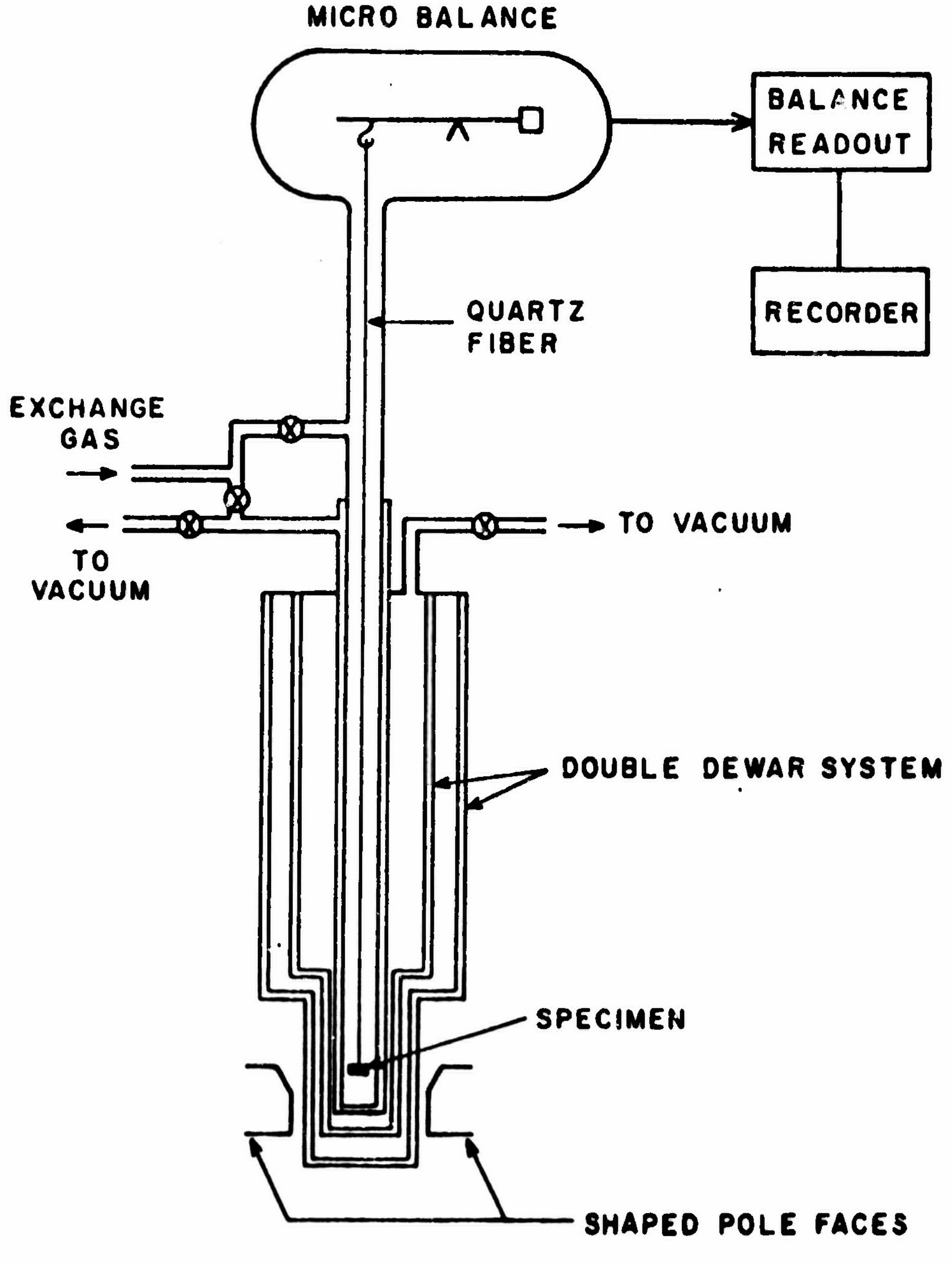

F. Mass Spectrometric Determination of Reaction Products

A Bendix-Time-of-Flight mass spectrometer was used to analyze possible gaseous decomposition products other than oxygen. In particular, chlorine and various chlorine oxides were of interest.

Initially the decomposition gases were collected in a cold trap during a DTA run, and then analyzed on the mass spectrometer. Later the DTA apparatus constructed in the laboratory, was connected directly to the inlet of the mass spectrometer and the offcoming gases analyzed at intervals during the decomposition.

G. Additional Analytical Methods

Optical microscope and BET analysis were used to obtain information on the surface structure and surface area of a few selected oxides.

A Phillips x-ray diffractometer and powder camera were used in complex structural analyses, in particular in conjunction with the pseudo-catalysts, Cr_2O_3, and CrO_3 in mixture with $KClO_3$.

As standard wet analysis for the intermediate and final reaction products during TGA runs the following procedure was used:

A TGA run was performed to a predetermined temperature, the residue then rapidly cooled, and submitted for wet analysis.

The wet analysis consisted of three titrations. (1) Cl^- was titrated according to the Volhard method.[20] (2) ClO_3^- was reduced by SO_2 to Cl^- and the total Cl^- content (from $Cl^- + ClO_3^-$) determined after Volhard. (3) ClO_3^- and ClO_4^- were reduced to Cl^- by fusion in alkali (Na + K) carbonates in a Pt crucible, and again the overall Cl^- content (from Cl^-, ClO_3^-, and ClO_4^-) determined by titration after Volhard.

The oxides, Fe_2O_3 and MgO, were irradiated in our hot cell facility shown in Figure 6. The hot cell consists of a circular aluminum rack which contains a center hole and holes around the periphery of the rack one inch from the center hole. The holes contain stainless steel test tube holders which are one sixteenth inches thick. A Co^{60} gamma ray source of 1,000 curies is placed in a pyrex test tube in the center holder. The sample to be irradiated is placed in a second pyrex test tube which is located in one of the peripheral holders. The samples were exposed to the atmosphere during irradiation. The magnesium oxide was irradiated for 17 hours which corresponds to a dose of 2.5×10^5 rads. The Fe_2O_3 was irradiated for 65 hours corresponding to a dose of 5×10^6 rads.

Figure 6

THE SAMPLE HOLDER OF THE GAMMA RAY HOT CELL

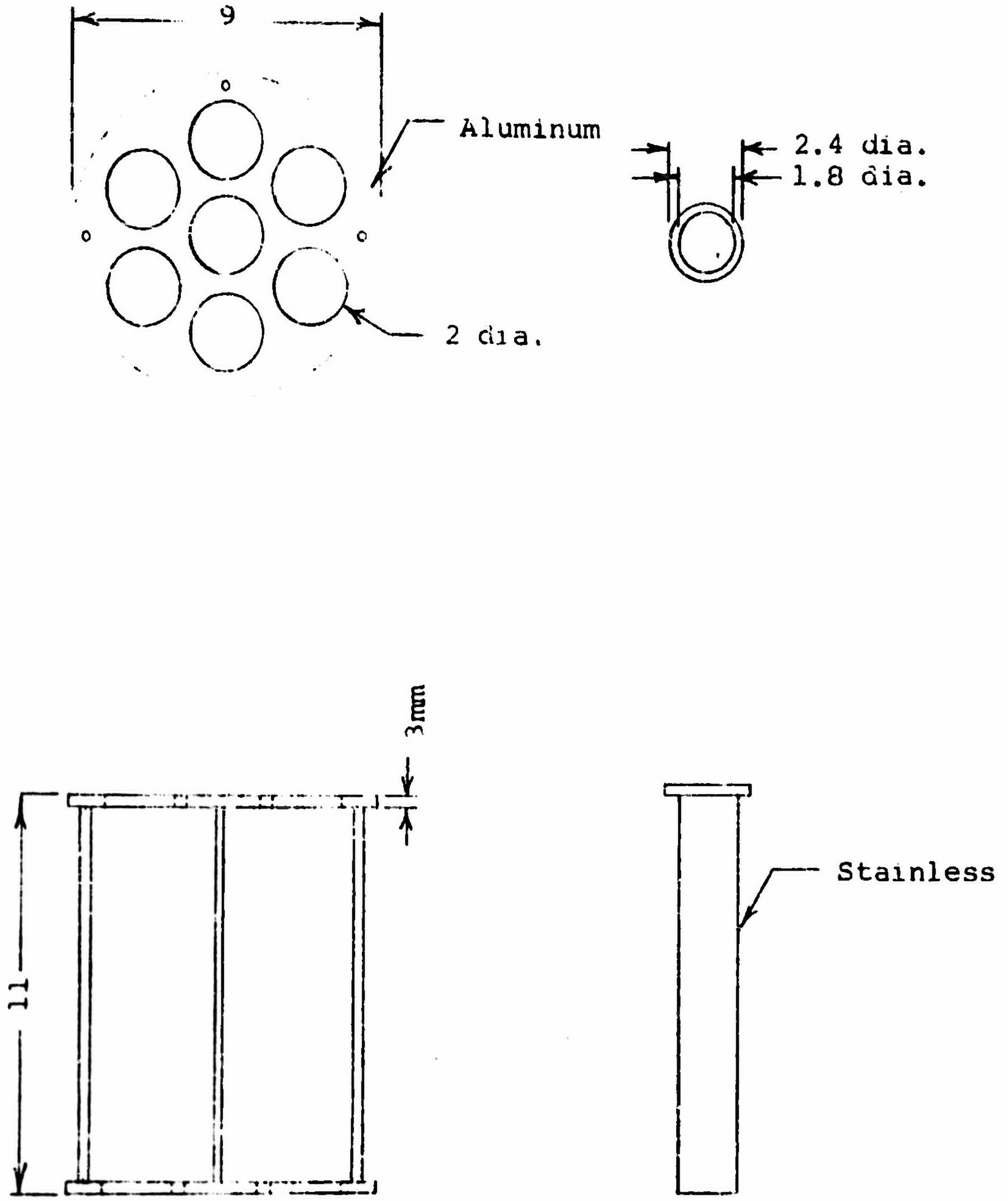

Scale 1/2 cm = 1 cm

EXPERIMENTAL RESULTS

A. Selection of Potassium Chlorate Sample

Preliminary experiments were carried out to determine if the reagent grade $KClO_3$ can be used directly in this investigation or if recrystallization is required due to the effects of impurities. To this end differential thermal analysis and thermogravimetric analysis experiments were carried out on the reagent grade material and compared to once recrystallized sample from distilled water. Figures 7 and 8 show the thermal analysis curves. It may be seen that there is little difference between the samples as indicated by the position and relative areas under the bands. This conclusion was confirmed by the thermogravimetric analysis experiments. On the basis of these results it was decided to use the reagent grade samples directly for the experimental program. The DTA curves show an endotherm and two exotherms at 368°C, 580°C and 610°C, respectively. The endotherm is due to melting and the exotherms to decomposition.

B. Ratio of Catalyst to Potassium Chlorate

Another factor which was considered concerned the mole ratio of catalyst to potassium chlorate. Several intimate mixtures of solid and powdered potassium chlorate were prepared, where the mole ratio ranged from 1/20 to 3/10. The differential thermal analysis curves in Figure 9 shows a very pronounced increase in catalytic activity in going from a ratio of 1/20 to 1/10 catalyst to chlorate. A further increase in concentration to a mole ratio of 3/10 shows no significant changes in the position of the

Fig. 7. DTA OF POTASSIUM CHLORATE DECOMPOSITION
(1, Recrystallized and 2, Original Material)
Air Atmosphere, Heat Rate = 10°C/min

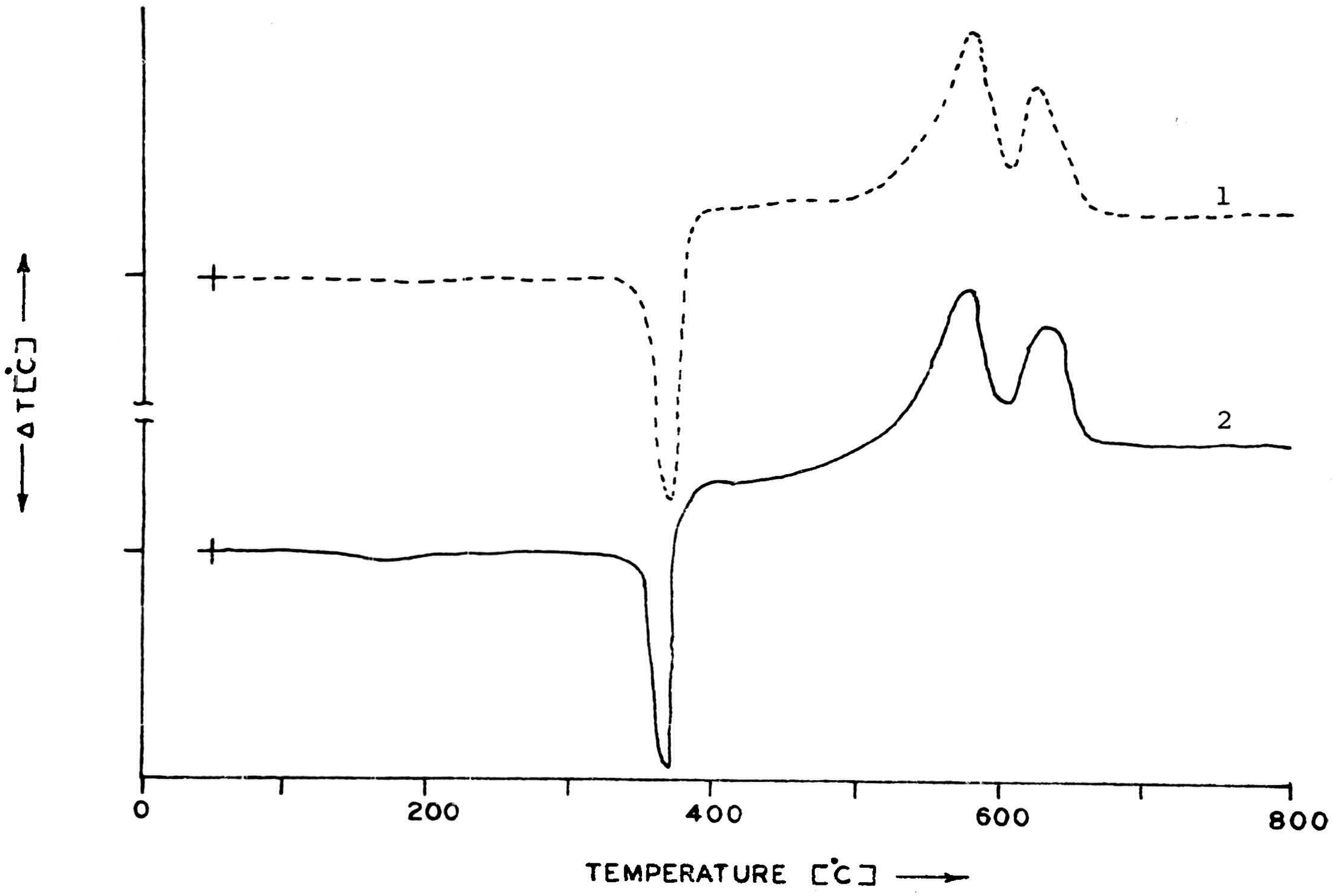

Fig. 8. THERMOGRAVIMETRIC CURVES OF REAGENT GRADE AND RECRYSTALLIZED $KClO_3$

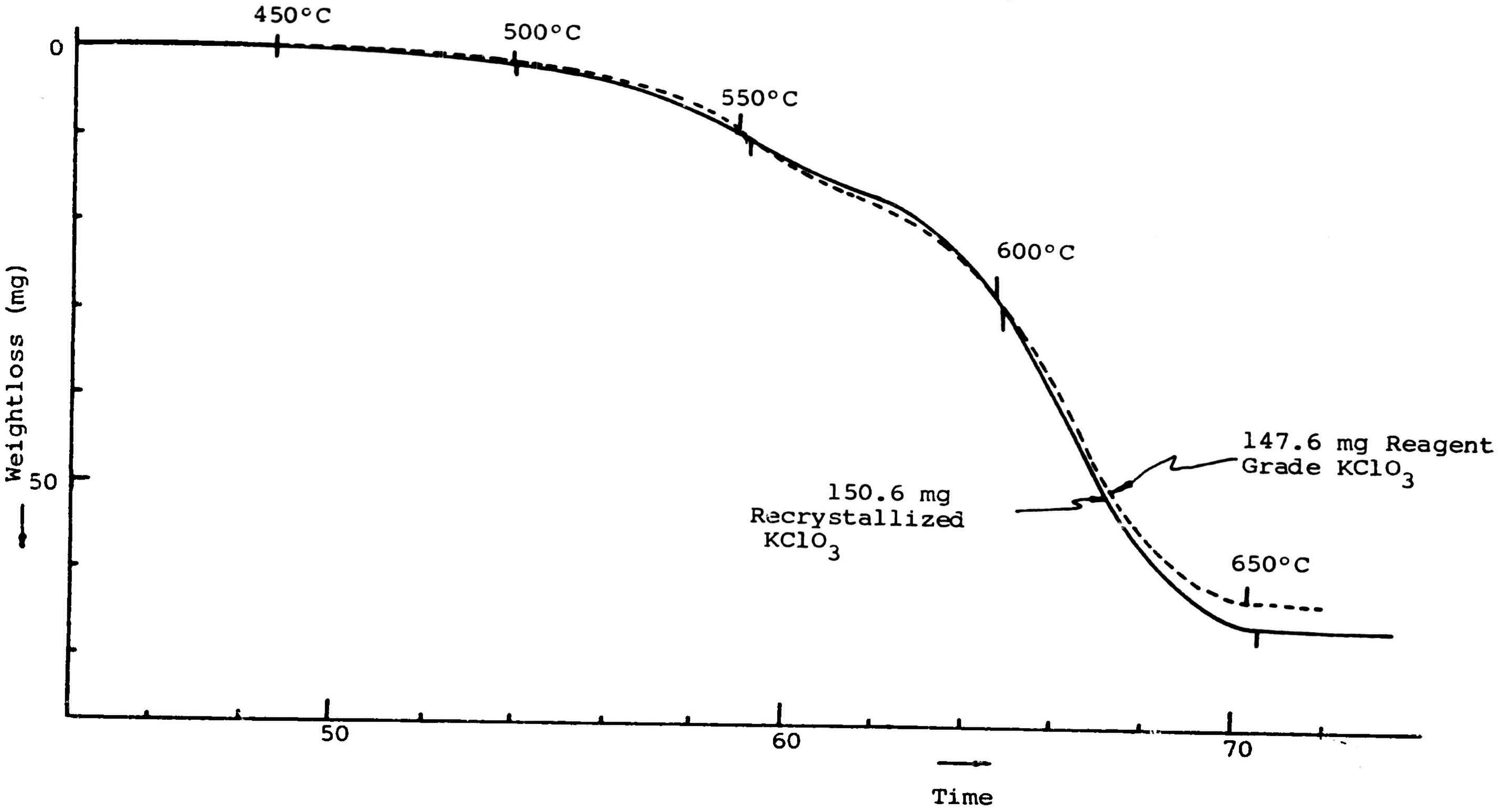

Fig. 9. DIFFERENTIAL THERMAL ANALYSIS OF THE CATALYTIC ACTION OF Fe_2O_3 ON THE DECOMPOSITION OF POTASSIUM CHLORATE
Heating Rate = 10°C/min
Atmospheric Pressure in Air

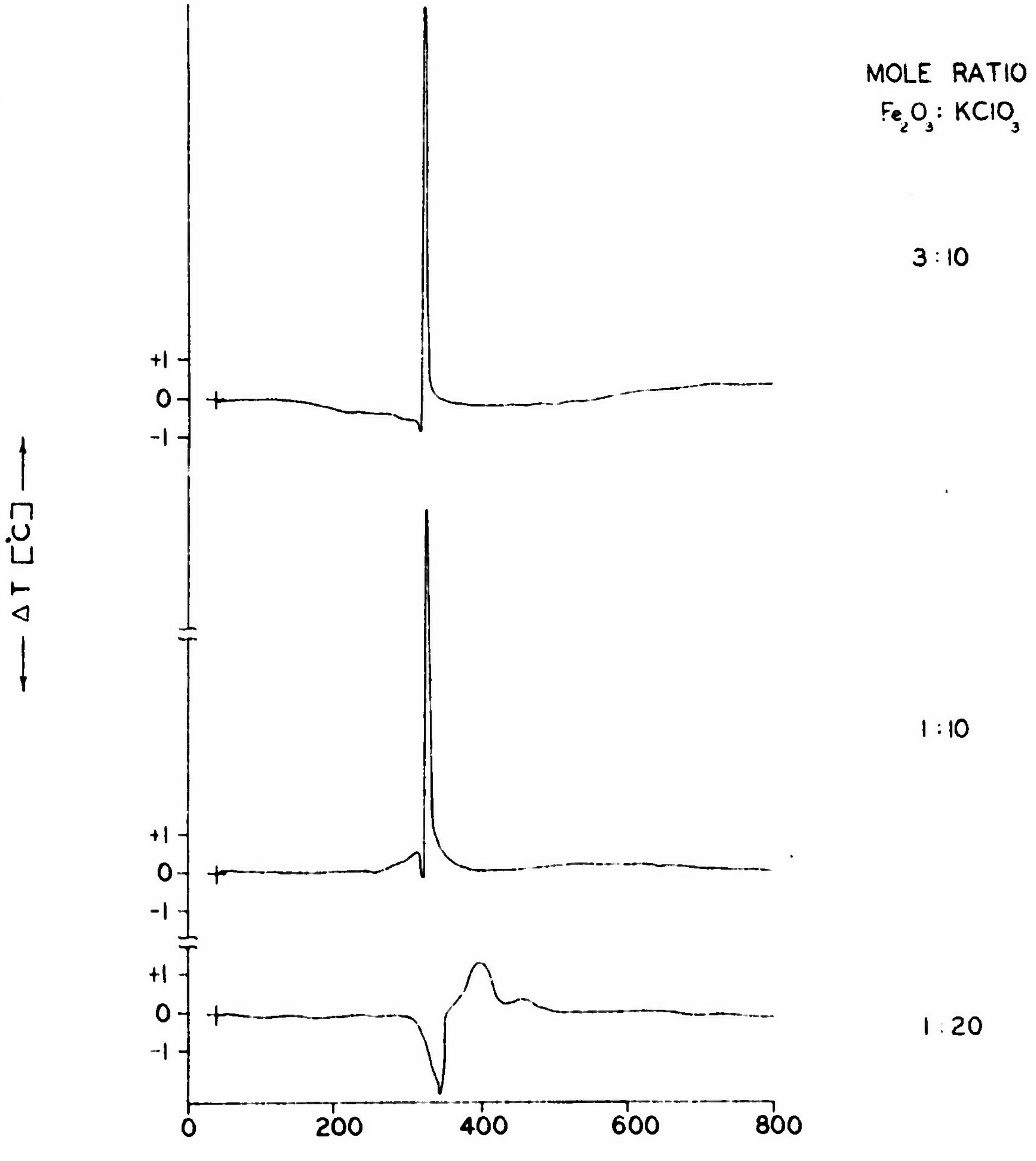

exotherm for decomposition. The mole ratio of 1 to 10 was, therefore, selected as the basis for the standard mixture to be used in this program. This mole ratio corresponds to one metal ion in the oxide to 5 potassium ions in the chlorate. The screen fraction of the oxides used in this work is 230/270.

C. The Influence of Gaseous Atmospheres

Some authors[16] claim reversibility of the reactions:

$$2KClO_3 \rightarrow 2KCl + 3O_2 \qquad (1)$$

and

$$4KClO_3 \rightarrow 3KClO_4 + KCl \qquad (2)$$

If this is true, the decomposition should be depressed in an oxygen atmosphere but should be increased in an inert gas flow. Figure 10 shows, however, that no significant change in the DTA curves could be obtained by using purified oxygen and/or nitrogen as the flow gas. During initial runs, oxygen and nitrogen taken directly from the tanks showed apparent catalytic action. Since a flow of air did not influence significantly the position of the peaks, it was first suspected that gases in the oxygen and nitrogen gas cylinders were moist, and the water gave rise to the catalytic action. Consequently, the gases were purified over activated molecular sieves. No catalytic action was then observed. However, when the purified gas stream was bubbled through water prior to entering the reaction chamber, again no catalytic effect was observed. This leads us to conclude that impurities in the gas cylinders other than water are responsible for the apparent catalytic action of the gases. Water vapor did not appear to affect the decomposition characteristics of $KClO_3$.

Fig.10. DIFFERENTIAL THERMAL ANALYSIS OF POTASSIUM CHLORATE IN DIFFERENT ATMOSPHERES

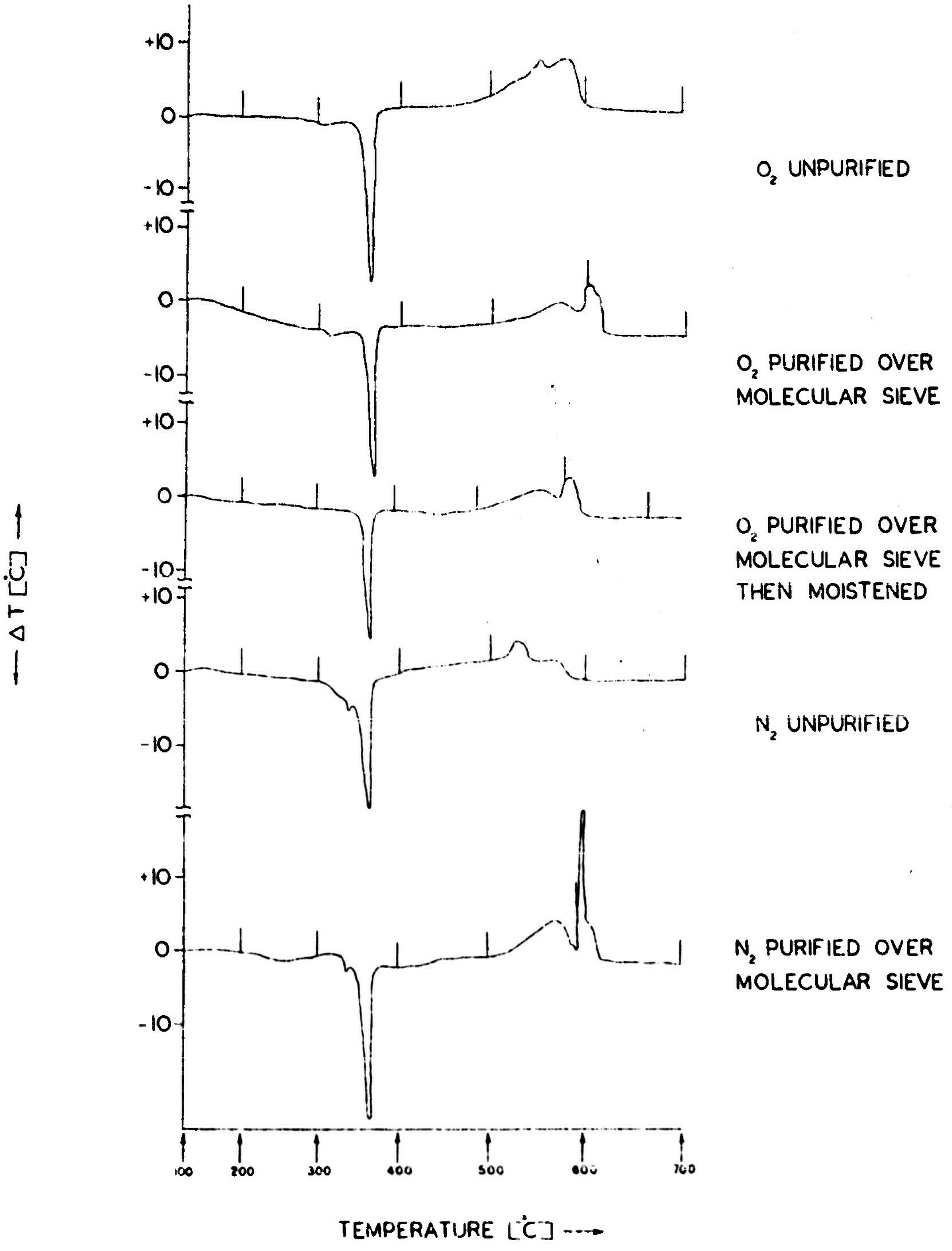

D. The Catalytic Activity of Metal Oxides with Respect to the Decomposition of Potassium Chlorate and Potassium Perchlorate

Figures 11 and 12 are differential thermal analysis and thermogravimetric analysis curves which show the catalytic effects of the complete series of oxides selected for this work on the thermal decomposition of potassium chlorate and perchlorate, respectively. The amount of catalyst used in all cases corresponded to a ratio of one metal cation of the oxide to 5 potassium ions of the chlorate and/or perchlorate. Tables 1 and 2 show the order of catalytic activity with respect to initial decomposition and at approximately 50% decomposition of $KClO_3$ and $KClO_4$. The order of catalytic activity is seen to be essentially the same for the thermal decomposition of both the chlorate and perchlorate although there are some exceptions from the point of view of the order of "p" character as compared to the N_2O work.[1] The exceptions, however, do not upset the general trend from the point of view of interpretation. They are: Fe_2O_3, CuO, ZnO and MgO. It is interesting to note that the temperatures at which decomposition initially occurs are quite close for both $KClO_3$ and $KClO_4$ in the presence of the following oxides, Cr_2O_3, CoO, Co_3O_4, and Cu_2O. See Table 3.

In the case of the catalysis of the decomposition of N_2O to N_2 and O_2 the key to the understanding of this mechanism came from electrical conductivity studies carried out at relatively low temperatures, below 400°C.[21] In this work it was

Table 1

INITIAL DECOMPOSITION

$KClO_3$		$KClO_4$	
Catalyst	Temp, °C	Catalyst	Temp, °C
Cr_2O_3	300	Cr_2O_3	325
CoO	350	Co_3O_4	375
Co_3O_4	350	Cu_2O	380
Fe_2O_3	375	CoO	380
Cu_2O	380	CuO	450
MnO_2	380	Fe_2O_3	450
CuO	380	MnO_2	460
NiO	385	Ag_2O	520
ZnO	400	NiO	520
Ag_2O	420	MgO	525
MgO	440	Al_2O_3	530
TiO_2	440	TiO_2	535
Al_2O_3	520	ZnO	565
No Cat.	530	No Cat.	600

Ratio of cation in metal oxide to potassium ion in chlorate (perchlorate) = 1:5

Fig. 11. SIMULTANEOUS THERMOGRAVIMETRIC ANALYSIS AND DIFFERENTIAL THERMAL ANALYSIS. THE CATALYTIC ACTIVITY OF METAL OXIDES ON THE DECOMPOSITION OF POTASSIUM CHLORATE

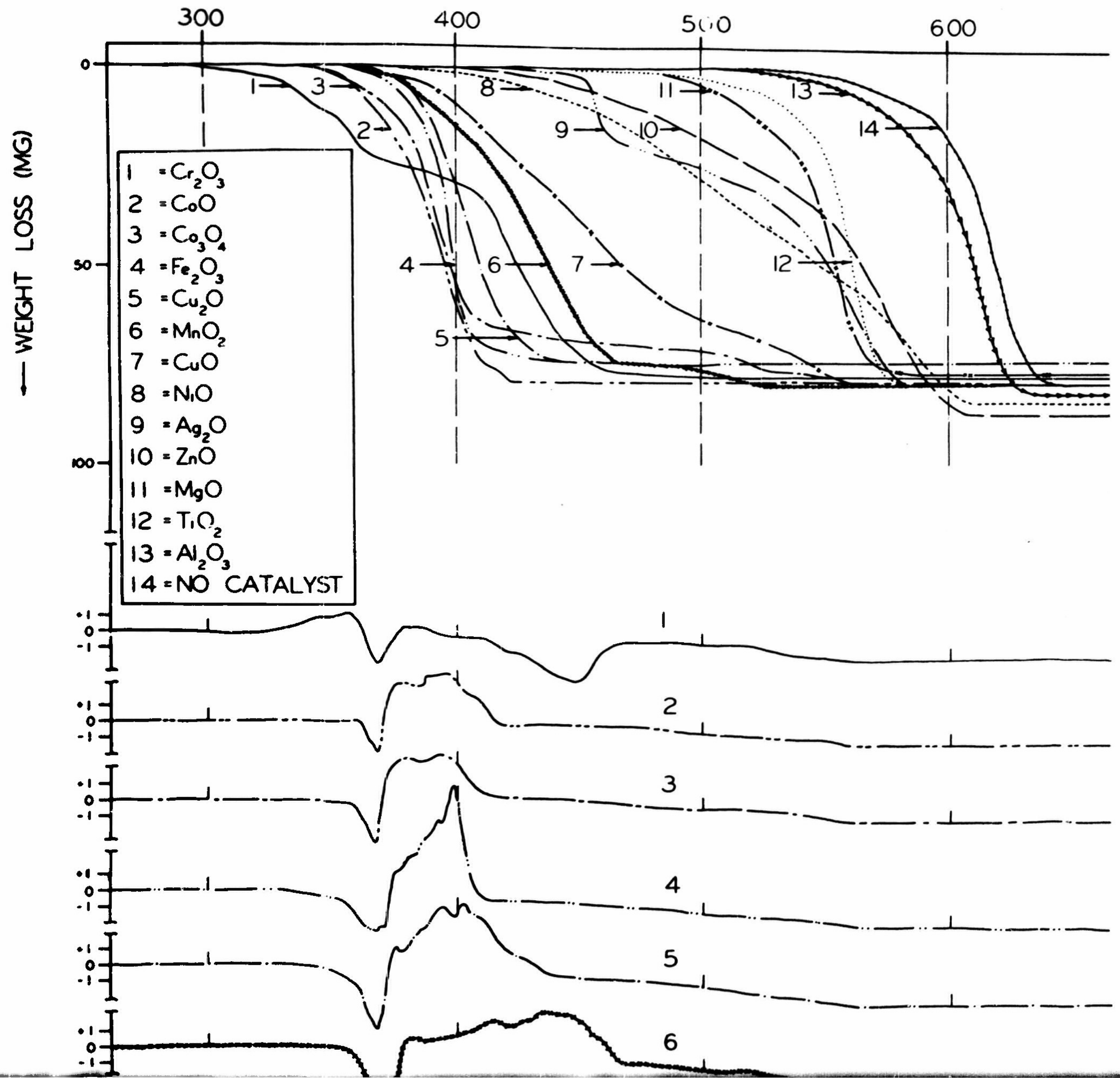

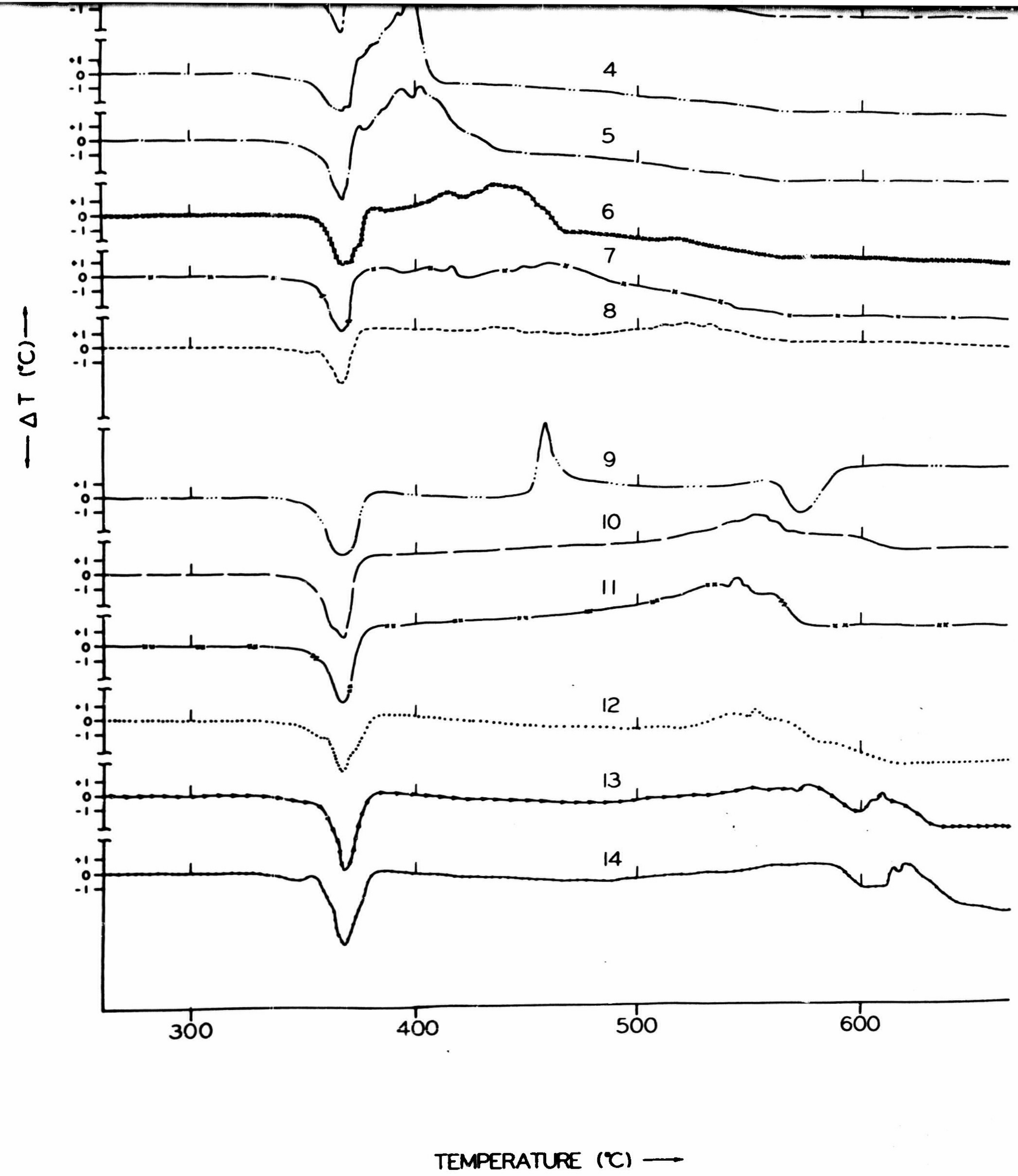

2

Fig. 12. SIMULTANEOUS THERMOGRAVIMETRIC ANALYSIS AND DIFFERENTIAL THERMAL ANALYSIS. THE CATALYTIC ACTIVITY OF METAL OXIDES ON THE DECOMPOSITION OF POTASSIUM PERCHLORATE

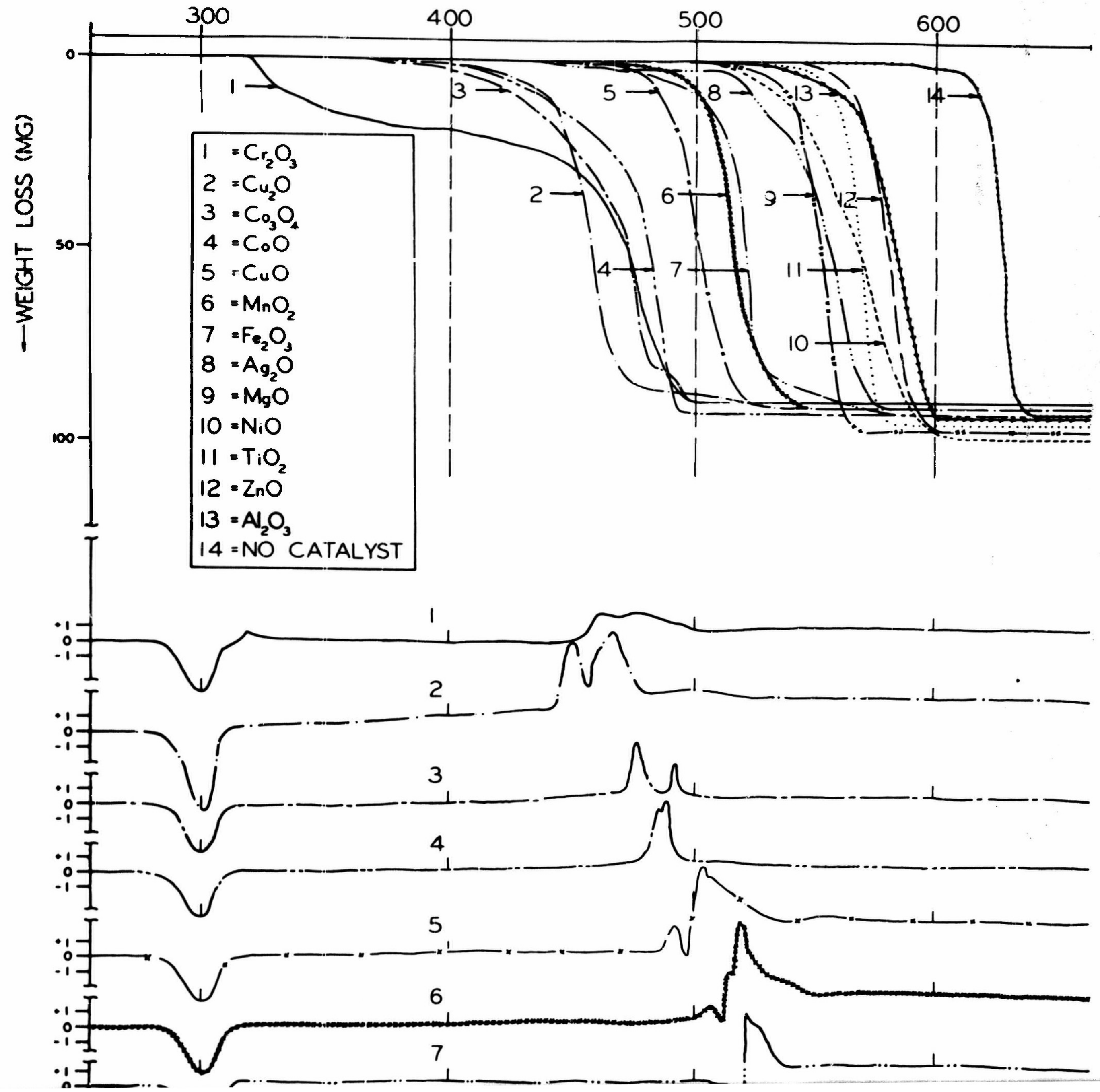

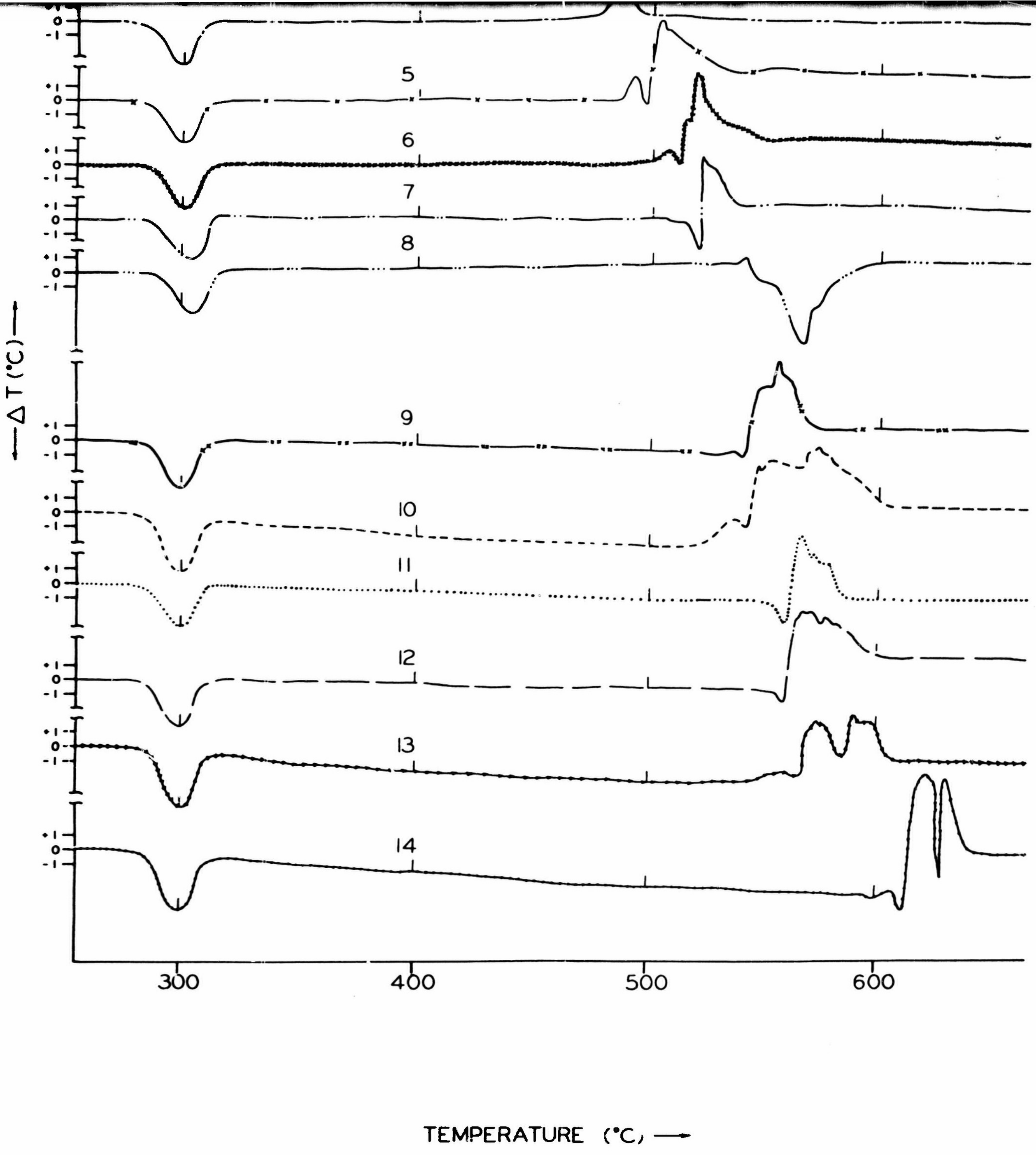

2

Table 2

DECOMPOSITION AT 50 mg WEIGHT LOSS

$KClO_3$		$KClO_4$	
Catalyst	Temp, °C	Catalyst	Temp, °C
CoO	400	Cu_2O	470
Co_3O_4	400	Cr_2O_3	480
Fe_2O_3	400	Co_3O_4	480
Cu_2O	415	CoO	490
Cr_2O_3	425	CuO	510
MnO_2	440	MnO_2	525
CuO	470	Fe_2O_3	530
NiO	540	MgO	565
Ag_2O	550	Ag_2O	570
ZnO	570	NiO	580
MgO	570	TiO_2	580
TiO_2	575	ZnO	585
Al_2O_3	615	Al_2O_3	590
No Cat.	625	No Cat.	635

Ratio of cation in metal oxide to potassium ion in chlorate (perchlorate) = 1:5

Table 3

COMPARISON OF CATALYTIC ACTIVITIES

$KClO_3$		$KClO_4$	
Catalyst	Temp, °C	Catalyst	Temp, °C
Cr_2O_3	300	Cr_2O_3	325
Co_3O_4	350	Co_3O_4	375
CoO	350	CoO	380
Cu_2O	380	Cu_2O	380

Ratio of cation in metal oxide: Potassium ion in chlorate (perchlorate) = 1:5

shown that the chemisorption of oxygen on NiO catalyst was accompanied by electron transfer.

$$N_2O + e \text{ (from catalyst)} = N_2 + O^- \text{ (ads)}$$

$$O^- \text{ (ads)} = 1/2\ O_2 + e \text{ (to catalyst)}$$

$$\text{or } O^- \text{ (ads)} + N_2O = N_2 + O_2 + e \text{ (to catalyst)}$$

This electron transfer process between the oxygen and catalyst was shown to be reversible as indicated by the equations above. Since the release of neutral O_2 depends on O^- giving up its electron to the catalyst the better the "p" conductor the higher the catalytic activity. The electrical conductivity evidence seemed to support this theory.

E. The Effects of Defect Structure on the Catalytic Activity of Ferric Oxide and Magnesium Oxide

Ferric oxide was selected for further investigation because of the high catalytic activity which it exhibited in the initial experiments and since it has "n" semiconducting properties as will be later confirmed, and MgO because it has "p" semiconducting character. It is known that the method of preparation, purity and thermal treatment, history and exposure to high energy radiation can markedly effect the defect structure and semiconducting properties of solid oxides. Experiments were, therefore, conducted which involved investigating the catalytic activity of a series of iron oxide and magnesium oxide samples which were heat treated, exposed to radiation or doped with impurity ions in order to change their structural and electronic properties. The object of these experiments was to investigate the effects of defect structure of the solid oxides on catalytic activity with respect to the thermal decomposition of potassium chlorate. The methods of preparation and conditions of heat treatment and radiation are given in the experimental section.

1. Effects of Method of Precipitation of Fe_2O_3

Figure 13 shows the differential thermal analysis curves for the decomposition of potassium chlorate in the presence of ferric oxides which have different histories and have been prepared by different methods. The uppermost curve shows the catalytic effect of reagent grade ferric oxide as received. It may be seen that there is some initial solid state decomposition indicated by the slight exotherm beginning at about 220°C. The small endotherm for melting is seen at 310°C. This is immediately followed by a single sharp exotherm due to the decomposition of the potassium chlorate at about 320°C. In the case of the sodium hydroxide precipitated ferric oxide the thermal analysis curve shows that there is a significant decrease in catalytic activity as indicated by the shift of the exotherm for decomposition to higher temperatures, in this case about 480°C. Increasing the amount of sample to a ratio of Fe_2O_3 (ppd in NaOH) to $KClO_3$ of 3.5 did not appear to alter the position of the exotherm on the DTA curve. This confirmed the previous results which indicated that increasing the amount of Fe_2O_3 beyond a mole ratio of 1 to 10 has little further effect on the catalysis of decomposition.

Fig. 13. DIFFERENTIAL THERMAL ANALYSIS OF DECOMPOSITION OF $KClO_3$ CATALYZED BY Fe_2O_3 IN ARGON

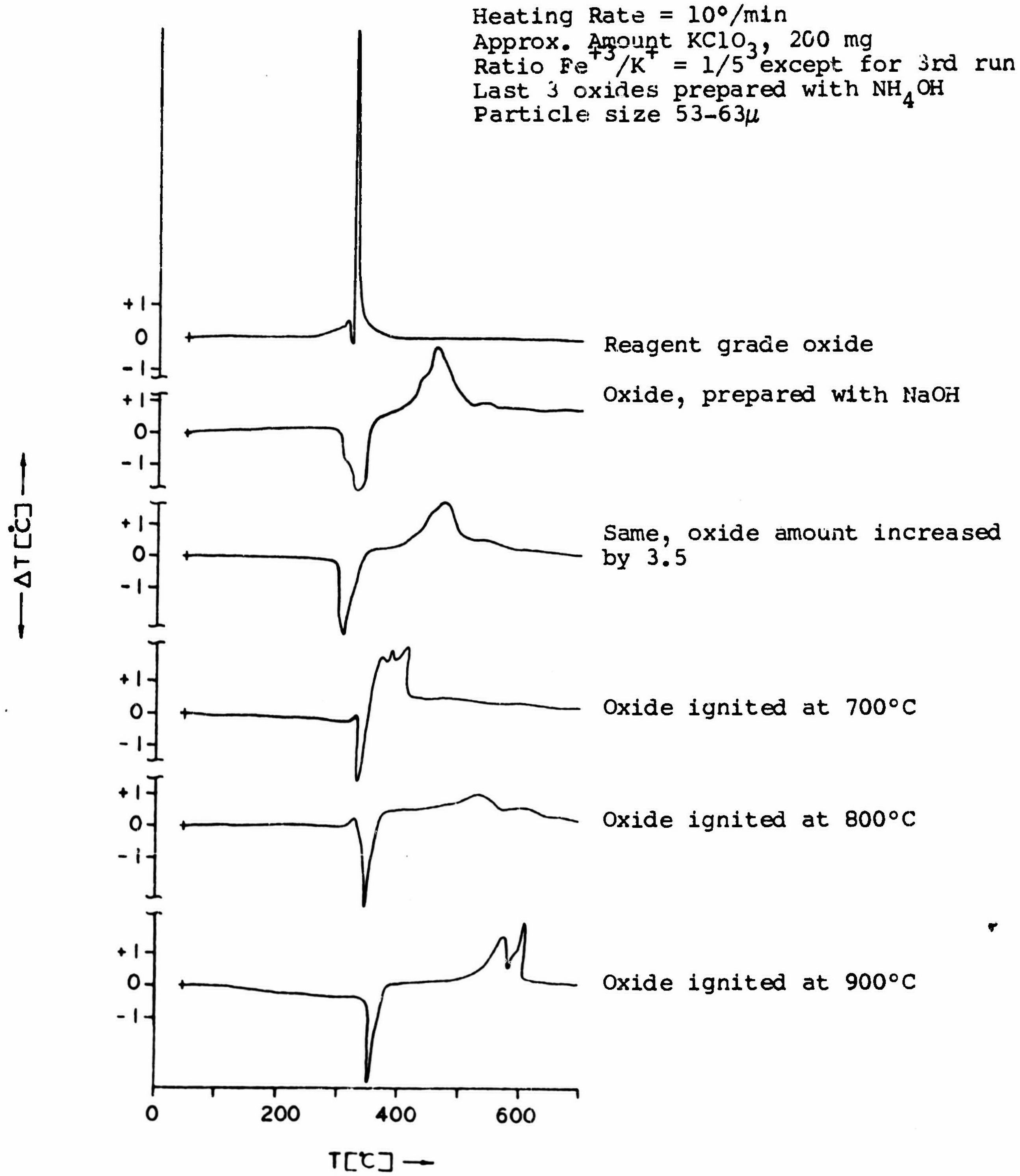

Heating Rate = 10°/min
Approx. Amount $KClO_3$, 200 mg
Ratio Fe^{+3}/K^{+} = 1/5 except for 3rd run
Last 3 oxides prepared with NH_4OH
Particle size 53-63μ

2. Effects of Heat Treatment

Ferric oxide prepared by precipitation in ammonium hydroxide solution was used to investigate the effect of heat treatment on its catalytic activity. Figure 13 shows the results of experiments in which the precipitate was heated at 700°C, at 800°C and 900°C. It can be seen from the differential thermal analysis curves that as the temperature was increased the catalytic activity significantly decreased. In the presence of the ferric oxide heat treated at 700°C, the melting point of the $KClO_3$ showed and a triple peaked exotherm between 310° and 420°C due to decomposition is seen. In the presence of the 800°C heat treated Fe_2O_3 the exotherm becomes quite broad and shows low peaks at 520°C and 620°C. The low exotherms are due to the slow rates of reaction. Heat treatment at 900°C appears to have substantially decreased the effectiveness of the catalyst as may be seen by comparisons with the DTA curves shown previously for pure $KClO_3$.

Samples of ferric oxide were also heat treated in oxygen and argon at atmospheric pressure. As seen in the case where the samples were heat treated in air, (page 50 ff) the catalytic activity generally decreased also in oxygen and in argon as the temperature was increased from 800°C to 1000°C. The argon heat treated samples, however, are more active than the oxygen heat treated samples at 800°C and 900°C. Heat treatment at 1000°C virtually eliminated, as well as equalized, the catalytic activity of both the oxygen and argon heat treated samples. Figure 14 shows the results.

The catalytic activity of MgO was investigated after heat treatment in argon and in oxygen. See Experimental section (page 20) for the preparation of the sample. It was found from thermogravimetric analysis that the trend in catalytic activity is apparently opposite to that encountered with Fe_2O_3. The results in Figure 15 show that the oxide heat treated in argon has lower catalytic effectiveness as is indicated in higher decomposition temperature of $KClO_3$ than the oxide heat treated in oxygen. The difference between the temperature of complete decomposition of the $KClO_3$ with magnesium oxide heat treated in argon and the magnesium oxide heat treated in oxygen is about 30°C. The oxygen heat treated magnesium oxide is the more active catalyst.

3. Effects of Gamma Ray Irradiation

Figure 16 shows the catalytic effect of reagent grade ferric oxide exposed to Co^{60} gamma rays on the decomposition of $KClO_3$. The dose rate was about 10^6 r/hr and the total exposure dose was 5×10^5 r. The samples were exposed in air at atmospheric pressure. The differential thermal analysis and thermogravimetric analysis curves demonstrate that irradiation resulted in a significant increase in catalytic activity with respect to the thermal decomposition of potassium chlorate. It may be noted that the weight losses seen in the thermogravimetric analysis curves correspond closely to the thermal

Fig. 14. THERMOGRAVIMETRIC ANALYSIS OF THE CATALYTIC ACTIVITY OF HEAT TREATED Fe_2O_3 ON THE DECOMPOSITION OF $KClO_3$ (Oxides Heated for about 1 hr. to the Temperatures Indicated)

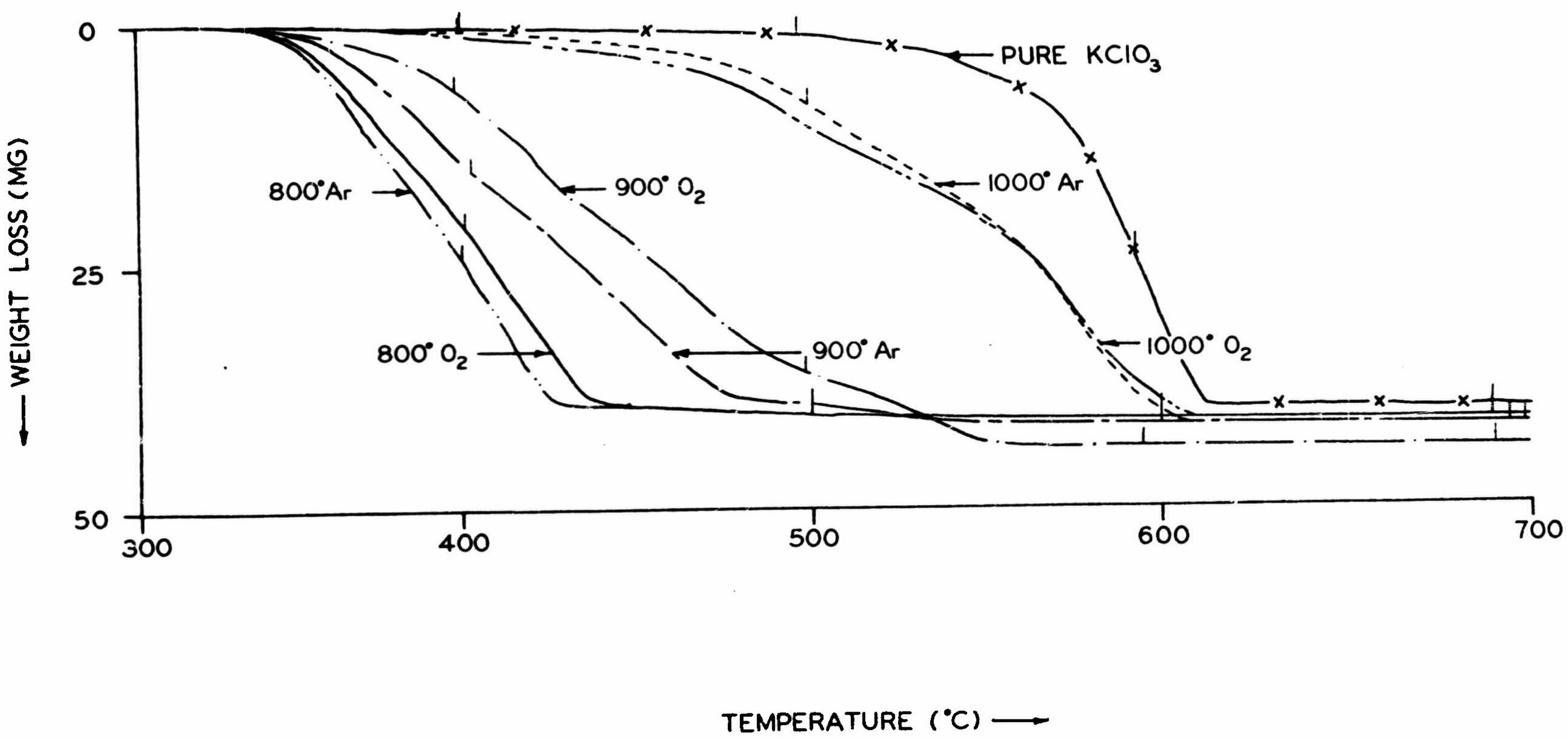

Fig. 15. CATALYTIC ACTIVITY OF MAGNESIUM OXIDE (1) HEAT TREATED IN ARGON (2) HEAT TREATED IN OXYGEN (Heated to above 750°C at 10°C/min) ((3) Reference Curve Without Catalyst)

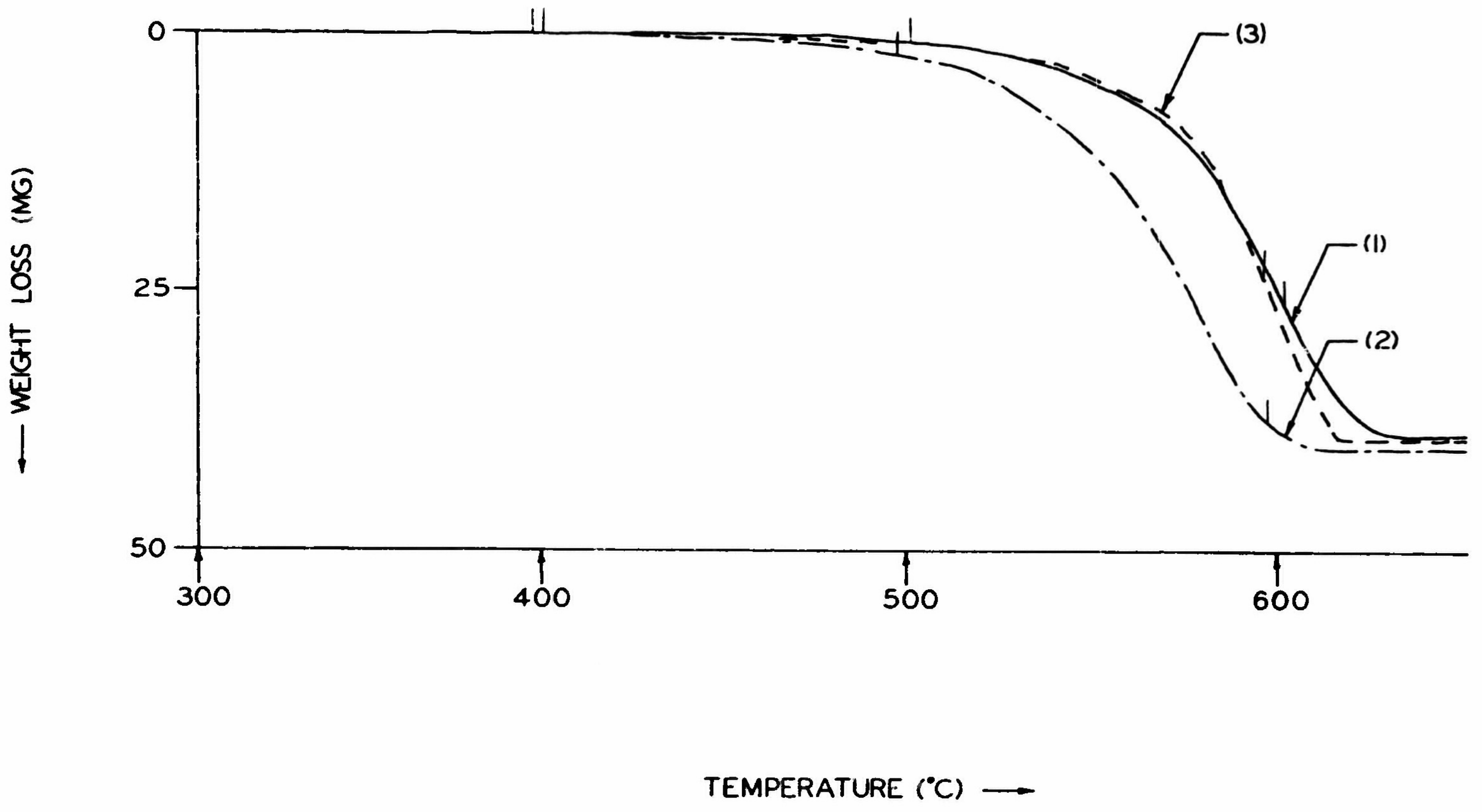

Fig. 16 INFLUENCE OF IRRADIATION ON THE CATALYTIC ACTIVITY OF Fe_2O_3 WITH RESPECT TO DECOMPOSITION OF $KClO_3$.

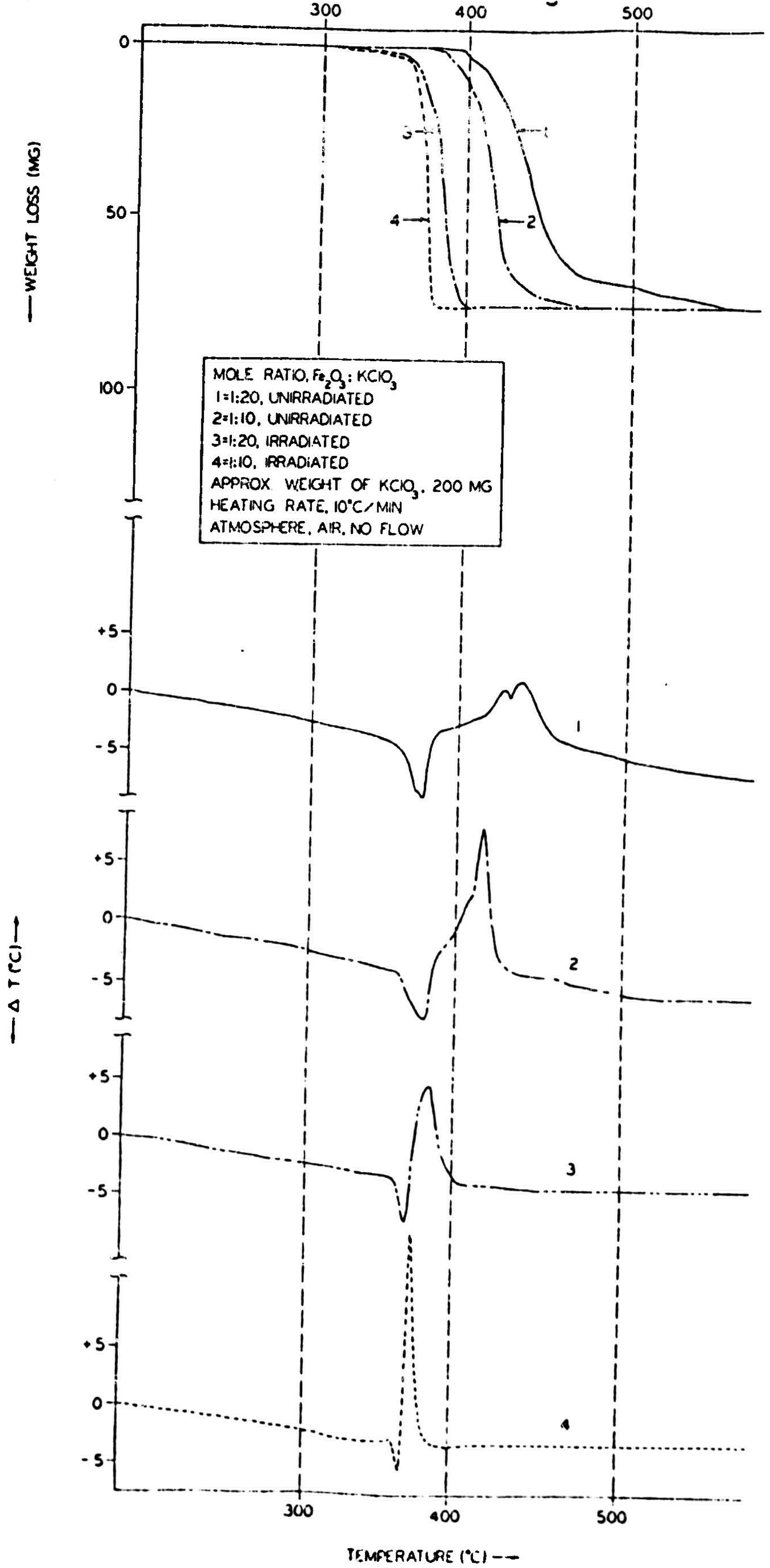

effects seen in the DTA curves. Again it is seen that there is an increase in catalytic activity in going from a mole ratio of $Fe_2O_3/KClO_3$ of 1:20 to 1:10. The double exotherm seen during the decomposition of the $KClO_3$ in the presence of the unirradiated Fe_2O_3 is combined into a single sharp exotherm at lower temperatures in the case of the irradiated Fe_2O_3.

Gamma ray irradiated magnesium oxide shows a similar deviation from normal behavior of the untreated oxide as in the case of the argon treated sample (Figure 17). It is significantly less active as a catalyst than the unirradiated material.

4. Effects of Doping on the Catalytic Activity of Fe_2O_3

Figure 18 shows simultaneous differential thermal analysis and thermogravimetric analysis curves of the decomposition of $KClO_3$ in the presence of doped and undoped ferric oxide. Sample preparation is described in the Experimental section. (Page 19)

The order of catalytic activity with respect to the overall reaction going from the most active to the least was the Zr^{+4} doped sample, Be^{+2}, undoped and Li^{+1} doped Fe_2O_3. If we examine the initial decomposition, the order of catalytic activity is Zr^{+4}, undoped, Be^{+2} and Li^{+1} ions. The thermal analysis curves show that the temperature range for complete decomposition decreases as the overall catalytic effect increases. In the case of the differential thermal analysis curves this is indicated

Fig. 17. INFLUENCE OF IRRADIATION ON THE CATALYTIC ACTIVITY OF MgO WITH RESPECT TO DECOMPOSITION OF $KClO_3$

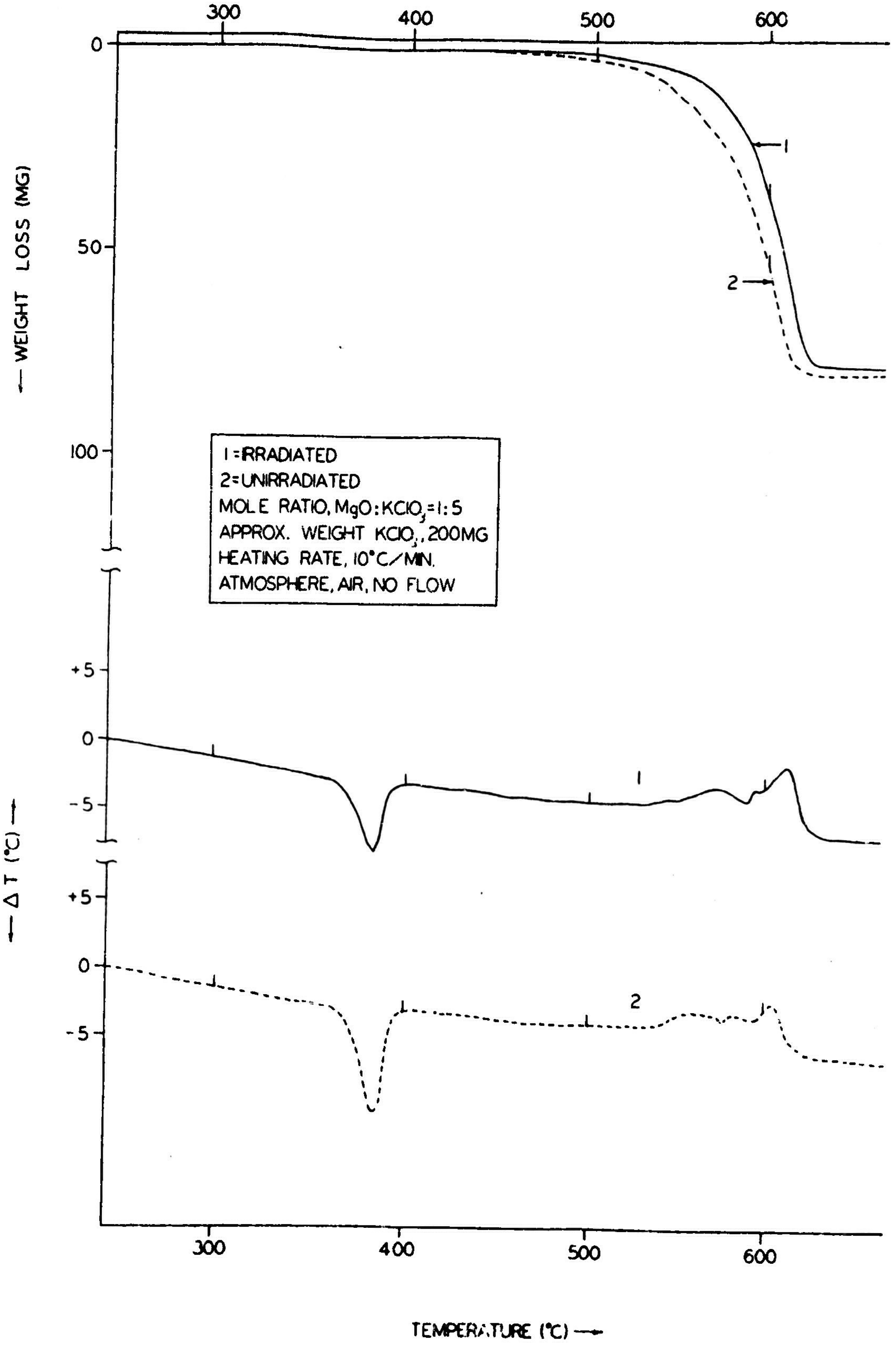

Fig. 18. THE INFLUENCE OF DOPING ON THE CATALYTIC ACTIVITY OF Fe_2O_3 WITH RESPECT TO THERMAL DECOMPOSITION OF $KClO_3$

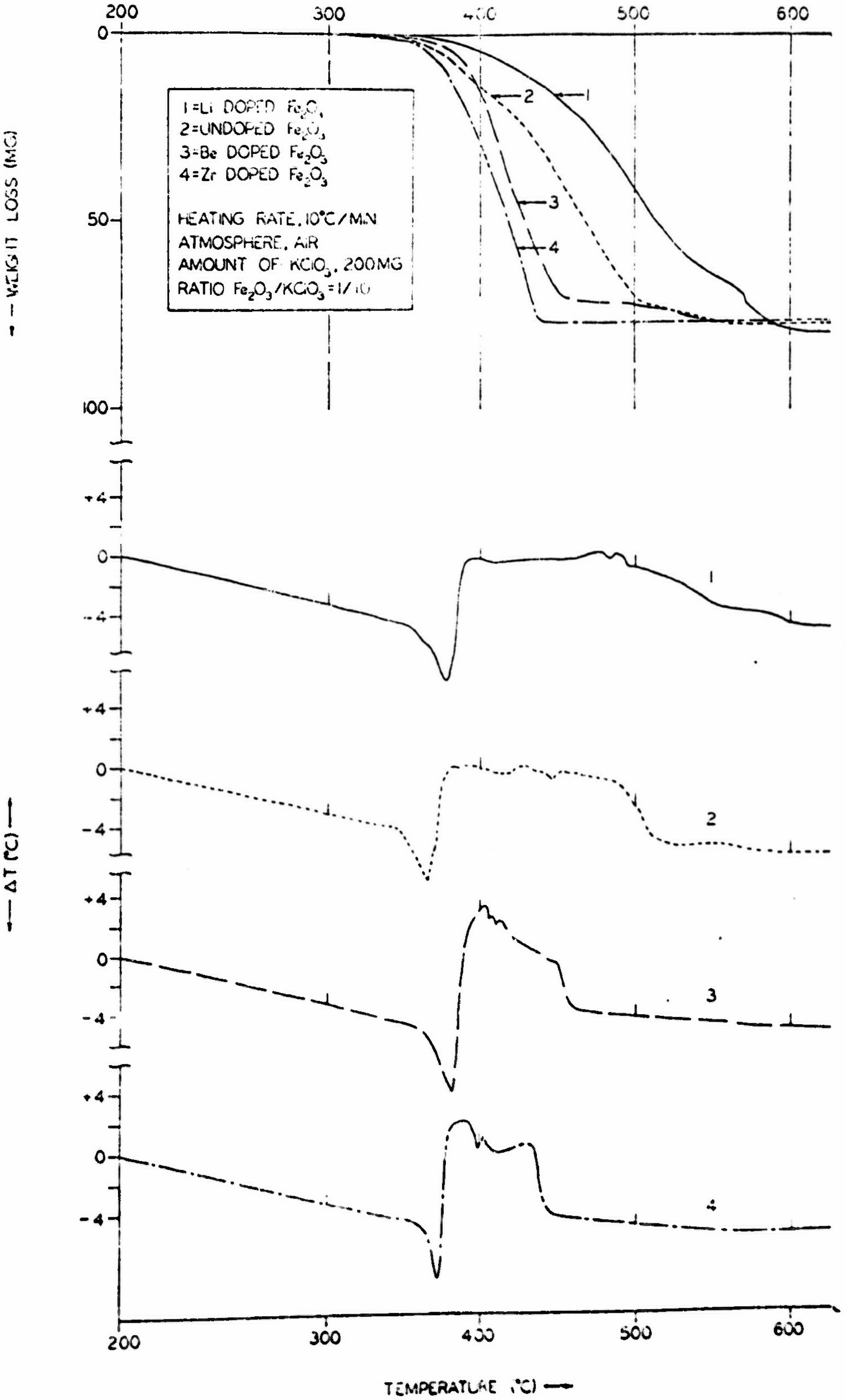

by the spread of the exothermal bands which also corresponds to the weight loss curves.

5. Effects of Potassium Chloride

It is necessary to know the effects which the reaction products might possibly have on the kinetics of decomposition of $KClO_3$. Experiments were therefore, carried out to evaluate the effects of potassium chloride on the decomposition of potassium chlorate. This information is also required in order to evaluate the catalytic effects of the oxides.

Figure 19 shows simultaneous thermogravimetric analysis and derivative thermogravimetric analysis curves of a 1:1 mixture of potassium chlorate and potassium chloride. In the case of the decomposition of $KClO_3$ alone there appears to be an initial rapid reaction followed by a decrease in the reaction rate and then a rapid decomposition. The derivative thermogravimetric curve shows a shoulder at about 550°C followed by another peak at 600°C. The reaction is complete at approximately 620°C. The derivative thermogravimetric curve is a simple smooth band with only one peak which ends about 10°C higher than for the pure potassium chlorate. The maximum reaction rate is also lower.

6. Pseudo-Catalytic Effects of Cr_2O_3 and CrO_3 on the Thermal Decomposition of $KClO_3$

When the catalytic effects of the selected series of metal oxides were investigated with respect to the decomposition of $KClO_3$ and $KClO_4$ it was found that Cr_2O_3 was the most effective apparent catalyst. However, a color change from the green

Fig. 19. DECOMPOSITION OF (1) POTASSIUM CHLORATE AND (2) A MIXTURE OF POTASSIUM CHLORATE AND CHLORIDE

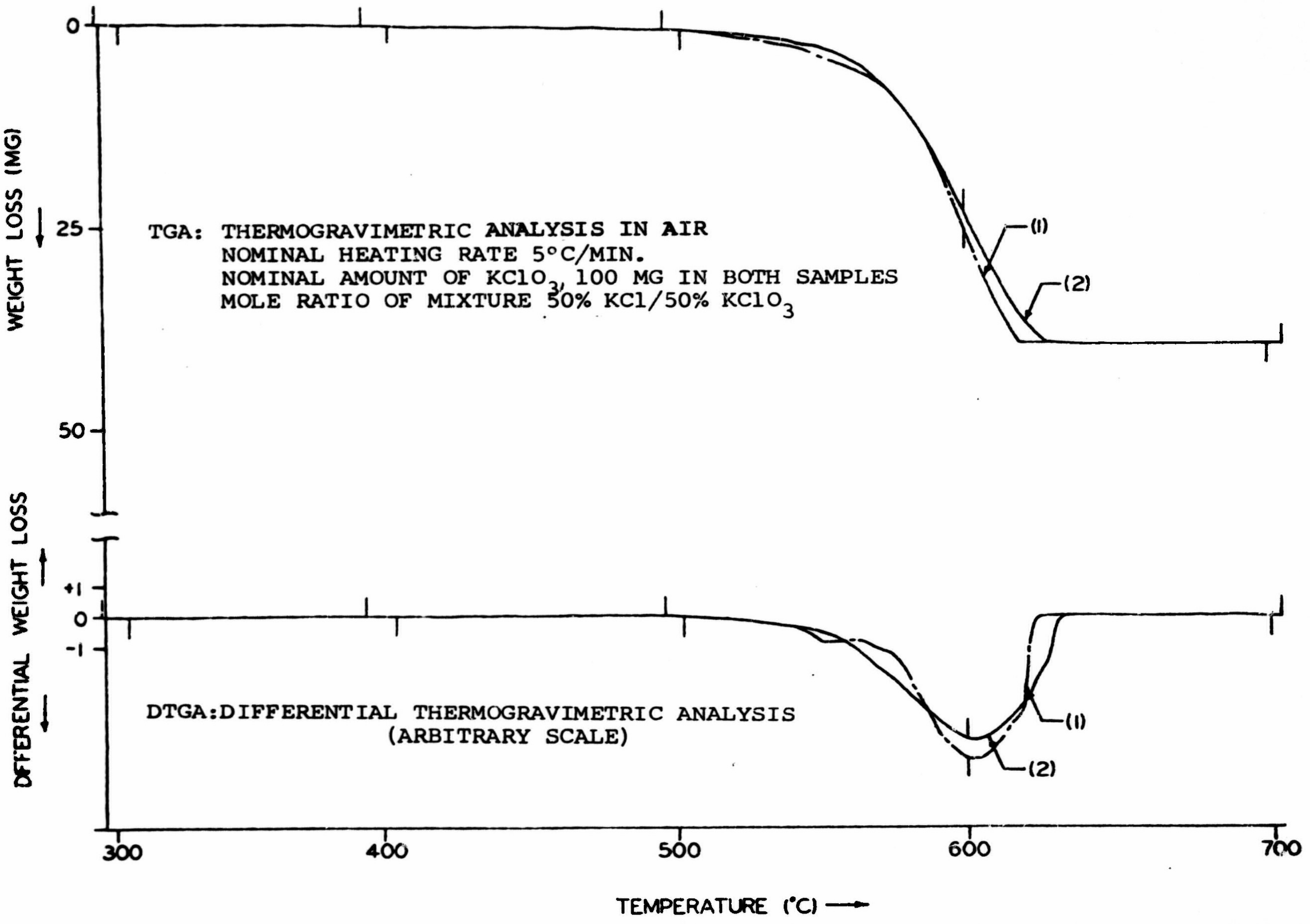

TGA: THERMOGRAVIMETRIC ANALYSIS IN AIR
NOMINAL HEATING RATE 5°C/MIN.
NOMINAL AMOUNT OF $KClO_3$, 100 MG IN BOTH SAMPLES
MOLE RATIO OF MIXTURE 50% KCl/50% $KClO_3$

DTGA: DIFFERENTIAL THERMOGRAVIMETRIC ANALYSIS
(ARBITRARY SCALE)

Cr(III) oxide to yellow in the residue indicated that Cr_2O_3 may have changed to a higher valent chromium oxide. In order to investigate this possibility in more detail a series of experiments was carried out with Cr_2O_3 and CrO_3. Thermogravimetric analysis and differential thermogravimetric analysis were carried out on mixtures of Cr_2O_3 and $KClO_3$ with a mole ratio of 1/10 and CrO_3 and $KClO_3$ at a mole ratio of 1/5. The results are shown in Figure 24. It may be seen that CrO_3 is significantly more active than Cr_2O_3. In the presence of CrO_3 the decomposition of $KClO_3$ is observed to begin at approximately 200°C. In order to determine if the catalytic activity is related to the decomposition of CrO_3, thermoanalysis experiments were conducted on the oxide alone under the same conditions as the decomposition runs. It may also be seen from Figure 24, that weight loss does not occur over the temperature range where CrO_3 catalyzes the decomposition of $KClO_3$. This oxide begins to decompose at approximately 290°C and that decomposition is complete at 510°C. The total weight change corresponds to the formation of Cr_2O_3. However, it is quite interesting to observe that an endotherm occurs on the DTA curve which corresponds almost exactly to a sharp decrease in weight in the thermogravimetric curves. This occurs at approximately 200°C which is very close to the reported melting point of CrO_3, 198°C.[22] A sharp exotherm corresponds to the rapid weight loss at 200°C. At 350°C the final region of weight loss occurs which corresponds to the decomposition of $KClO_3$ in the presence

Fig. 20. SIMULTANEOUS THERMOGRAVIMETRIC ANALYSIS AND DIFFERENTIAL THERMAL ANALYSIS. COMPARISON OF THE CATALYTIC ACTIVITIES OF Cr_2O_3 AND CrO_3 ON THE DECOMPOSITION OF $KClO_3$

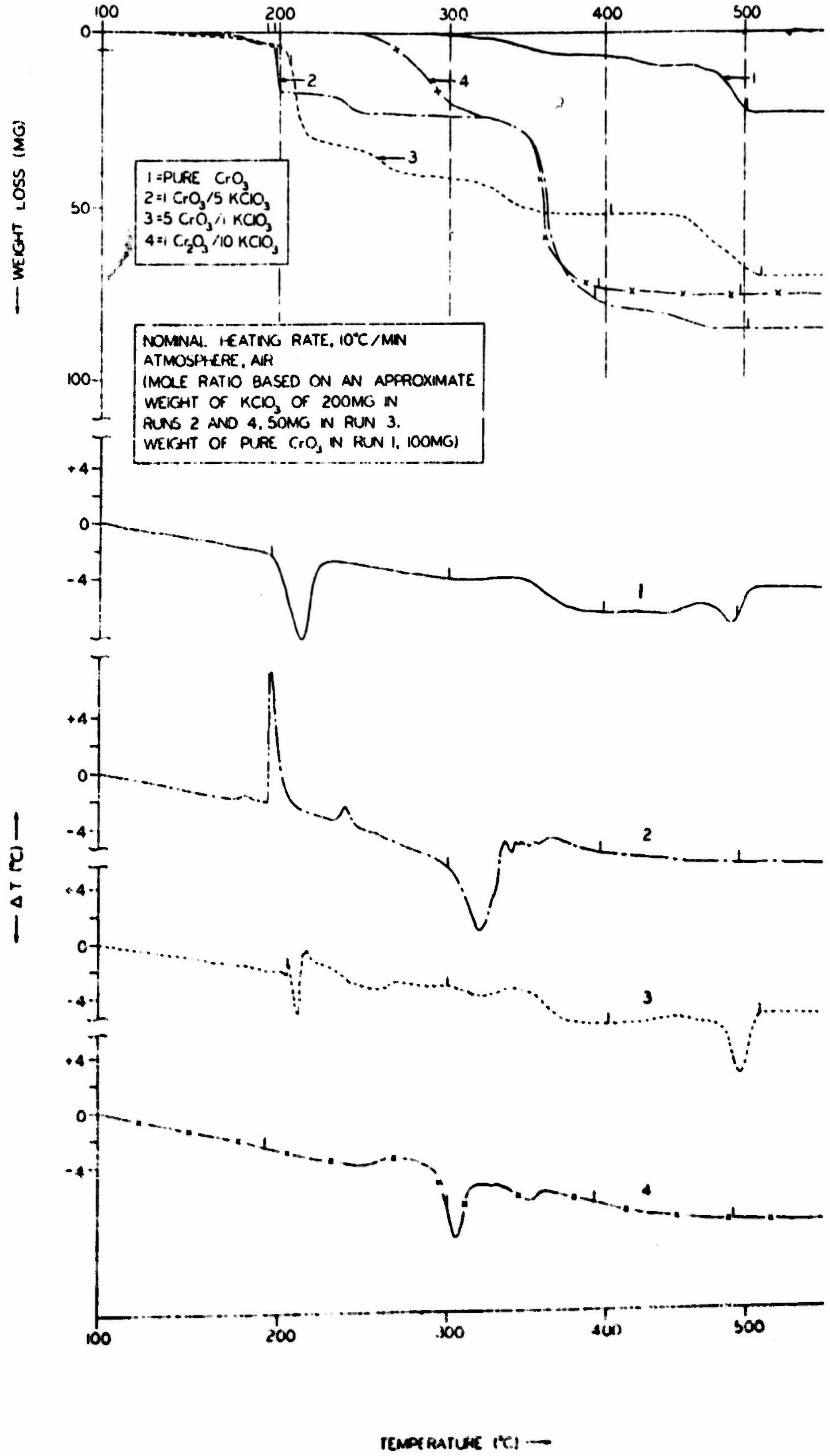

of Cr_2O_3. Decomposition is complete at 510°C. Endotherms seen at 305°C are probably due to the melting of potassium chlorate.

The total weight loss in case of $CrO_3/KClO_3$ (Curve 2) corresponds to the overall reaction:

$$2\ CrO_3 + 10\ KClO_3 \rightarrow K_2Cr_2O_7 + 8\ KCl + 14\ 1/2\ O_2 + Cl_2$$

There are at least five decomposition steps, where CrO_3 is the additive, the initiation step begins much below 200°C, and the second sharp decrease in weight is apparently triggered by the melting of CrO_3. (Compare curves 1 and 2) The average weight loss at this point is approximately 7.3% of the total weight of the mixture. This reaction is distinctly exothermic as is seen in the sharp peak in the DTA curve of the mixture of mole ratio 1:5.

Since this step of decomposition is rather pronounced, it is probable that stable intermediates are formed at this point. The stoichiometry, however, is rather difficult to evaluate and the mechanism of the several steps of reaction seems to be complex. This is indicated from the fact that a mole ratio 5/1 of $CrO_3/KClO_3$ shows similar stepwise decomposition at similar temperatures, (curve 3) whose proportions of weight losses are however different from those in curve 2. The overall weight loss in curve 3 corresponds to the equation:

$$10\ CrO_3 + 2\ KClO_3 \rightarrow K_2Cr_2O_7 + 4\ Cr_2O_3 + Cl_2 + 8\ 1/2\ O_2$$

The final step is most likely due to weight loss of residual CrO_3 according to:

$$2\ CrO_3 \rightarrow Cr_2O_3 + 1\ 1/2\ O_2$$

since it coincides with the weight loss range of the last step of pure CrO_3 decomposition (compare curve 1).

In case of Cr_2O_3 as the additive, the total weight loss corresponds to the equation:

$$Cr_2O_3 + 10\ KClO_3 \rightarrow K_2Cr_2O_7 + 8\ KCl + 2\ ClO_2 + 11\ O_2$$

The formed ClO_2 decomposes partially to $Cl_2 + O_2$.

The decomposition steps which occur before the melting point of $KClO_3$ are consistent with the stoichiometry of the equation:

$$Cr_2O_3 + 3\ ClO_3^- \rightarrow Cr_2O_7^{-2} + Cl^- + 2\ ClO_2 + 1/2\ O_2$$

the theoretical weight loss at this point is 10.96%, while experimentally an average weight loss of 10.51% was observed. The formed $K_2Cr_2O_7$ then catalyzes further the $KClO_3$ decomposition as soon as the latter begins to melt. This seems to be also the case with CrO_3 as judged from the similarity of curves 2 and 4 within this range.

F. Reaction of Sulfur with Potassium Chlorate in the Presence of Oxide Catalysts

A series of experiments were conducted to determine the reactivity of sulfur vapor with solid potassium chlorate in the presence of the solid oxide catalysts. The experimental technique used was differential thermal analysis, where the reactants were separated into two layers separated by a layer of aluminum oxide in the sample tube. The thermocouples were located in the top layer which was usually potassium chlorate with and without catalyst and in the aluminum oxide reference sample at a depth corresponding to that of the thermocouple in the $KClO_3$. Figure 21 shows the results of these experiments for the various fuel-oxidant-catalyst combinations. The reaction exotherms occur at relatively low temperatures between 200°C and 300°C. This reaction, of course, would be expected to be enhanced in an intimate mixture of sulfur and potassium chlorate since hot spots would develop during the pre-ignition process. Another interesting observation is that in the presence of the iron oxide catalyst the exotherm is significantly enhanced. Duplicate runs were done for all experiments. The temperatures of the exotherms apparently do not change appreciably in the presence of the oxide catalysts. In the presence of CrO_3 catalyst a sharp exotherm is also noticed at about 200°C, which also corresponds to the other DTA curves of mixtures of CrO_3 and $KClO_3$.

G. Isothermal Decomposition of $KClO_3$ and $KClO_3/KCl$ Mixtures

The thermal analysis results indicated that the reaction product potassium chloride can significantly change the rate of decomposition of potassium chlorate. In order to investigate this in more detail, experiments were performed over a series of constant temperatures involving pure $KClO_3$ and various known mixtures of $KClO_3$ with reagent grade KCl.

Figures 22 and 23 show series of isotherms for pure $KClO_3$ and $KCl/KClO_3$ mixtures in various mole ratios. It is clear that

Fig. 21. COMBUSTION OF SULFUR WITH POTASSIUM CHLORATE AND POTASSIUM CHLORATE-CATALYST MIXTURES

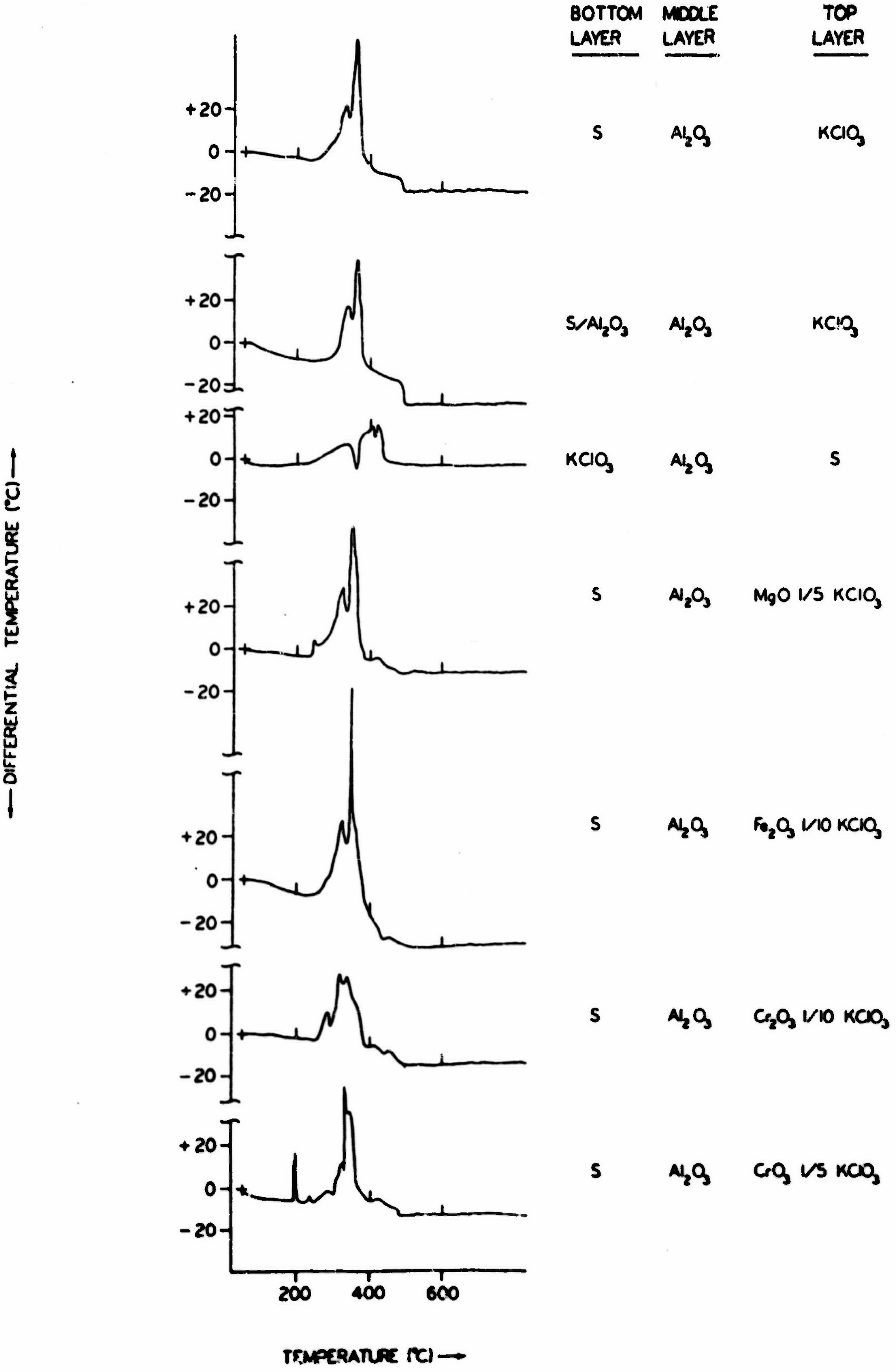

Fig. 22. Isothermal Decomposition of Pure Potassium Chlorate

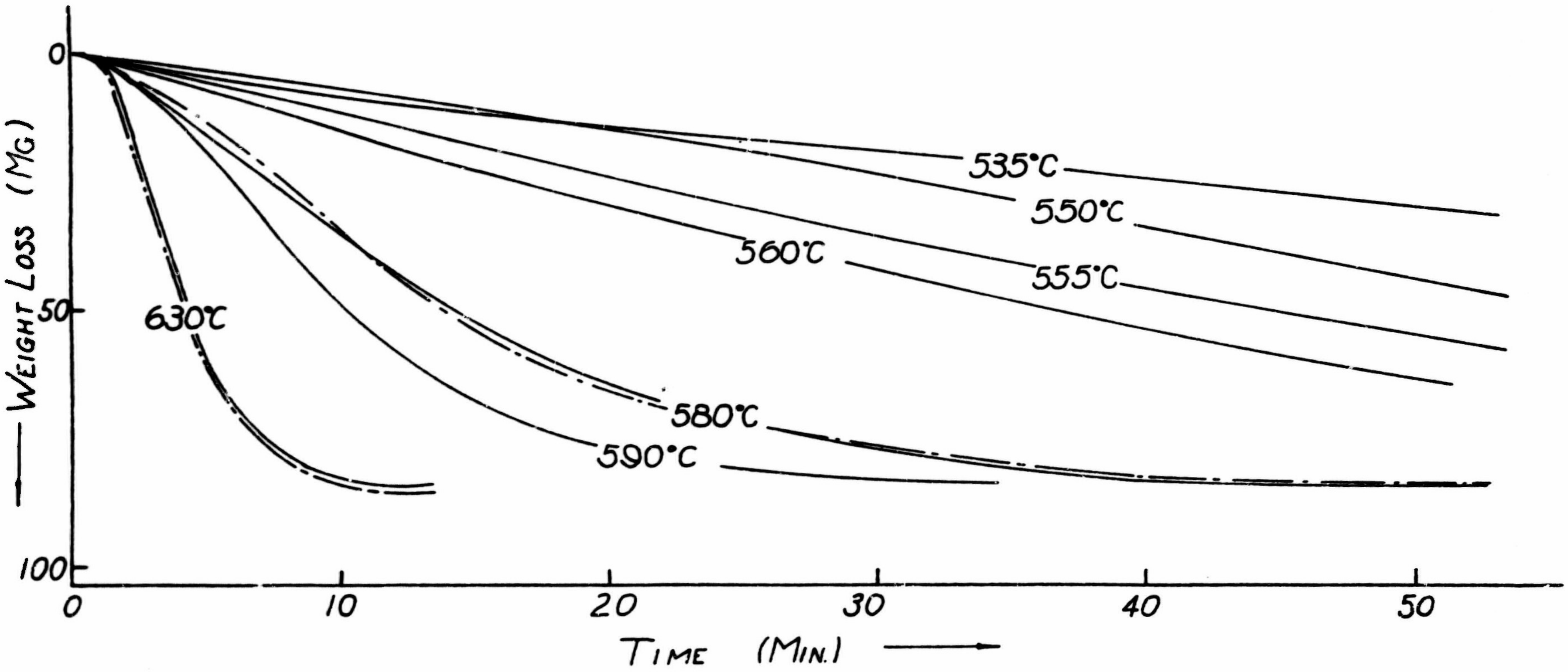

Fig. 23. ISOTHERMAL DECOMPOSITION OF $KClO_3$-KCL MIXTURES
MOLE RATIO - 1:1

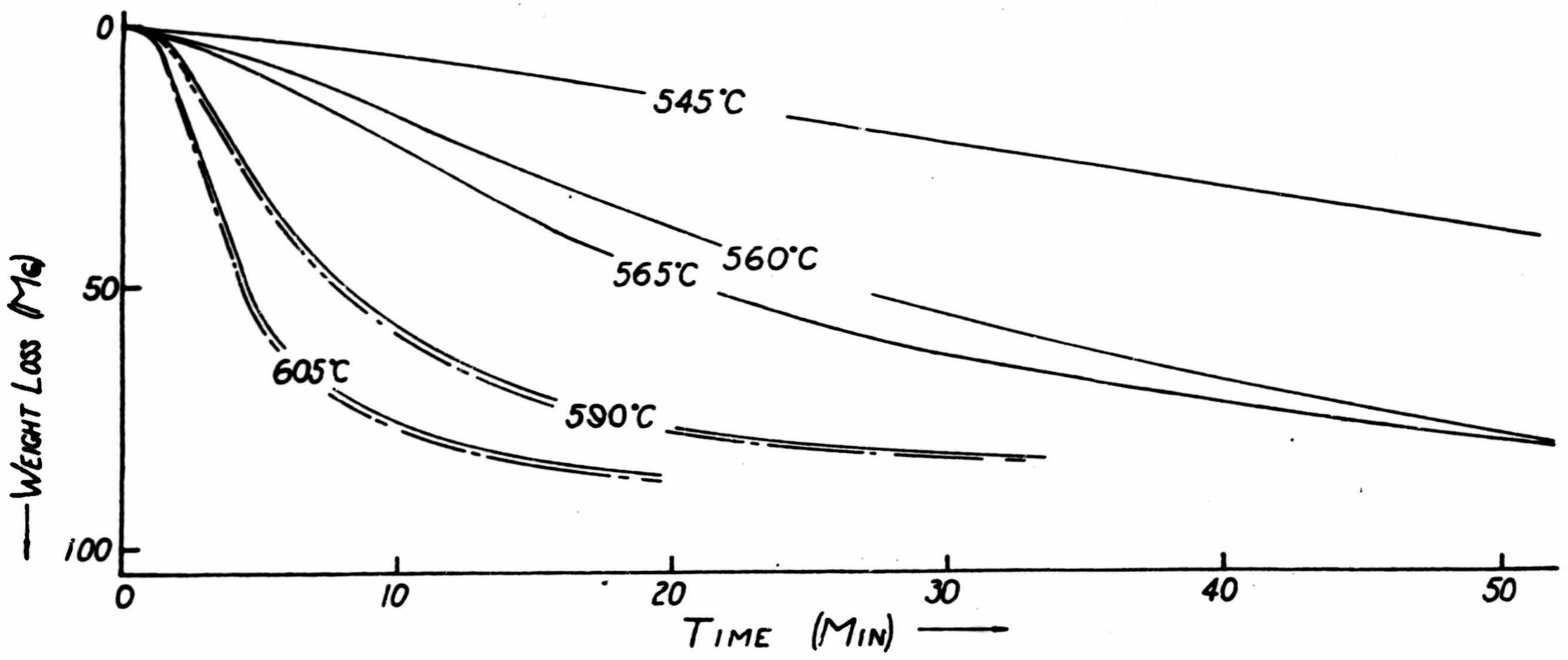

the rate of decomposition is increased in the presence of KCl. These experiments were carried out in air at atmospheric pressure. Table 4 gives some of the values for the rates of reaction as a function of extent of reaction.

Figure 24 shows a comparison of isotherms of various mixtures with the pure material at similar temperatures. It appears that the comparative reaction rates are lowest in case of the pure $KClO_3$, highest at a mole ratio, $KCl/KClO_3$, of 1:5, while again they are lower at smaller ratios, 1:4, 1:1. In separate experiments it was found that KCl is soluble in $KClO_3$ in the mole ratio of about 1:2.5, $KCl/KClO_3$ at 400°C. This information is of importance because of the effect that KCl has on the reaction rates.

H. Structural Studies

1. Electrical Conductivity

a. Untreated Oxides

One of the principal objectives in this program was to correlate the semiconducting properties of solids and their catalytic activity. In order to do this several of the oxides whose catalytic activity was investigated in more detail were pressed into pellets and then electrical conductivities evaluated as a function of temperature. The particles of oxides were screened into close sieve fractions so that the particle size range would be as close as possible for the various samples prior to pressing. The oxides on which these measurements were

Table 4

ISOTHERMAL RATES OF REACTION AS A FUNCTION OF EXTENT OF REACTION

Run No.	Ratio $KCl:KClO_3$	Average Temperature	Slope		
			At 1/4 Decomposition (mg/min)	At 1/2 Decomposition (mg/min)	At 3/4 Decomposition (mg/min)
1	0:1	631	13.3	15.5	9.0
2	0:1	637	16	17.3	10.5
3	0:1	573	3.55	4.1	2.4
4	0:1	591	5.25	6.0	3.05
5	0:1	553	0.98	1.1	0.5
6	0:1	535	0.52	0.47	
7	0:1	581	3.8	3.8	1.85
8	0:1	550	0.93	1.05	0.65
9	0:1	557	0.94	0.97	0.47
10	1:3	607	18.2	17.0	7.9
11	1:3	604	18.8	18.3	9.4
12	1:3	588	8.13	7.8	4.0
13	1:3	596	9.8	9.7	5.1
14	1:4	616	20.5	34.5	8.4
15	1:4	618	26.0	59.0	13.8
16	1:4	591	7.5	7.5	4.2
17	1:4	589	5.85	5.9	3.7
18	1:4	562	2.44	2.1	1.22
19	1:4	567	3.0	2.23	1.40
20	1:1	605	15.8	11.5	6.7
21	1:1	603	15.7	10.5	5.4
22	1:1	591	8.65	6.0	2.98
23	1:1	590	9.5	6.27	3.17
24	1:1	561	2.1	1.6	1.0
25	1:1	567	2.92	2.1	1.2
26	1:1	538	0.7	0.55	0.36
27	1:5	603	16.1	14.5	10.1
28	1:5	563	2.63	2.16	1.42
29	1:5	390	9.7	7.45	4.68
30	1:5	593	8.8	7.0	4.55
31	1:5	609	20.25	24.75	9.25
32	1:5	567	3.08	2.55	1.75

Fig. 24. COMPARISON OF ISOTHERMS OF PURE $KClO_3$ AND $KCl:KClO_3$ MIXTURES

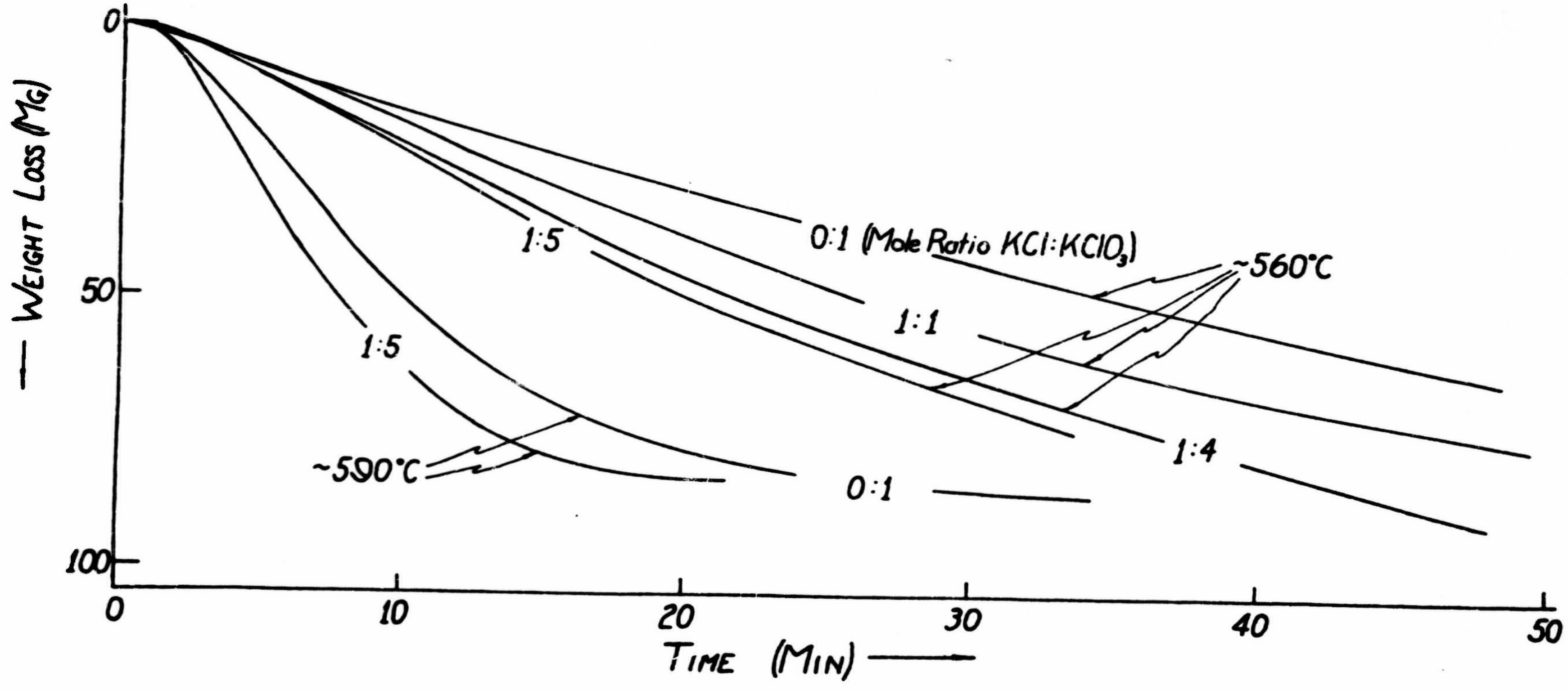

made are Cr_2O_3, MgO, Fe_2O_3 and TiO_2 in air at atmospheric pressure. Figure 25 shows the results. The conductivities in decreasing order is Cr_2O_3 (highest values) followed by Fe_2O_3 and TiO_2 and MgO. The TiO_2 and MgO conductivity curves cross at about 380°C.

b. Effects of Heat Treatment (Fe_2O_3)

Figure 26, shows the electrical conductivity as a function of temperature of a heat treated pellet of Fe_2O_3 powder. The same sample was used in these experiments so that variations in samples were eliminated. The heat treatment involved subjecting the sample alternately to argon and to oxygen atmospheres at 950°C. The electrical conductivity of the pellet was measured as a function of temperature after the above heat treatment in different atmospheres. The data show that the pre-treatment in argon with an overall heating time above 500°C of 100 min induces relatively high electrical conductivities in argon as seen in curve 1. If the conductivity of the samples after this argon heat treatment, is measured in oxygen at temperatures up to 350°C, the conductivity does not change appreciably as seen in curve 2.

If, on the other hand, the sample is heat treated in oxygen to about 950°C (heating time above 500°C is about 107 min), the determined overall conductivity is significantly reduced over the temperature range of 25°C to 400°C as shown in curve 3.

Fig. 25. ELECTRICAL CONDUCTANCE OF OXIDE PELLETS AS A FUNCTION OF TEMPERATURE

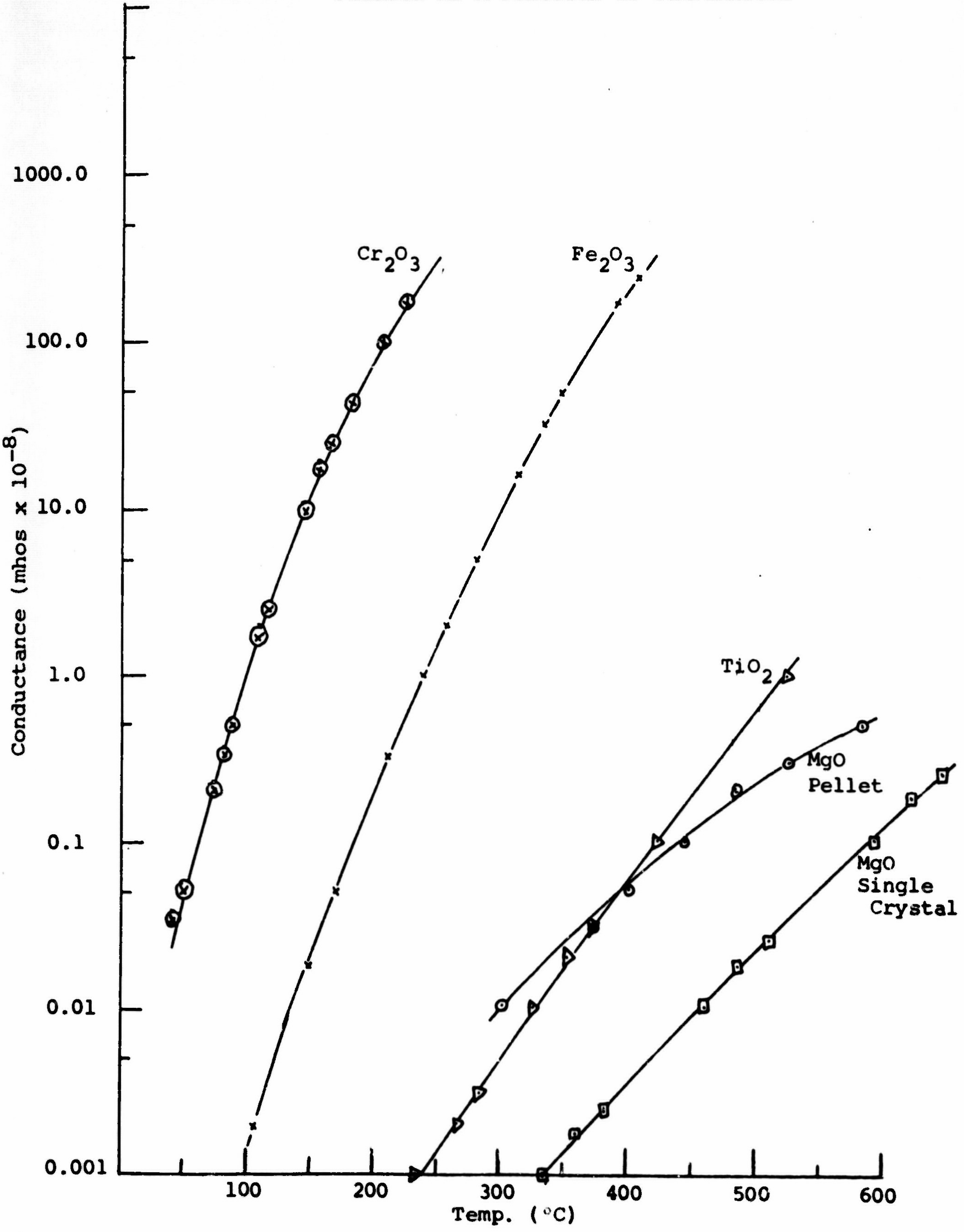

Fig. 26. ELECTRICAL CONDUCTANCE OF AN Fe_2O_3 PELLET AS A FUNCTION OF TEMPERATURE

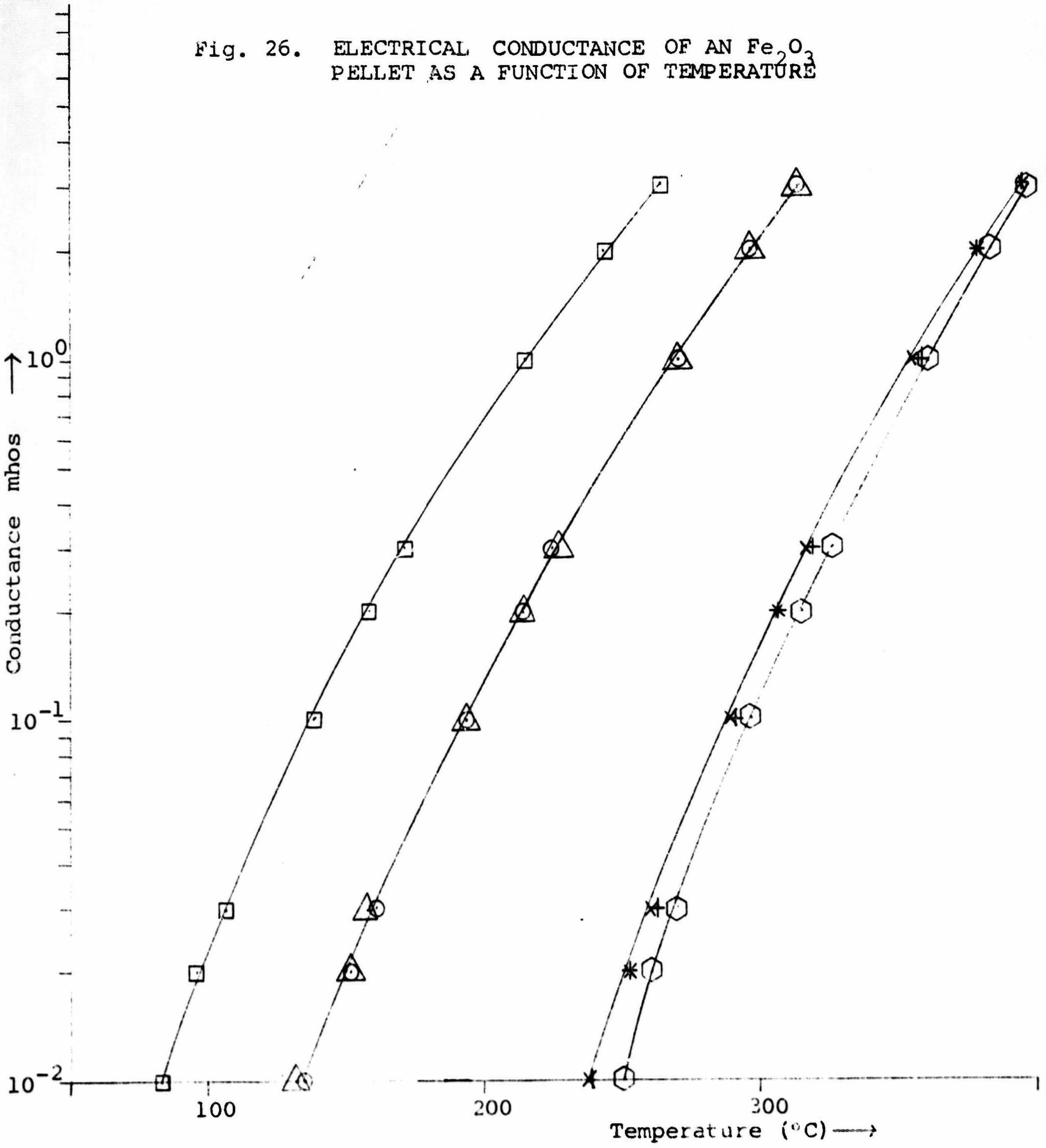

		Heat Treatment		Heating Duration Above 500°C in min	Atmosphere of Conductivity Experiments
No.	Symbol	To Temperature (°C)	In Atmosphere		
1		950	AR	100	AR
2		950	AR	100	O_2
3		950	O_2	107	O_2
4		950	AR	87	AR
5		935	O_2	132	O_2
6		935	O_2	132	AR

The process is qualitatively reprocudibly, i.e., heat treatment in argon increases the conductivity of the Fe_2O_3 sample (curve 4), and heat treatment in oxygen decreases the overall conductivity (curve 5).

The atmosphere does apparently not change the conductivity significantly, if the sample is subjected to argon and/or oxygen during the conductivity runs up to at least 400°C. This is seen by comparing curves 5 and 6, and curves 1 and 2. In order to obtain direct correlations between catalytic activity and electrical conductivity, a portion of the argon and oxygen heat treated samples which were used in the thermogravimetric experiments seen in Figure 14 were also used in the electrical conductivity studies. These samples were pressed into pellets at 30,000 psi for the electrical conductivity measurements. The conductivity curves are shown in Figure 27 which are plots of the logarithm of the electrical conductivity vs temperature. This plot confirms the finding that pre-treatment in oxygen under the conditions used in the work resulted in a significant decrease in electrical conductivity.

c. Effects of Irradiation (Fe_2O_3)

Electrical conductivity measurements were also carried out on gamma ray irradiated and unirradiated Fe_2O_3. The data did not reveal any significant differences. Since, however, there were significant differences in catalytic activity between the samples an attempt was made to measure

Fig. 27. ELECTRICAL CONDUCTANCE MEASURED IN AIR OF Fe_2O_3 HEAT TREATED AT 900°C IN (1) ARGON AND (2) OXYGEN AS A FUNCTION OF TEMPERATURE

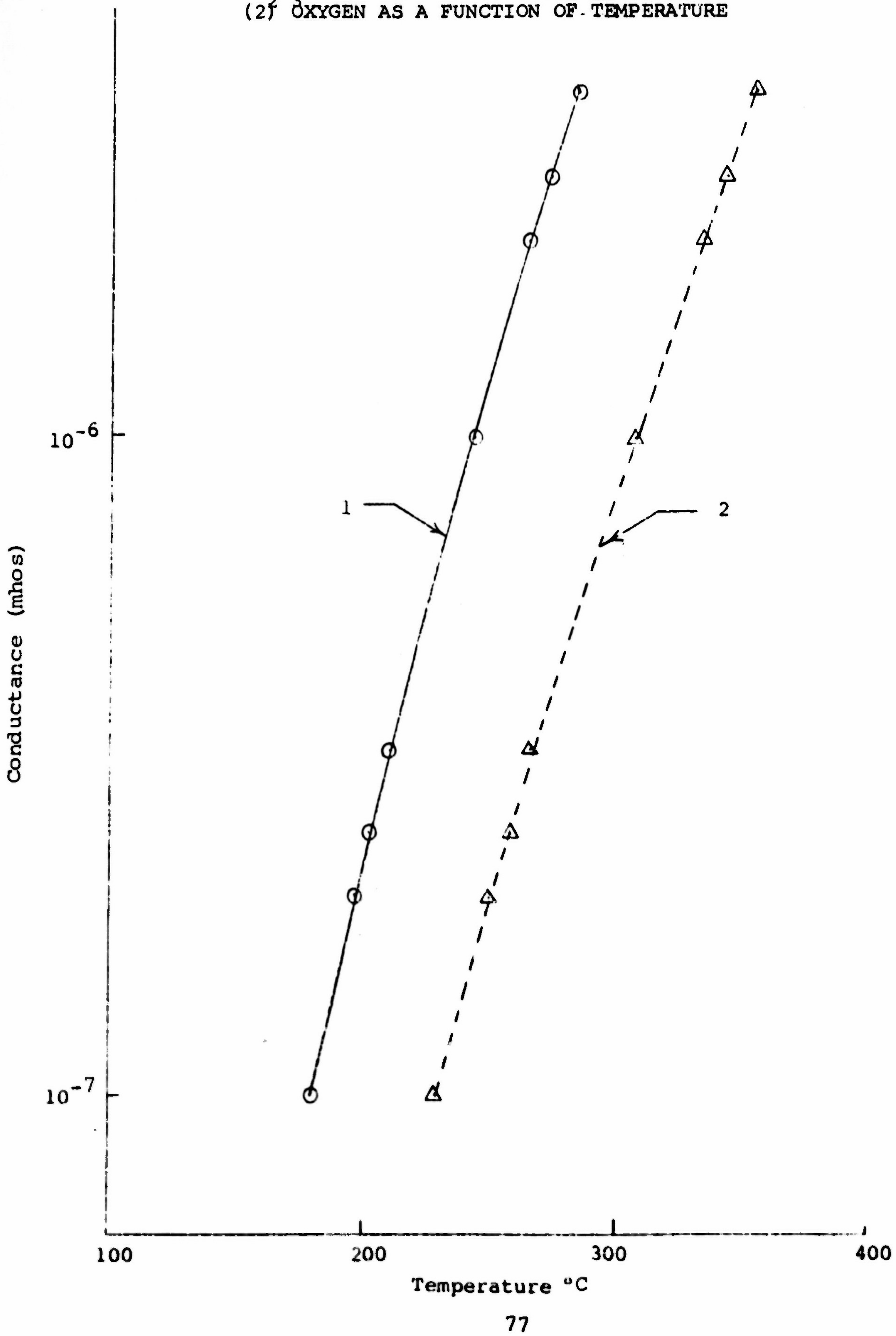

in a preliminary way the contact potentials of the oxides. The reason for using this technique is that the contact potential is a very sensitive method for revealing changes in the electrical properties of solids. It was found that the potential difference between the clean gold electrode and the irradiated Fe_2O_3 powder placed on the gold electrode varied from 75 to 85 μ volts. The values in the case of the unirradiated sample was 150 to 160 μ volts.

d. Effects of Doping (Fe_2O_3)

Figure 28 shows the effects of doping with altervalent ions, on the electrical conductivity of Fe_2O_3 as a function of temperature. The doping ions were Li^+ and Zr^{+4}. It can be seen from the figure that the electrical conductivity of the Zr^{+4} ion doped Fe_2O_3 is highest over the entire temperature range. There is a cross over in the curves of the Li^+ ion and undoped samples at approximately 350°C. Over the low temperature range the electrical conductivity was higher for the Li^+ doped sample, but over 300°C the conductivity of the Li^+ doped sample was lower than the doped sample.

e. Effect of Heat Treatment (MgO)

Figure 29 shows the effects of heat treatment in oxygen and argon on the electrical conductivity of a single crystal of magnesium oxide as a function of temperature. The two uppermost curves show the results of measurements carried out during cyclic heating and cooling in oxygen and argon, respectively. There do not appear to be any significant

Fig. 28. ELECTRICAL CONDUCTANCE OF DOPED Fe_2O_3 IN AIR AS A FUNCTION OF TEMPERATURE

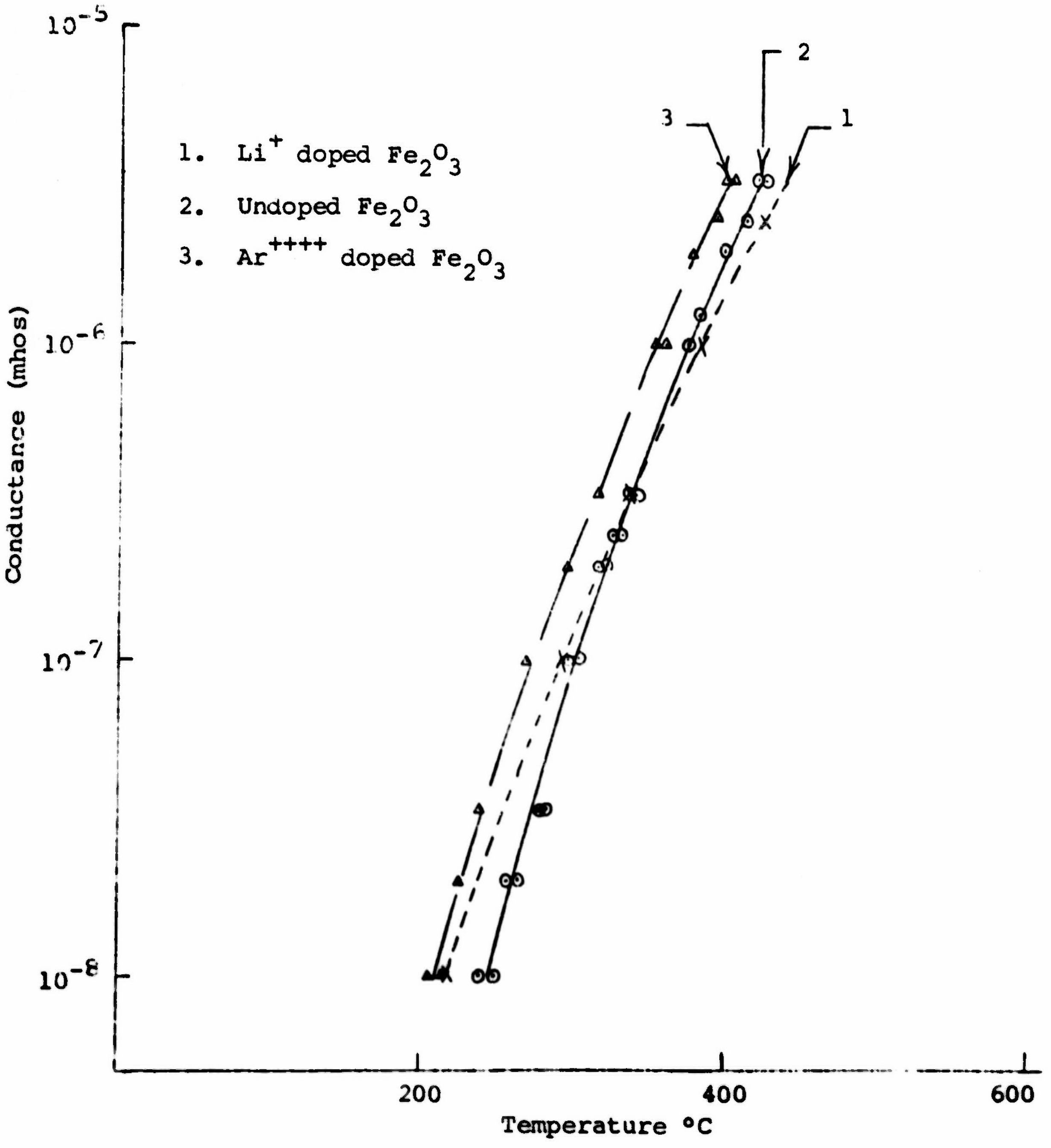

Fig. 29. ELECTRICAL CONDUCTANCE IN A SINGLE CRYSTAL OF MAGNESIUM OXIDE HEAT TREATED IN DIFFERENT ATMOSPHERES
Heating Rate Nominally 10°C/min

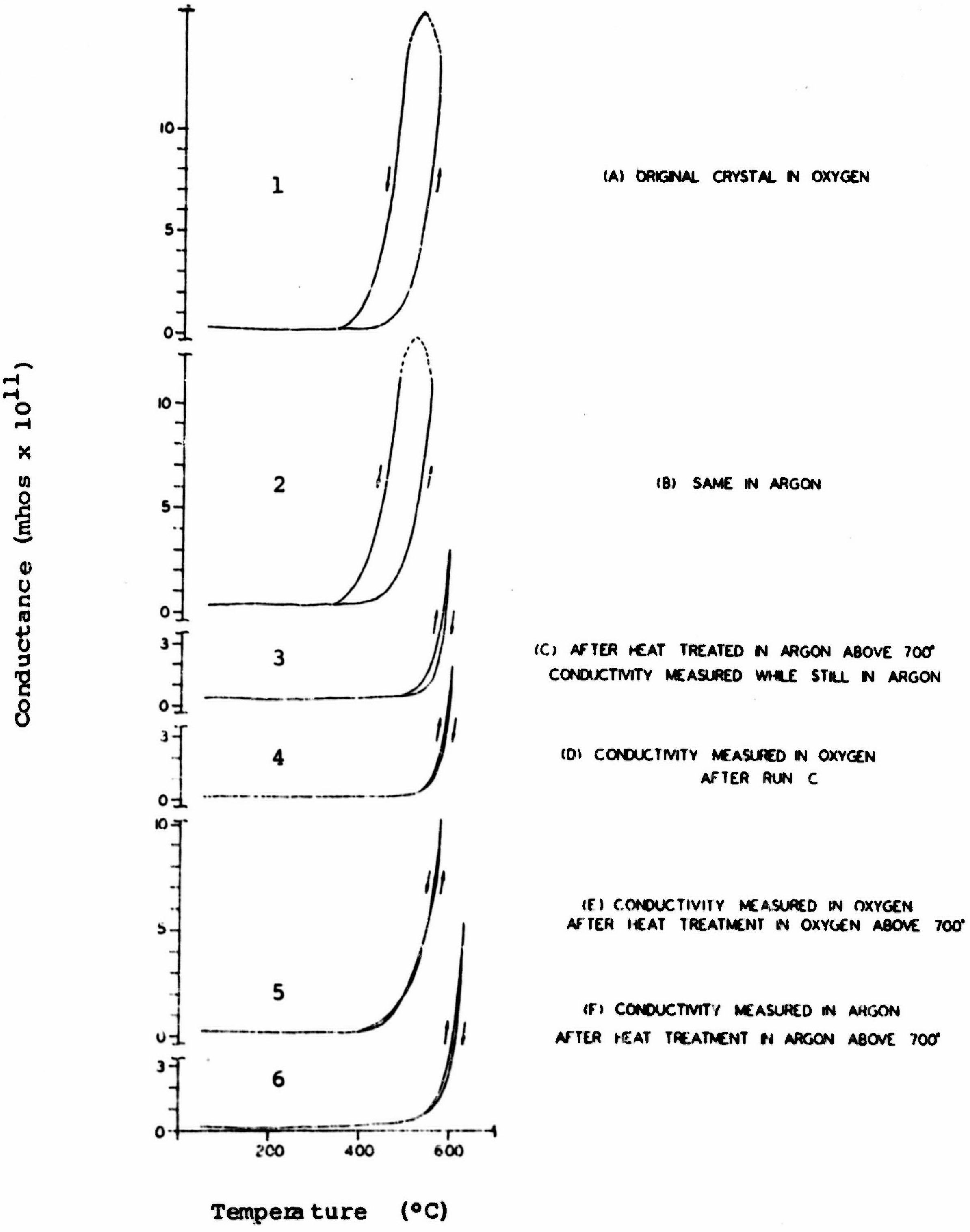

differences between these curves. Curve C shows the conductivity in argon after heat treatment in argon above 700°C. If the electrical conductivity measurements of sample C were made in oxygen there is again no significant difference as seen by comparing curves C and D. There is, however, a significant increase in conductivity as seen in curve E if the sample is heat treated above 700°C in oxygen prior to the conductivity measurements. The corresponding curve obtained in argon with the same crystal is shown in curve F.

f. Effects of Irradiation (MgO)

Figure 30 shows the logarithm of conductance of MgO pellets pressed from MgO powder as a function of inverse temperature. There are variations in the absolute values between different pellets of the same MgO material. This is probably due to differences in pellet packing and/or contact between pellets and Pt-electrodes. Also, the measurement of the relatively high resistance of MgO is less accurate than in the case of Fe_2O_3 which has lower resistivities. The slopes in the MgO curves are, however, comparable within reasonable error limits. It is quite obvious that the slopes of curves of irradiated MgO are steeper than those of non-irradiated pellets.

2. Magnetic Susceptibility

Samples which differed in preparation and thermal history were investigated by magnetic susceptibility. The measurements were made at 25°C. It is seen from Table 5 that magnetic

Fig. 30. ACTIVATION ENERGY FROM ELECTRICAL CONDUCTIVITY IN MgO PELLETS

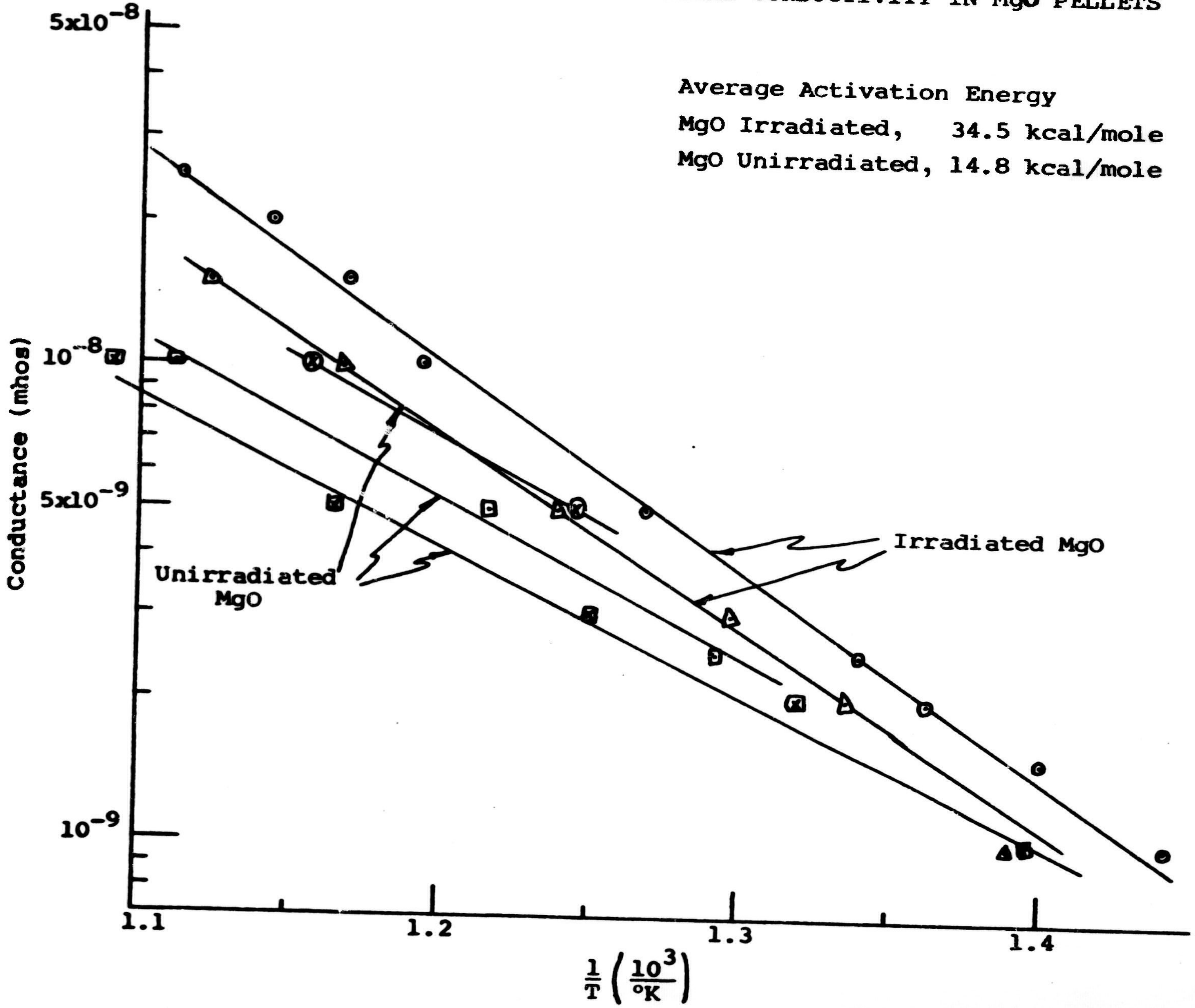

Table 5

MAGNETIC SUSCEPTIBILITY OF SEVERAL Fe_2O_3 SAMPLES AT 25°C

Samples	$\chi \cdot 10^5$
1	7.24
2	9.28
3	2.28
4	2.11
5	3.67
Literature	2.06

Sample 1 = B & A Reagent Grade

Sample 2 = Prepared with NaOH

Sample 3,4,5 = Prepared with NH_4OH and Ignited at 700, 800 and 900°C, respectively.

susceptibilities depend very much on the sample history.

Another series of heat treated and doped Fe_2O_3 samples showed definite trends. (Tables 6 and 7) The samples tempered at similar temperatures in argon had higher magnetic moments than those in oxygen. The magnetic moments of doped Fe_2O_3 samples showed the order $Zr^{4+} > Be^{2+} >$ undoped $> Li^{+}$. Conductivity trends of these oxides appear to correspond to magnetic susceptibilities.

3. Electrical Conductivity of $KClO_3$ and $KClO_3$ on Contact with Fe_2O_3 and MgO

It is rather difficult to measure the conductivity of $KClO_3$ in contact with the catalyst oxides, because at the temperatures in question the $KClO_3$ is in the molten state.

Figure 31 shows the conductivity of a $KClO_3$ pellet up to its melting point. It is seen that the conductivity is relatively high, and is even higher than that of an Fe_2O_3 pellet.

If Fe_2O_3 pellets are used as electrodes in a melt of $KClO_3$, the electrical conductivity is similar to Fe_2O_3 alone (Figure 32), as is found, if the Fe_2O_3 pellets are connected by a Pt wire during melting of $KClO_3$.

In a separate experiment the electrical conductivity of a magnesium oxide single crystal crucible was compared with, and without $KClO_3$ within the crucible (Figure 33). Preliminary investigations did not show significant differences, and these experiments were not further pursued.

Table 6

MAGNETIC MOMENTS OF Fe_2O_3 HEAT TREATED IN DIFFERENT ATMOSPHERES

Sample Treatment	Magnetic Moment (Bohr Magneton)
Prepared at 700°C in Air	3.81
Heated at 800°C in Argon	3.75
Heated at 800°C in Oxygen	3.65
Heated at 900°C in Argon	3.75
Heated at 900°C in Oxygen	3.69
Theoretical sample completely ionized, as Fe^{+++}	5.9
Same, as Fe^{++} or Fe^{++++}	4.9

Table 7

MAGNETIC MOMENTS OF DOPED Fe_2O_3

Doping Cation	Magnetic Moment (Bohr Magneton)
Zr^{++++}	4.27
Be^{++}	4.15
Undoped	3.81
Li^{+}	3.76

Concentration of doping cations 1/2 mole %. Magnetic moments are measured at room temperature.

Fig. 31. COMPARISON BETWEEN ELECTRICAL CONDUCTANCE OF $KClO_3$ and Fe_2O_3 PELLETS

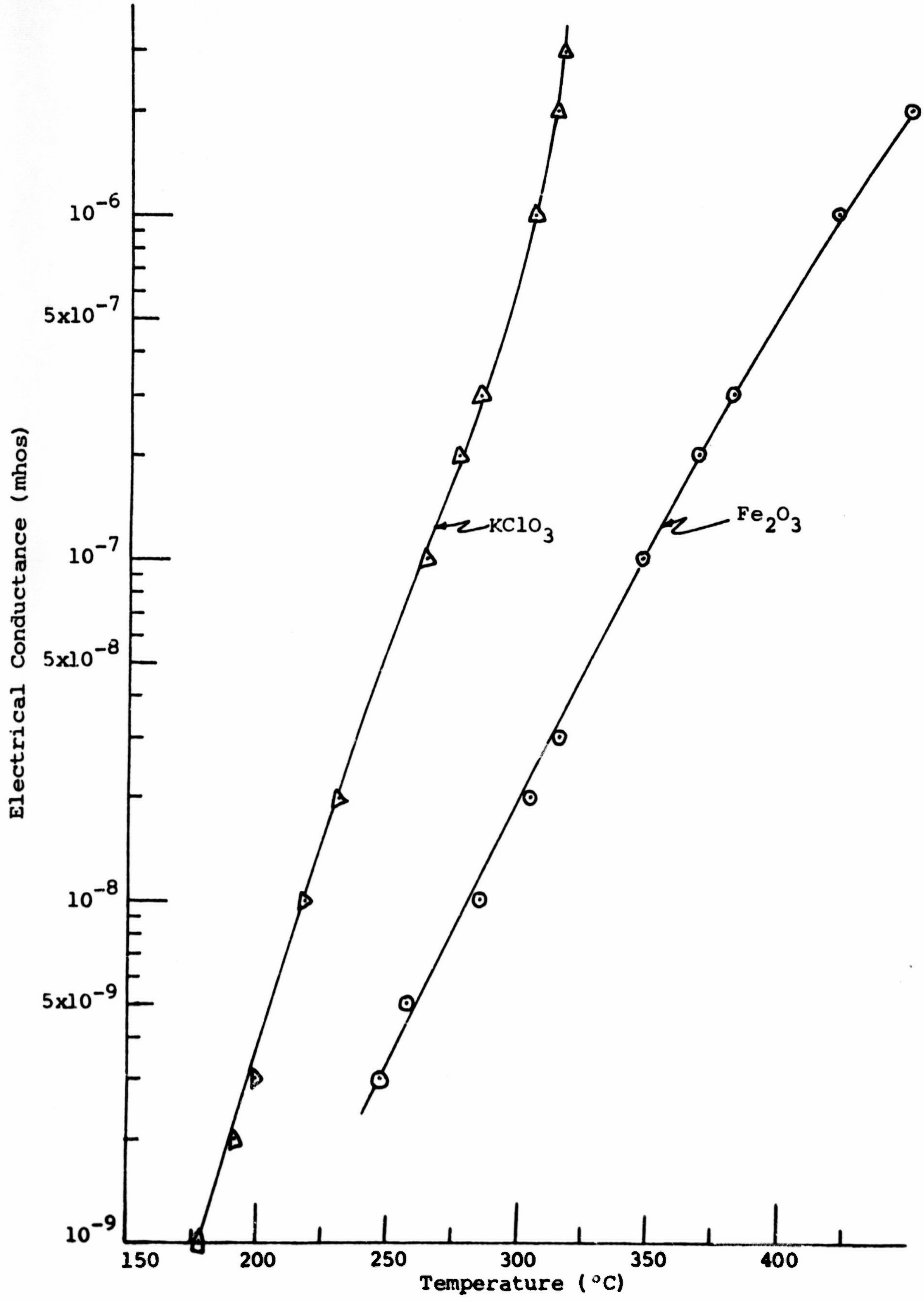

Fig. 32. ELECTRICAL CONDUCTANCE OF THE SYSTEM Pt – Fe_2O_3 – $KClO_3$ – Fe_2O_3 – Pt

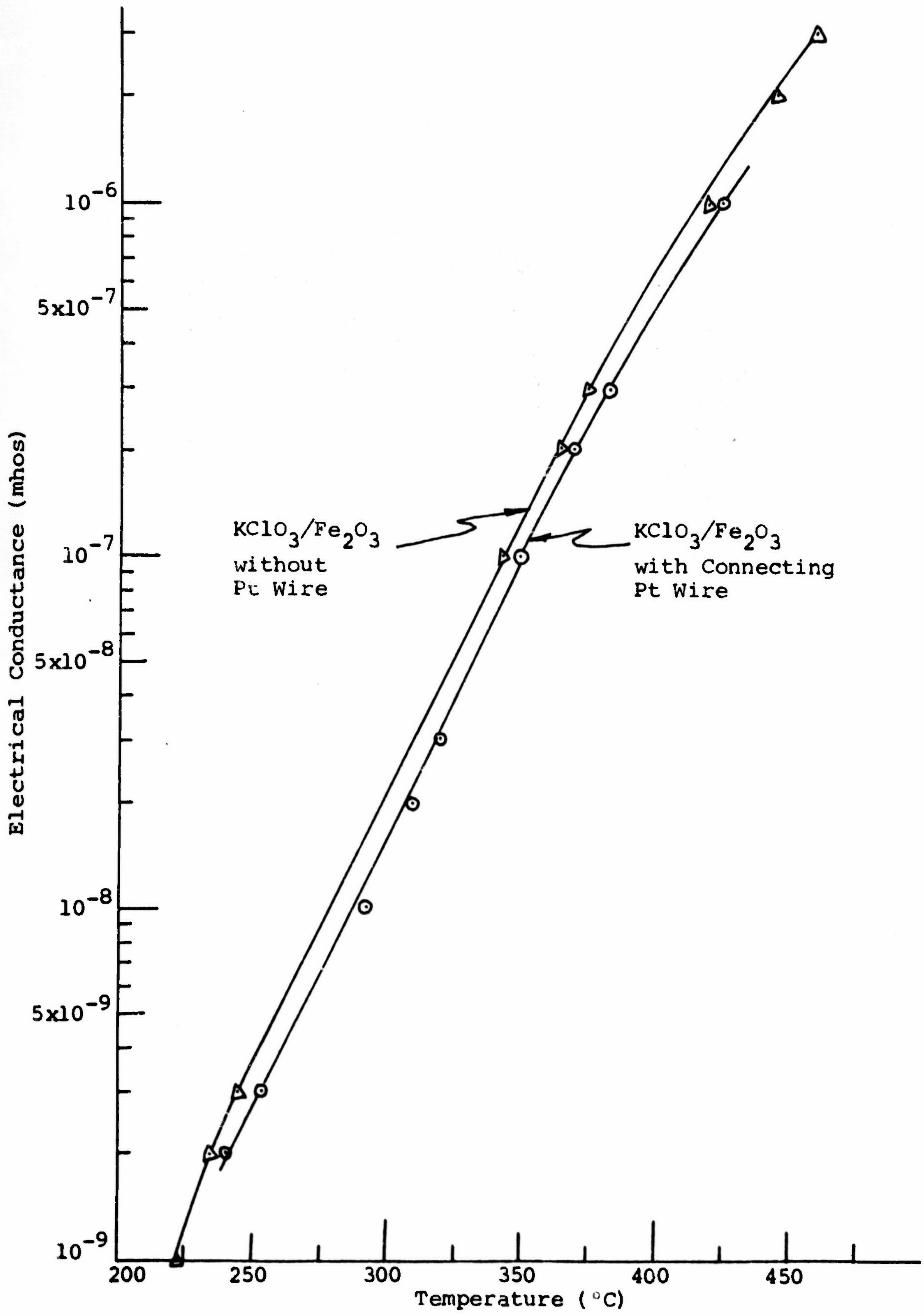

Fig. 33 MgO SINGLE CRYSTAL CRUCIBLE BETWEEN PLATINUM ELECTRODES

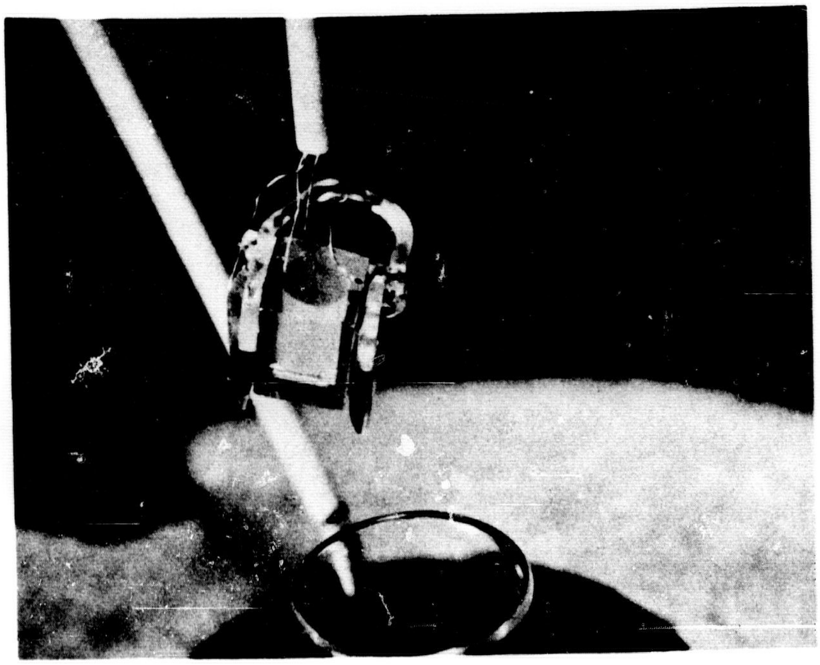

I. Analysis of Selected Oxides and Reaction Products

1. Analysis of Iron Oxides

The first series of iron oxides which was investigated with respect to their preparation and thermal history was analyzed for impurities as well as Fe^{3+} and Fe^{2+} ions. Tables 8 and 9 refer to semiquantitative spectro-chemical analysis and show that sample 2 which was prepared using NaOH, has many impurities, in particular, sodium.

Figure 34 shows that sample 2 has larger crystals than sample 1, and a BET surface analysis (Table 10) reveals lower surface area of sample 2 than of sample 1.

Table 11 lists x-ray intensities of 5 different Fe_2O_3 samples in comparison with intensities of various known Fe_2O_3 and Fe_3O_4 phases.

Since the doped iron oxides showed rather interesting trends in their catalytic activity with respect to the decomposition of potassium chlorate it was thought advisable to have the oxides analyzed for the added cationic impurities. Table 12 shows the results in weight percent. It is apparent that Li^+ is present in the lowest amount. This is understandable based on the solubility of lithium hydroxide.

X-ray analysis of these Fe_2O_3 samples did not show significant differences from the pure sample.

Table 8

SEMIQUANTITATIVE SPECTROCHEMICAL ANALYSIS OF Fe_2O_3 SAMPLES

Element	Sample 1	Sample 2
Ca	--	W
Cr	--	W
Cu	T	T
Fe	VS	VS
Mg	FT	FT
Na	--	S

VS = very strong (10-100%)
S = strong (1-10%)
W = weak (0.01-0.1%)
T = trace (1-10 ppm)
FT = faint trace (0.1-1 ppm)

Sample 1 = B and A reagent grade Fe_2O_3

Sample 2 = Fe_2O_3 prepared with NaOH

Table 9

ANALYSIS OF Fe^{3+} AND Fe^{2+}

	Amount	
Sample	Fe_2O_3	FeO
1	98.72	0.96
2	72.93	0.57

Sample 1 = B and A reagent grade

Sample 2 = Fe_2O_3 prepared with NaOH

Table 10

BET-SURFACE ANALYSIS

Sample	Area (m^2/g)
Fe_2O_3 (B & A)	12.82
Fe_2O_3 (A)	3.82
Cu_2O	1.68

Fig. 34 MICROSCOPIC PICTURES OF Fe_2O_3 SAMPLES 1 AND 2

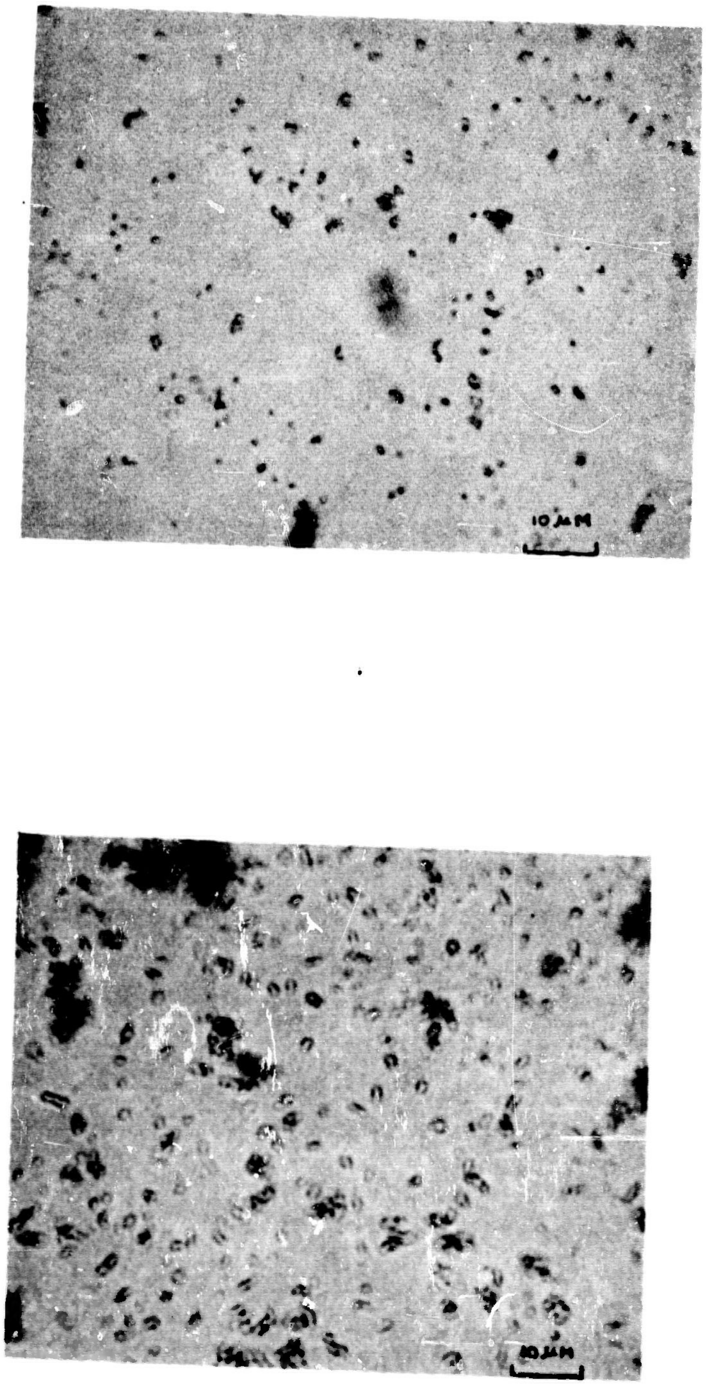

Table 11

INTENSITIES AND SPACINGS OF X-RAY TRACES OF Fe_2O_3

	I/I_o								
d(Å)	S1	S2	S3	S4	S5	α	γ	δ	Fe_3O_4
3.67-3.70	29	38	32	33	36	70	--	--	--
2.98	--	--	33	30	35	--	--	--	60
2.95	--	--	--	--	--	--	34	--	--
2.78-2.80	--	100	22	23	50	--	19	--	40
2.69-2.71	100	86	100	100	100	100	--	--	--
2.63	--	38	--	--	--	--	--	--	--
2.51-2.53	77	52	72	60	83	80	100	80	100
2.43	--	--	--	--	--	--	--	--	30
2.18-2.21	19	24	26	21	27	--	--	100	--
2.10	10	--	--	--	--	--	--	--	60
1.99	--	48	--	--	--	--	--	--	--
1.84-1.85	29	24	38	33	36	10	--	--	--
1.69-1.71	39	43	50	45	50	80	12	100	45
1.60-1.61	13	--	10	5	--	40	33	--	70
1.48-1.49	26	24	28	33	40	70	53	80	80
1.45-1.46	29	33	28	24	38	80	--	--	--

LEGEND: d = x-ray spacings in Å

I/I_o = relative intensities in per cent

α, γ, δ, Fe_2O_3 = 3 phases of Fe_2O_3. Data are taken from literature.

S_1 - S_5 = Fe_2O_3 samples 1 - 5 (see also Table 1 for S_1 and S_2.

S_3 = Prepared with NH_4OH, Ignition at 700°C.

S_4 = Prepared with NH_4OH, Ignition at 800°C.

S_5 = Prepared with NH_4OH, Ignition at 900°C.

Table 12

ANALYSIS OF DOPED Fe_2O_3

Dopant	Weight (%)	Precision Estimate (%)
Li	0.0050	±0.0003
Be	0.0170	±0.0006
Cr	0.40	±0.02
Zr	1.34	±0.03

2. Analysis of Decomposition Products of Pure $KClO_3$ During TGA

In order to more completely understand the mechanisms of reactions, the thermogravimetric analysis experiments were stopped after heating the samples to a series of predetermined temperatures. At these temperatures the samples were rapidly cooled and the solid residue was analyzed to determine the decomposition products. The results of this series of experiments are shown in Figure 35 where the mole % of reactant and of the principal reaction products are plotted as a function of temperature. The curve pertaining to the amount of $KClO_3$ passing through a minimum at about 595°C corresponds approximately to the maximum amount of $KClO_4$ at 590°C. As the temperature is increased above 600°C the relative amount of $KClO_4$ decreases while the curve pertinent to the amount of $KClO_3$ goes through another slight maximum at 620°C. The product KCl increases slowly as the sample is heated to 575°C after which its rate of formation rapidly increases.

3. Analysis of Reaction Products in $KClO_3$ Decomposition Reactions Involving Cr_2O_3 and CrO_3

It was found that Cr (III) and Cr (VI) oxides were apparently the most reactive catalysts for the decomposition of potassium chlorate. There were, however, indications that these oxides also underwent irreversible reactions. The yellow color of the reaction products and discrepancies in overall weight loss of the mixtures suggested that potassium chromates or dichromates were formed during the decomposition of $KClO_3$.

Fig. 35. DECOMPOSITION PRODUCTS OF $KClO_3$ AND WEIGHT LOSS AS A FUNCTION OF TEMPERATURE DURING THERMOGRAVIMETRIC ANALYSIS

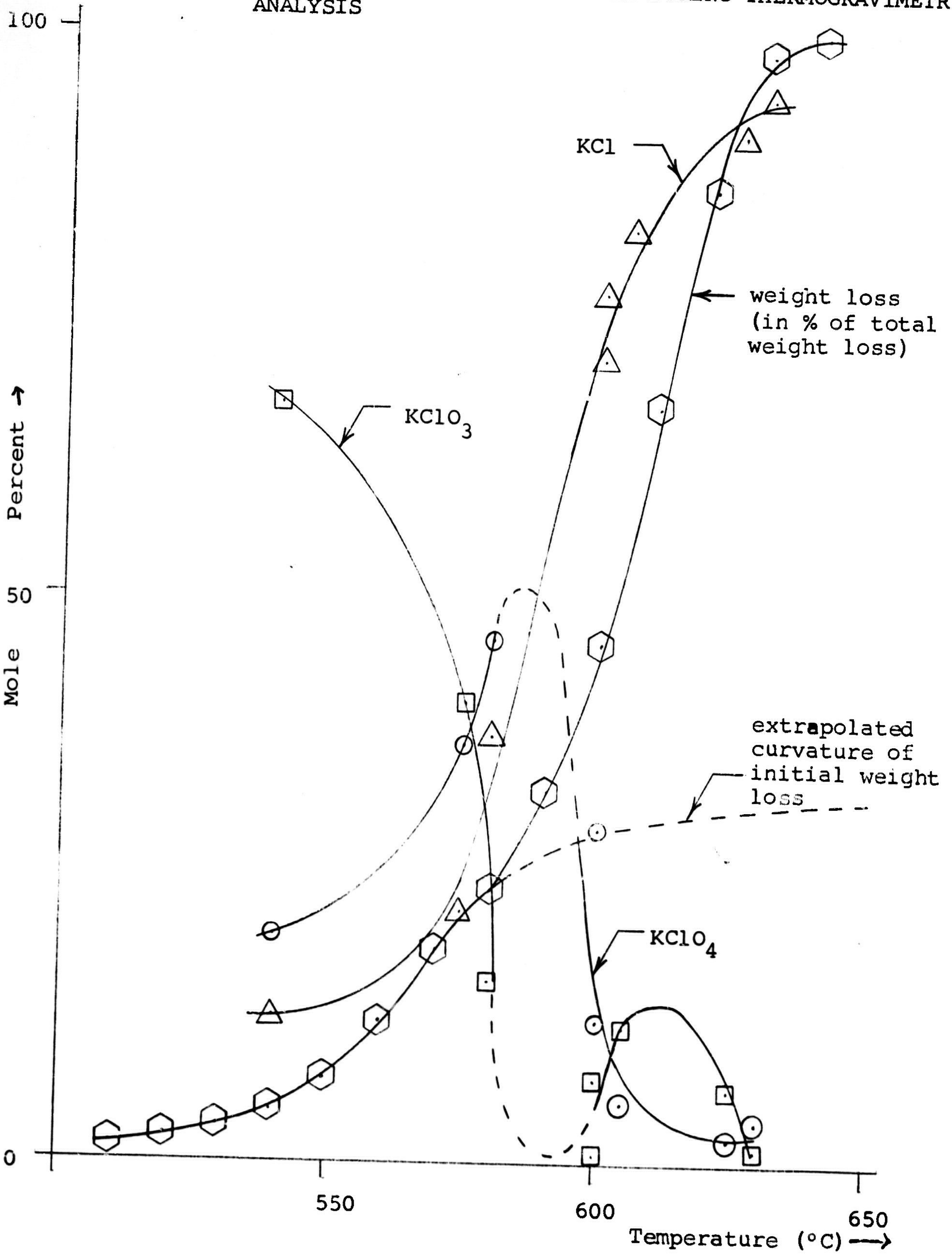

In order to obtain more information on the possible mechanism of this reaction, TGA experiments were performed at several temperatures, and x-ray analyses were carried out on the reaction products. Table 13 summarizes the results. In the case of CrO_3 there is apparently no evidence of formation of Cr_2O_3. If the sample is heated above 270°C, lines appear in the x-ray spectrum which indicate the formation of potassium dichromate, $K_2Cr_2O_7$. (See also Figure 36).

It was also observed in the reaction of chromium oxides with potassium chlorate that a yellow-greenish gas was liberated on heating indicating the probable release of chlorine and/or chlorine oxides. To verify this, a systematic mass spectrometric analysis of the gaseous decomposition products was conducted as a function of temperature. The preliminary data indicated that chlorine and chlorine oxides were formed during the reaction. See Figure 37. The mass spectrometric analysis shows the formation of Cl_2, ClO_2 and traces of ClO and ClO_3. More quantitative studies proved that formation of ClO_2 prevails at lower temperatures as is seen from Figure 38. With increasing temperatures, however, formation of ClO_2 decreases, while chlorine, Cl_2 and oxygen, are formed predominantly at increasing temperatures. Where CrO_3 is the catalyst, Cl_2 is principally formed during the decomposition of $KClO_3$; ClO_2 is present only in trace quantities. (Figure 37) There are however, indications that a new phase is formed which does not correspond to KCl, $KClO_3$, CrO_3, $K_2Cr_2O_7$ or

Table 13

RATIO OF RELATIVE INTENSITIES OF REACTION PRODUCTS IN THE DECOMPOSITION OF $KClO_3$ MIXED WITH Cr_2O_3 AS A FUNCTION OF TEMPERATURE

T°C	I_{KCl}/I_{KClO_3}				$I_{K_2Cr_2O_7}/I_{Cr_2O_3}$	
	2.22/2.79	3.146/2.79	2.22/4.41	3.14/4.41	4.83/2.66	3.68/2.66
225	0	0	0	0	0	0
270	0.25	0.26	0.74	0.78	0.65	0.59
300	0.78	0.38	3.6	1.8	3	2
340	1.15	1.06	4.5	4.1	6.7	4.7
365	8.4	5.2	10.5	6.5	∞	∞
485	15	9	15	9	∞	∞

Fig. 36. THE RATIOS OF X-RAY INTENSITIES OF (1) $K_2Cr_2O_7/Cr_2O_3$ and (2) $KCl/KClO_3$ AS FUNCTION OF TEMPERATURE DURING THE DECOMPOSITION OF $KClO_3$ IN THE PRESENCE OF Cr_2O_3

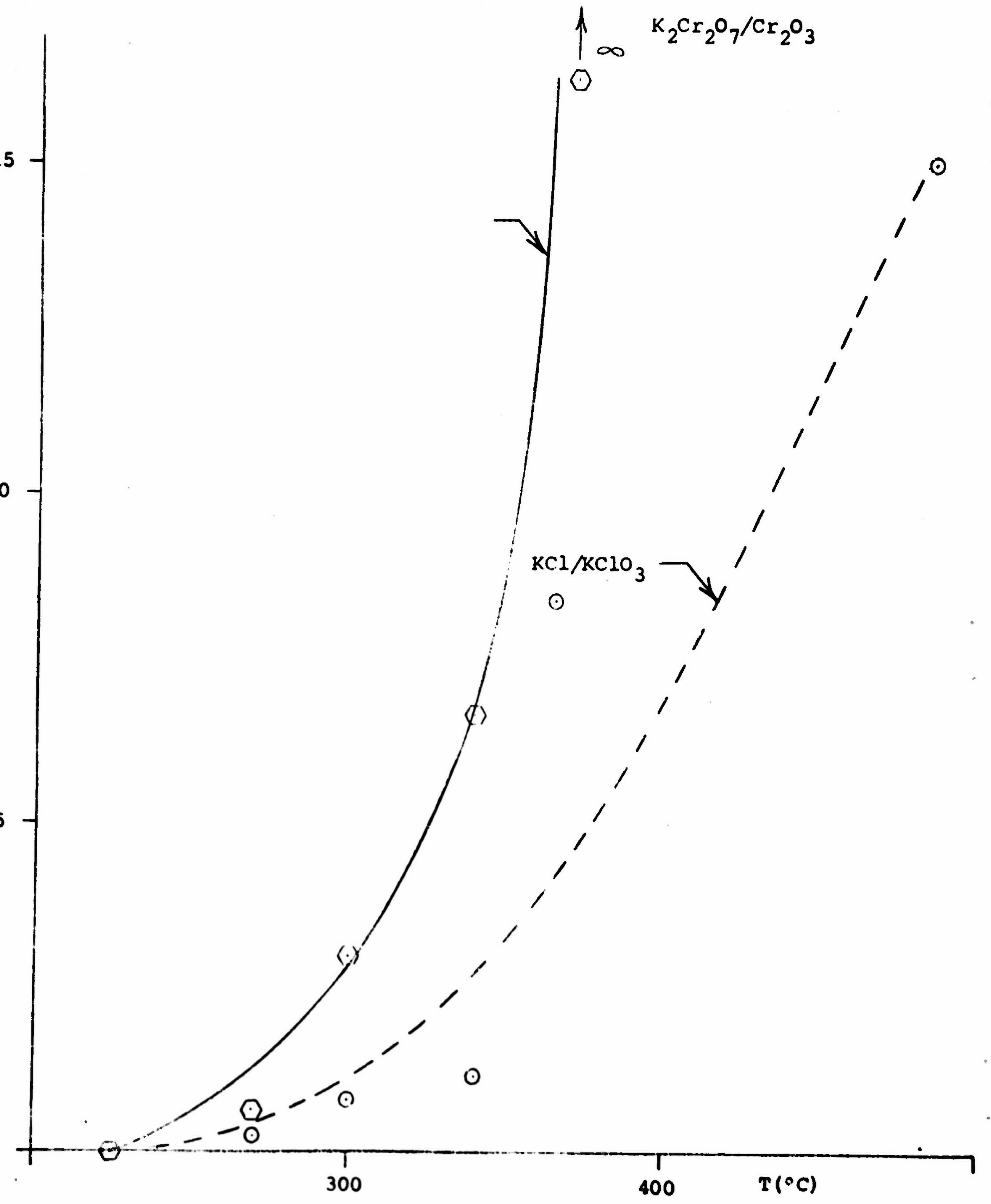

Fig. 37. MASS SPECTROMETRIC TRACES OF DECOMPOSITION PRODUCTS OF (1) $KClO_3$-Cr_2O_3, and (2) $KClO_3$-CrO_3 MIXTURES

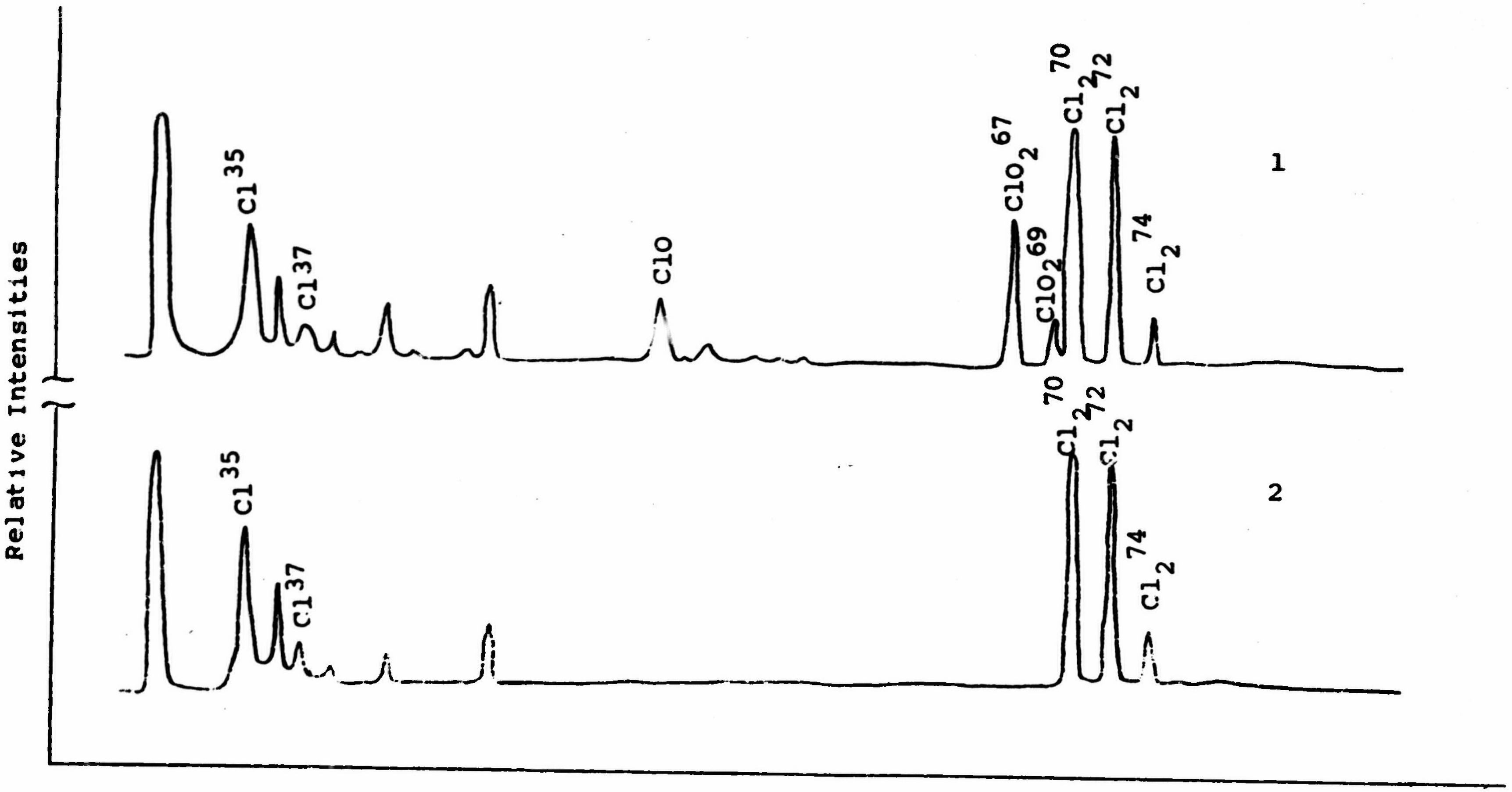

Fig. 38. MASS SPECTROMETRIC ANALYSIS OF DECOMPOSITION PRODUCTS Cl_2, and ClO_2, FROM A MIXTURE OF $KClO_3/Cr_2O_3$ DECOMPOSED ON HEATING AT 10°C/MIN

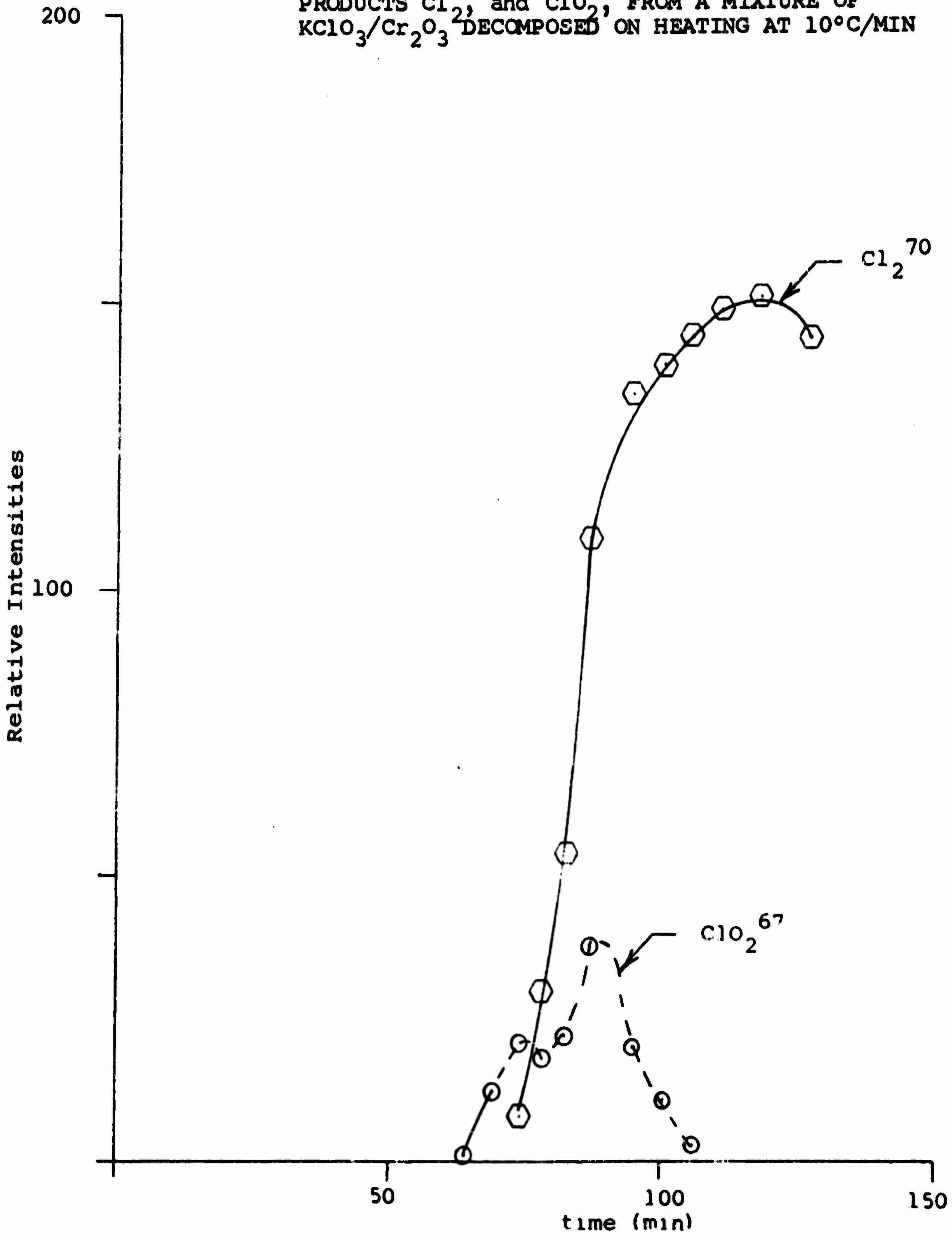

the Cr_2O_3 phases. There are some x-ray lines present which correspond to an intermediate formation of K_2CrO_4. These lines disappear at higher temperatures. The mechanism of formation of this as an intermediate phase is, however, not quite understood, since K_2CrO_4 is more stable than $K_2Cr_2O_7$.

DISCUSSION

A. Decomposition of Potassium Chlorate

The final decomposition products of $KClO_3$ are rather simple, KCl and O_2. The mechanism of reaction, however, is not a settled question, although, there have been a number of publications on this point.[7,16,17]

The differential thermal analysis curves which we have obtained are in agreement with the results of Markowitz[10] and show 3 peaks. The first peak at 370°C is endothermal and is due to fusion. The third and fourth peaks at approximately 580°C and 620°C are exothermal, and are due to thermal decomposition. The decomposition reaction is known to involve disproportionation, which results in the formation of KCl and $KClO_4$. Since $KClO_4$ is more stable than $KClO_3$, it can be expected to decompose over a higher temperature range than the disproportionation reaction of $KClO_3$. It is reasonable, therefore, to conclude that the first exotherm is due to the disproportionation reaction and the second exotherm to the thermal decomposition of the potassium perchlorate. The reactions may be written as:

$$2\ KClO_3 = KCl + KClO_4 + O_2 \qquad \text{(1) 1st exotherm}$$

$$KClO_4 = KCl + 2O_2 \qquad \text{(2) 2nd exotherm}$$

Examination of the TGA curves, and in particular the combined TGA and corresponding derivative curves, appear to confirm this interpretation since the weight loss at the first inflection point of the TGA curve comes at about 25% of the total weight change. This corresponds to the minimum on the derivative TGA curve. See Figure 19. The theoretical value should be about 33% of the total weight loss to form KCl and O_2, which is not expected to be observed experimentally, because of overlap between the decomposition of $KClO_3$ and $KClO_4$. The analytical results confirm the overlap between the two reactions. The correlation between the final exotherm and the thermal decomposition of $KClO_4$ is, also, strongly indicated from the finding that the final exotherm follows the maximum for the formation of $KClO_4$ at about 600°C. It is shown from the analytical curves in the Result section, in which the TGA experiment was stopped over various intervals and the products analyzed. Figure 35 In some cases, it may be noted, in DTA curves of the decomposition of $KClO_3$, that the final exotherm appears to have a slight break. It was shown by Freeman and Anderson,[23] in a previous publication, that this is due to the precipitation of potassium chloride during the decomposition of $KClO_4$. Another point which should be considered in interpreting the DTA curves of $KClO_3$ is that the exotherm for disproportionation is shown to be approximately the same in area as the exotherm for the decomposition of $KClO_4$, whereas, only one-third of the oxygen is lost during disproportionation. The reason for the comparatively large exotherm for the disproportionation reaction is due to its relatively high heat of reaction, compared to the thermal decomposition of $KClO_4$, where the exothermicity is essentially due to the precipitation of KCl The heat of reaction for the decomposition of one mole of potassium perchlorate to potassium chloride and oxygen under standard conditions at 25°C is about -0.58 kcal. If the heat of fusion of potassium perchlorate is considered this would increase the value to approximately -3 kcal. For this disproportionation reaction involving 2 moles of $KClO_3$ with the liberation of 1 mole of oxygen, the heat of reaction under standard conditions at 25°C is approximately -20.8 kcal. These values are, of course, only approximately since the calculations are made at 25°C, but they show why there is a pronounced exotherm for the disproportionation reaction. Table 14 lists the thermodynamic values used for these calculations.

Table 14

STANDARD THERMODYNAMIC PROPERTIES

		ΔH_f°	ΔF_f°	S°
$KClO_3$	(c)	- 93.50	-69.29	34.17
$KClO_4$	(c)	-103.6	-72.7	36.1
KCl	(c)	-104.18	-97.592	19.76
O_2	(g)	0.0	0.0	0.0
O	(g)	59.2	55.0	38.5

Some authors have written the thermal decomposition of potassium chlorate as a reversible reaction.[7,16] In this work, however, it was shown by experiments, in various gaseous atmospheres, including oxygen and nitrogen (Figure 10) that there is no shift in the DTA peaks, indicating that the reaction is non-reversing with respect to oxygen. This is in agreement with the results reported in reference 17, where it was shown that even at pressures as high as 1200 atm., no $KClO_4$ is formed by the direct reaction of $KClO_3$ with molecular oxygen.

An interesting observation was made, that by adding potassium chloride to potassium chlorate the initial peak in the derivative thermogravimetric analysis curve is eliminated and that this curve appears as a single continuous band with a lower maximum rate of reaction. See Figure 19 Although, sufficient work was not carried out to fully interpret these results, it appears that the presence of chloride inhibited the initial disproportionation reaction. Figure 39 shows the temperature dependency plot on a semilogarithmic scale of decomposition rate vs 1/T which demonstrates the importance of the presence of potassium chloride on the rates of reaction. The data were taken from Figure 19 and are presented also in Table 15. The derivative weight loss curve in Figure 39 is used to demonstrate the effects of chloride since it is much more sensitive to detecting changes than the integral curve. There are several possibilities which may account for this effect. One possibility is that mechanistically the disproportionation reaction is bi-molecular and that KCl, which is in solution in the molten reaction mixture acts as a diluent, thus reducing the concentration of the chlorate reactant. Another possibility is that the rate controlling step is the rupture of chlorine-oxygen bonds to form chloride and atomic oxygen and that this reaction is reversing with respect to chloride and atomic oxygen. The atomic oxygen concentration, at the temperatures of the experiment are extremely low and

Fig. 39. PLOT OF DECOMPOSITION RATE, dw/dt, VS THE INVERSE TEMPERATURE, 1/T, FOR DECOMPOSITION OF (1) PURE $KClO_3$ and (2) A MIXTURE OF 50% $KClO_3$ with KCl

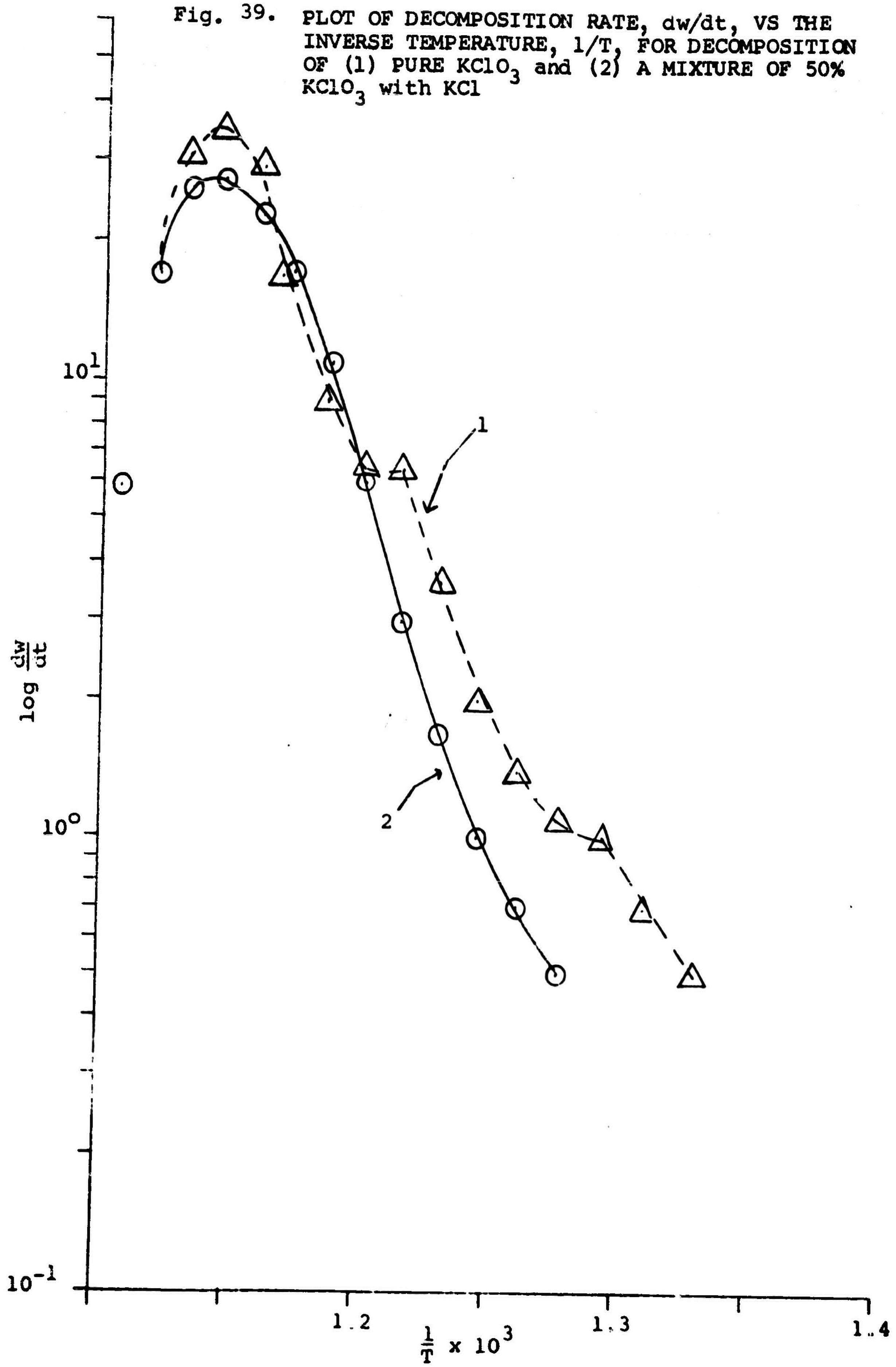

Table 15

RATE OF WEIGHT LOSS AS FUNCTION OF TEMPERATURE

Pure $KClO_3$		$KClO_3$/KCl (Ratio 1:1)	
$\frac{1}{T} \times 10^3$	$\frac{dw}{dt}$	$\frac{1}{T} \times 10^3$	$\frac{dw}{dt}$
1.328	0.5	1.277	0.5
1.310	0.7	1.261	0.7
1.293	1.0	1.245	1.0
1.277	1.1	1.230	1.7
1.261	1.4	1.215	3.0
1.245	2.0	1.200	6.0
1.230	3.7	1.186	11.0
1.215	6.5	1.172	17.5
1.200	6.5	1.159	23.0
1.186	9.0	1.145	27.5
1.172	17.0	1.132	26.0
1.159	29.7	1.120	17.0
1.145	35.5	1.107	5.8
1.132	31.0	1.095	0
1.120	3.5		

consequently it is not expected that molecular oxygen should have a significant effect on the reaction. However, it is possible, when having a steady-state concentration of atomic oxygen, that increasing the chloride concentration appreciably may have a reversing effect. A point in favor of this mechanism is that a calculation of the bond energy for the chlorine oxygen bond in chlorate is 55.6 kcal/mole, which is essentially the value for the activation energy for the decomposition of potassium chlorate. The calculation for bond energy is based on the following relationships:

$$KClO_3\ (s) \rightarrow KCl\ (s) + 3/2\ O_2 \qquad (3)$$

$$3/2\ O_2 \rightarrow 3O \qquad (4)$$

adding Equations (3) and (4) one obtains

$$KClO_3\ (s) \rightarrow KCl\ (s) + 3O \qquad (5)$$

The heat of reaction for Equation (3) under standard conditions at 25°C is -10.7 kcal, and the heat of formation for atomic oxygen, under the same conditions, is 59.2 kcal/mole. Since Equation (4) involves the formation of three moles of atomic oxygen the heat of reaction for Equation (4) is 177.6 kcal. Adding the heats of reaction for Equations (3) and (4) gives us the heat of reaction for equation (5) which is 166.9 kcal. Since equation (5) involves the rupture of three oxygens and we are interested in a single chlorine-oxygen bond rupture, the heat of reaction (5) must be divided by three to obtain the bond energy for the chlorine-oxygen bond in the chlorate ion. Doing this, the value turns out to be 55.5 kcal. It should be pointed out, however, that further work is required to clarify the mechanism of the effect of chloride on the disproportionation reaction. For example, if the reversing mechanism is true then it may be expected that potassium chloride would react with atomic oxygen to form potassium chlorate. The atomic oxygen can be formed in a microwave or radio-frequency field in the presence of potassium chloride. The formation of potassium chlorate can be determined analytically. The free energy change for this process appears to be favorable, based on the heat of reaction of Equation (5). Since the entropy change is a relatively high positive number (103 eu.), it is expected that at sufficiently high temperatures the free energy change for the reaction may be unfavorable. This, of course, is based on strictly thermodynamic considerations, which does not take into account the activated complex and entropy of activation, which could have a marked effect on the above possibilities.

In view of the effects that chloride was shown to have on the decomposition of potassium chlorate, experiments should also be conducted to determine the effects of potassium perchlorate on the decomposition of the chlorate. This approach is necessary to evaluate the complex kinetics of the thermal decomposition of potassium chlorate. It is not surprising that the non-isothermal treatment gave spurious results in view of the fact that the solubilities of the products of reaction have important effects on the kinetics, and since the reaction becomes rapidly exothermal. However, there is an approach that one may use to evaluate the activation energy for the initial decomposition reaction using a modified form of the Freeman and Carroll equation.[18] The basic equation is:

$$\frac{\Delta \log \frac{dw}{dt}}{\Delta \log W_r} = n - \frac{\frac{E^*}{2.3R} \Delta \left(\frac{1}{T}\right)}{\Delta \log W_r} \qquad (6)$$

where:

$\frac{dw}{dt}$ = rate of reaction at a constant heating rate

n = order of reaction

$W_r = \Delta w_c$ (weight change at completion of reaction)
$-\Delta w$ (change in weight at any given time)

E^* = activation energy

T = absolute temperature

Equation 6 may be rearranged to give,

$$\Delta \log \frac{dw}{W_r^{\,n} dt} = \frac{-E^*}{2.3R} \Delta \left(\frac{1}{T}\right) \qquad (7)$$

For a first order reaction which is assumed in this case the expression is:

$$\Delta \log \frac{dw}{W_r dt} = \frac{-E^*}{2.3R} \Delta \left(\frac{1}{T}\right) \qquad (8)$$

or

$$\Delta \log \frac{df}{dt} = \frac{-E^*}{2.3R} \Delta \left(\frac{1}{T}\right) \qquad (9)$$

where:

$$df = \frac{dw}{W_r dt} \qquad (10)$$

If $\Delta(\frac{1}{T})$ is maintained constant then for a first order reaction, if one plots $\Delta \log \frac{df}{dt}$ vs Δw, a horizontal straight line of zero slope should be obtained. If the products of reaction and/or temperature effects influence the reaction rate then the activation energy may be more accurately determined by extrapolating to $\Delta w = 0$. At this point the influences of the reaction products are minimized and the most accurate value of the activation energy may be calculated for the initial reaction. The results of this plot are shown in Figure 40. Table 16 gives the data for the plot. The activation energy calculated from the y intercept is 51 kcal/mole which is in fair agreement with some reported isothermal data.[7] This technique was used in a previous publication to obtain the kinetics of the oxidation of magnesium.[24]

Isothermal decomposition studies were conducted at temperatures above 550°C. It appears that above 550°C the presence of chloride may have an accelerator effect on the rate of decomposition. This is in accord with the derivative TGA curve (Figure 19) which shows that there is a temperature region above 550°C where the rate of decomposition of $KClO_3$ is more rapid in the presence of KCl. The apparent inhibition of the disproportionation reaction occurs below 550°C as is also seen in Figure 19. Figure 39 and Table 15 present the rate data.

Arrhenius plots of the isothermal decomposition rates at 50% and 75% decomposition are rather peculiar (Figure 41). (At 1/4 decomposition the curve shapes are similar as at 1/2 and 3/4 decomposition). All $KCl/KClO_3$ mixtures apparently follow Arrhenius law as is evident in straight lines of the semi-logarithmic plot of the slope vs 1/T. Pure $KClO_3$, however, shows at these decomposition stages a curvature indicating a more complex mechanism where the apparent activation energy decreases with increasing temperature. There seem to be a optimum rate at an intermediate mole ratio $KCl/KClO_3$ (Figure 42). In case of pure $KClO_3$ the rates are lowest. At a ratio $KCl/KClO_3 = 1/3$ the rates are relatively high, and decrease again at larger ratios of $KCl/KClO_3$.

Fig. 40. THE MODIFIED FREEMAN-CARROLL PLOT OF THE DECOMPOSITION OF POTASSIUM CHLORATE

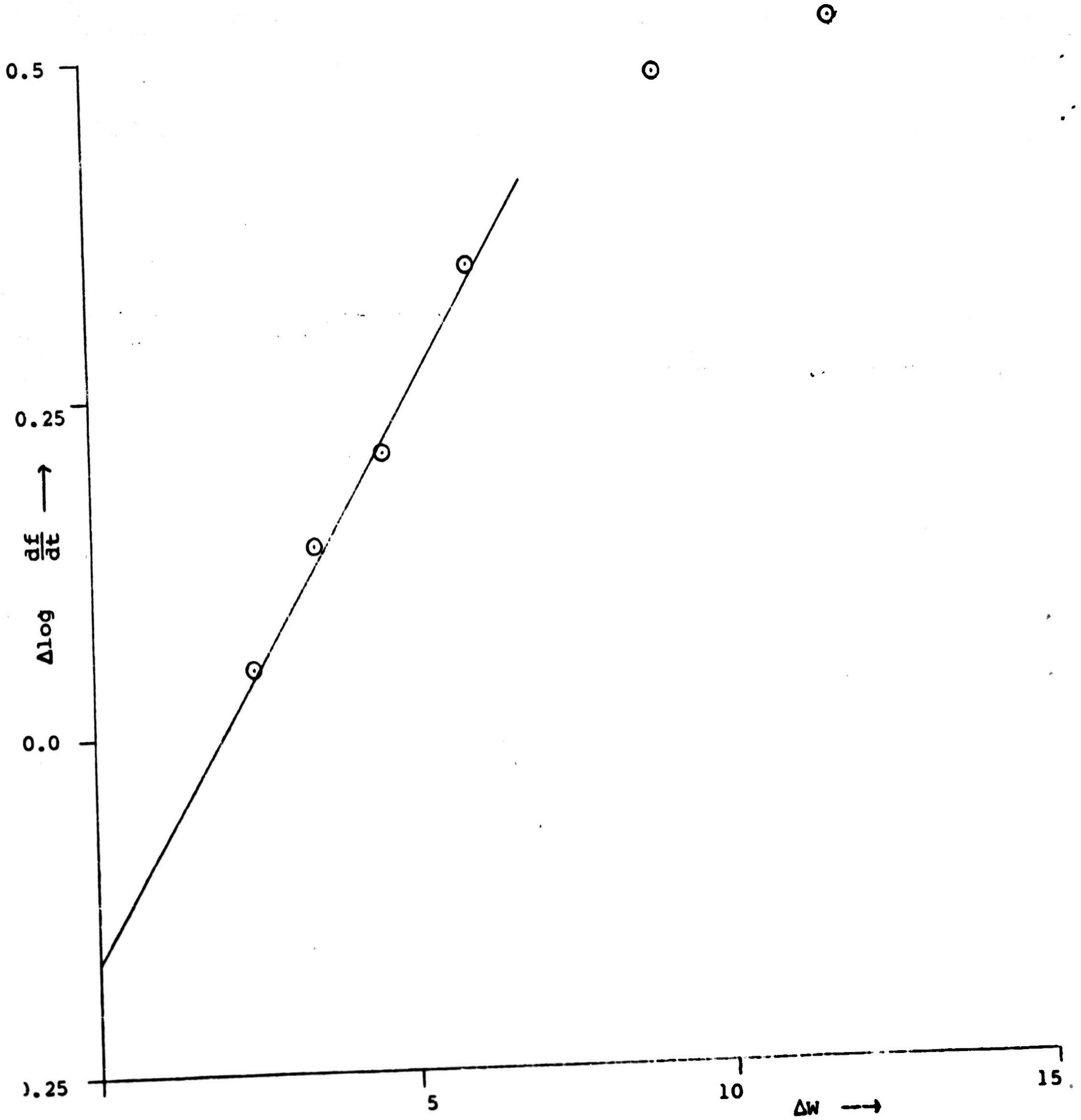

Table 16

COMPUTATION OF THE FREEMAN-CARROLL PARAMETERS

Δw (mg)	$\frac{dw}{dt}$	W_r	$\frac{df}{dt}$	$\Delta \log \frac{df}{dt}$
1.9	1.0	11.1	0.0901	
2.5	1.1	10.5	0.0952	0.024
3.5	1.4	9.5	0.1474	0.190
4.6	2.0	8.4	0.2381	0.208
6.0	3.7	7.0	0.5286	0.347
9.0	6.5	4.0	1.6250	0.487
11.8	6.5	1.2	5.4167	0.522

Δw_c = 13 mg = total weight loss for initial reaction

$\Delta \frac{1}{T} = 1.55 \times 10^{-5}$ ($°K^{-1}$)

$\frac{df}{dt} = \frac{dw}{W_r dt}$

Fig. 41. ISOTHERMAL DECOMPOSITION RATES AT DIFFERENT STAGES OF DECOMPOSITION

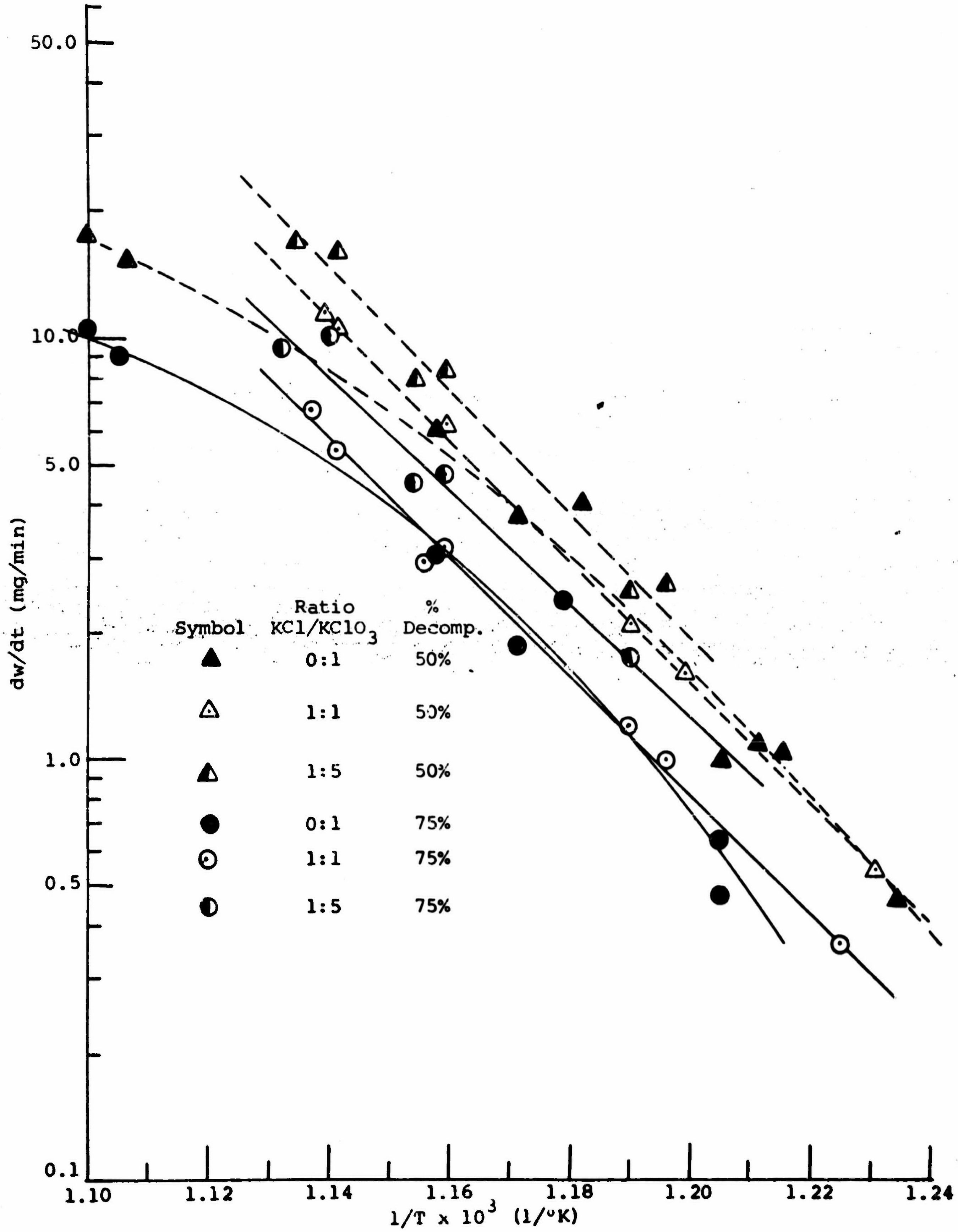

Fig. 42. ISOTHERMAL DECOMPOSITION RATES AS A FUNCTION OF KCl/$KClO_3$ RATIO AT ONE-HALF DECOMPOSITION

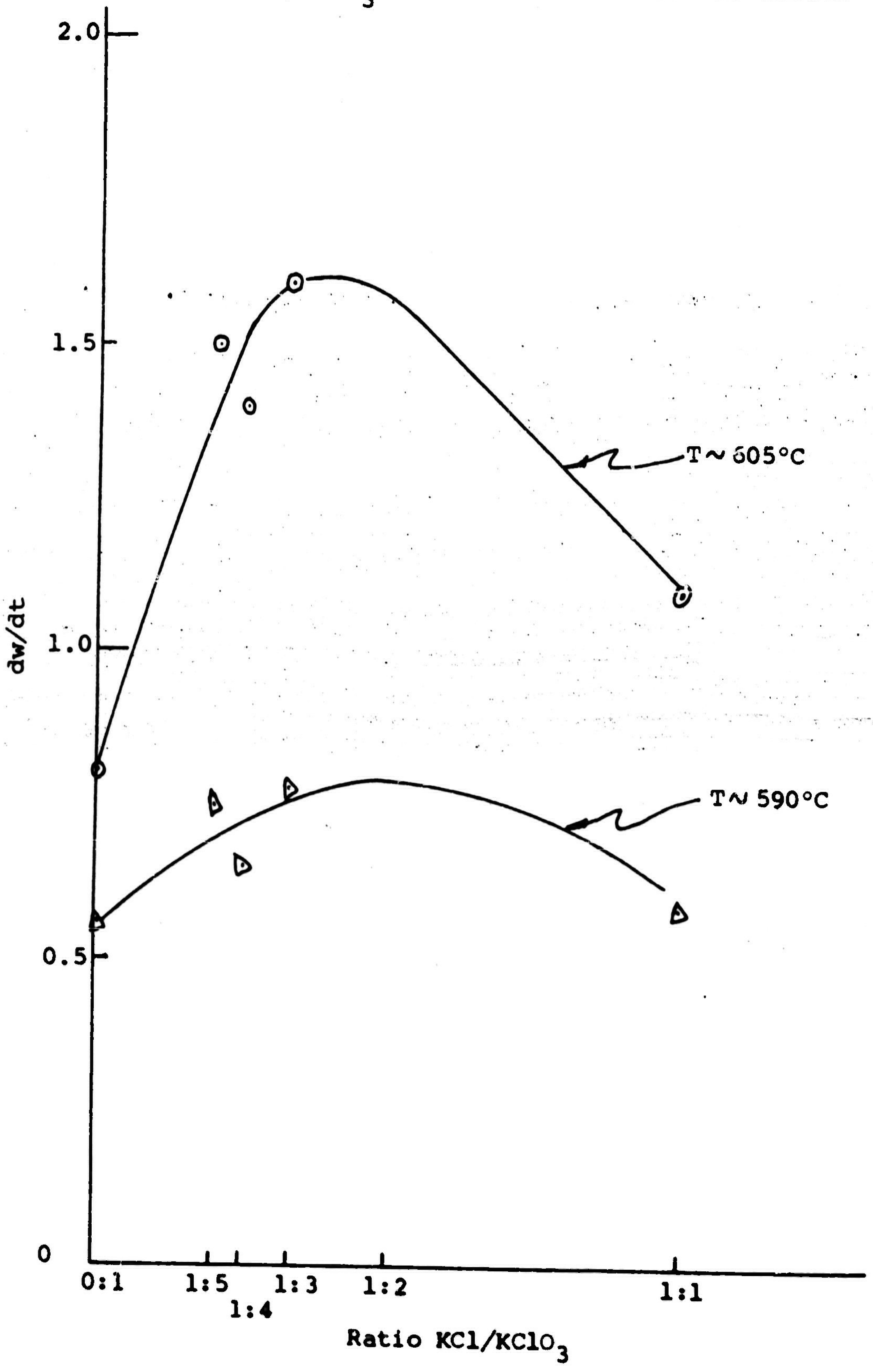

This behavior suggests strongly that the disproportionation reaction (1) is apparently suppressed by KCl, however, reaction (3) proceeds more readily at higher temperatures, if catalyzed by KCl in solution. The catalytic action of KCl is born out by the observation[16] that KCl of different histories influences the decomposition of $KClO_3$ differently. It was found that reagent grade KCl has a different apparent catalytic effect on $KClO_3$ decomposition than KCl obtained originally from decomposition of pure $KClO_3$.

It is certain that KCl does not catalyze in the solid state, since it is in solution at the initiation of the reaction. Yet it is quite possible that different impurity contents of the KCl additives create different polarization centers within the $KCl/KClO_3$ solutions, thus giving rise to different catalytic effects. The low temperature inhibition and higher temperature catalytic effects should receive further mechanistic consideration.

Fundamental to these interpretations is the solubility of KCl in the reaction mixture. Experiments were conducted in which it was found that KCl is soluble to an appreciable extent in molten $KClO_3$ at temperatures below 400°C. Visual observation of $KCl/KClO_3$ mixtures showed that KCl is soluble, up to a mole ratio of approximately 1:2.5 $KCl/KClO_3$ at 400°C. At higher temperatures, however, decomposition to KCl increases the amount of KCl which eventually precipitates out.

The sequence of reactions that may occur during the decomposition of potassium chlorate is as follows:

$$KClO_3 \rightarrow KClO_2^{\cdot} + O \qquad (11)$$

Since $KClO_2$ will be very unstable it can be expected to decompose very rapidly to KCl and oxygen

$$KClO_2 \rightarrow KCl + O_2 \qquad (12)$$

at lower temperatures

$$KClO_3 + O \rightarrow KClO_4 \qquad (13)$$

$$KClO_4 \rightarrow KCl + 2O_2 \qquad (14)$$

The activation energy indicates that reaction 5 may be rate controlling since the bond energy for the Cl-O bond was calculated as shown earlier to be 55.6 kcal which is reasonably close to the experimentally determined value of 51 kcal/mole.

B. Catalytic Effects of Metal Oxides

1. Survey of Oxides

The results of experiments conducted to evalute the relative catalytic activity of a selected series of metal oxides with respect to the thermal decomposition of potassium chlorate and perchlorate is seen in Figures 11 and 12. These oxides were in large part selected because it permitted comparisons to be made with the results of a similar approach taken on the thermal decomposition of N_2O.[1] In this reference, the order of catalytic activity was correlated to the "p" semiconducting character of the oxides. It was found that on going from "p" character to insulator to "n" character the catalytic activity decreased. In this study it was found that there was no general agreement with these findings. One main point is that in the case of potassium chlorate decomposition it is apparent that the "n" type semiconductors are the most active catalysts and that the catalytic activity increases as either the "n" or "p" semiconducting character increases. Tables 1 and 2 summarize the orders of catalytic activity for the decomposition of the chlorate and perchlorate. The perchlorate was considered because it is formed during the disproportionation of $KClO_3$.

The order of catalytic activity is seen to be essentially the same although there are some exceptions. The exceptions, however, do not upset the general trend from the point of view of interpretation. The exceptions are: Fe_2O_3, CuC, ZnO and MgO. It may be noted that the temperatures at which decomposition initially occurs are quite close for both $KClO_3$ and $KClO_4$ in the presence of the following catalysts, Cr_2O_3, CoO, Co_3O_4 and Cu_2O. See Table 17. This is interesting since the bond energy for the ClO bond in the ClO_4^- ion is appreciably higher than for the Cl-O bond in the ClO_3^- ion. From the color change in the decomposing sample containing Cr_2O_3 it may be concluded that Cr_2O_3 is oxidized during the very initial stage of decomposition to form CrO_3, or rather $K_2Cr_2O_7$ as will be discussed later.

For the purposes of interpretation it appears that the oxides may be separated into two general categories. The first category being the transition metal oxides and the second category being the remainder of oxides. If one calculates the heat of reaction per metal ion of the lower valent oxide to form the high valent oxide, the following order of heat of reaction is determined.

Table 17

HEATS OF REACTION

Reactions	Heat of Reaction per Mole of Metal ion in Lower Valent Oxide Kcal/mole
$\frac{Cu_2O}{2} + 1/4\ O_2 = CuO$	-17.2
$CoO + 1/6\ O_2 = \frac{Co_3O_4}{3}$	-13.0
$\frac{Cr_2O_3}{2} + 3/4\ O_2 = CrO_3$	-2.3
$MnO + 1/2\ O_2 = MnO_2$	-32.5

$MnO_2 > Cu_2O > CoO > Cr_2O_3$

The values are given in Table 17. Interestingly, the order of increasing catalytic activity follows the order of decreasing heat of reaction. Since the entropy effects may be expected to be small for the solid state processes compared to the enthalpy changes, the order of decreasing heat of reaction should also correspond to approximately the free energy changes associated with these reactions. If the rate controlling step in the heterogeneous catalysis of potassium chlorate is the transfer of electrons from the solid oxide to the chlorate ion as indicated by the hypothetical initial surface reaction in Equation (15) below, then one may expect that the greater the decrease in free energy in going from the lower to the higher oxide, the more favorable will be the catalytic process.

$ClO_3^- + e$ (solid catalyst) $\rightarrow ClO_2^- + O^-$ (adsorbed) (15)

However, the contrary was observed. This suggests that it is the reverse process which is rate controlling. Specifically, the results suggest that the rate controlling step is probably the transfer of electrons from the oxidant, or more likely dissociation products of the chlorate to empty levels in the d band structure of these oxides. The mechanism may be indicated by the following equations.

$ClO_3^- + e$ (solid catalyst) $\rightarrow ClO_2^- + O^-$ (adsorbed) (15)

$O^- \rightarrow O$ (adsorbed) $+ e$ (solid catalyst) (16)

$2O$ (adsorbed) $\rightarrow O_2$ (gas) (17)

$O + O^-$ (adsorbed) $\rightarrow O_2$ gas $+ e$ (solid catalyst) (18)

Reaction 16 is expected to be rate controlling based on the above discussion. The order of catalytic activity of the remainder of the oxides increases as the "p" character of the oxide is increased.

The similar mechanism may apply to the initial decomposition of potassium perchlorate. If the rate controlling step of the catalytic reaction is the transfer of electrons from the chemisorbed O^- to the catalyst in the case of the ClO_3^- and ClO_4^- this may account for the similarity in the initial decomposition temperatures for some of the catalysts. Since little further work was done with the $KClO_4$ this, of course, must be taken as merely speculation at this time.

Selective conductivity measurements on the oxides pressed into pellets from the reagent grade oxides (Figure 25) confirm the idea that it is the ease with which charge carriers (electrons) are transferred between oxide catalysts and oxidant which is responsible for the order in catalytic activity. Specifically, the order in electrical conductivity, $Cr_2O_3 > Fe_2O_3 > MgO$, corresponds to the order in catalytic activity.

2. Effects of Electronic Defect Structure

Results on the effects of thermal and preparatory history of Fe_2O_3 samples with reference to their catalytic activity confirmed the interrelationship between defect structure and sample history.

If the ferric oxide is slightly decomposed, the stoichiometry will not change appreciably, but the electronic defect structure may be considerably altered. For example, slight decomposition has the effect of adding electrons to the solid oxide, then reducing the concentration of positive holes in the valence band of the oxide. After all of the positive holes are filled, electrons will go into the conduction band of the oxide in a higher energy state. Based on these considerations, samples were prepared by precipitation with NH_4OH and ignition to 700°C, 800°C, and 900°C. Figure 9 shows the DTA of these samples as compared to the originally used reagent grade Fe_2O_3 sample. Portions of the sample were heated in air to 700°C, 800°C and 900°C. From Figure 9 it is obvious that the catalytic reactivity decreases with increasing temperature of oxide ignition. Figure shows the correlation between the temperature of the heat treatment and catalytic activity. The sample ignited at 700°C is most reactive, the reaction seems to be threefold as indicated by three distinct exotherms. The $KClO_3$ decomposition exotherm shifts to higher temperatures with the oxides treated at 800°C and 900°C.

The magnetic susceptibility of the iron oxide samples decreases slightly with the temperature of the heat treatment in going from 700°C to 800°C, but increases in going from 800°C to 900°C. See Table 5. An increase of the magnetic susceptibility upon heat treatment could be expected, if the Fe_2O_3 decomposes to some extent to form Fe_3O_4. This would have a marked effect in increasing the magnetic susceptibility of the oxide particles since the overall susceptibilities are of the order of 10^{-5}. However, at the reaction temperature of 320°C and higher the ferromagnetic phase may be in large part destroyed. Consequently, the magnetic susceptibility of the 900°C heat treated particles may fall in line with the general decreasing trend in catalytic activity with increases in the temperature of the heat treatment. The three oxide samples should be analyzed with respect to the content of Fe^o, Fe(II), Fe(III) and possibly Fe(IV), in order to more completely interpret the results.

The relative x-ray intensities (Table 11) seem to indicate lines corresponding to an Fe_3O_4 phase. This appears more pronounced in the sample heated to 900°C than in the other samples (treated at low temperatures) although some of the lines reported in the literature for Fe_3O_4 are missing. It is obvious from this discussion that methods of Fe_2O_3 preparation can significantly change the catalytic activity as well as affect magnetic susceptibility. Figure 43 also shows a plot of the magnetic susceptibility *vs* ignition temperature. Methods of preparation are likely to account for the large discrepancies between the magnetic susceptibilities of the reagent grade Fe_2O_3 and the literature values.

A significant observation is that the rate of decomposition of $KClO_3$ as seen in Figure 14 in the presence of Fe_2O_3 heat treated at 800°C and 900°C in Ar is more rapid than if the heat treatment was carried out in oxygen at the same temperatures. At 1000°C there is little difference between the samples. These results were correlated to magnetic susceptibility and electrical conductivity measurements of portions of the same treated oxide samples.

Magnetic susceptibility measurements at room temperature indicate that the magnetic moments in Bohr magnetons of the argon treated Fe_2O_3 are only slightly higher than the magnetic

Fig. 43. EFFECT OF HEAT TREATMENT ON CATALYTIC ACTIVITIES AND MAGNETIC SUSCEPTIBILITIES OF IRON OXIDES (Mole Ratio $Fe_2O_3/KClO_3$ = 1:10, Particle Size 53-63μ)

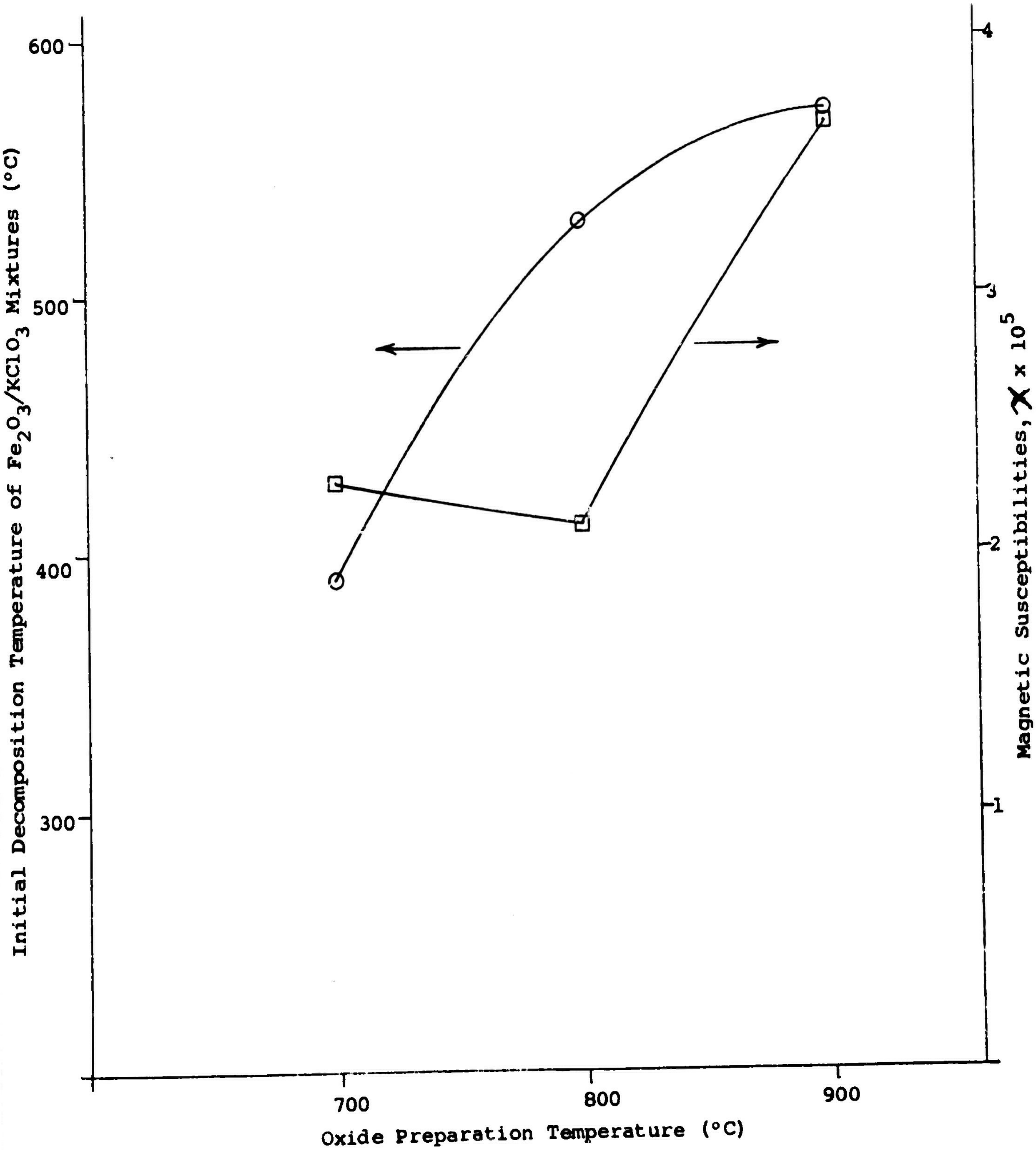

moments of the oxygen-treated material. See Table 6. The untreated Fe_2O_3 has the highest magnetic moment. In all cases, however, the magnetic moments are smaller than 5.9 Bohr magnetons calculated for Fe^{+++} ions indicating that the Fe_2O_3 is not a completely ionic crystal.

The significance of these values in terms of correlations with catalytic activity is uncertain because of the very slight differences in magnetic susceptibility. Possibly the high values due to heat treatment in argon can be due to greater thermal decomposition of the oxide in argon than in oxygen. This would add the electrons released from the oxide ion being connected to neutral oxygen to the conduction band of the solid. This of course accounts for the observed increases in catalytic activity.

It was shown in the Results section, that the oxygen treated samples have appreciably lower electrical conductivities than the argon treated samples in contrast to the almost negligible changes in magnetic susceptibilities. The lower conductivity is consistent with the interpretation that the Fe_2O_3 is an n-type semiconductor, and gives direct support to a theory of catalysis based on an electron transfer mechanism. Based on the result that Fe_2O_3 is an n-type conductor we may consider that at the high temperature to which the Fe_2O_3 was exposed some loss of oxygen occurs in argon. This would have the result of increasing the concentration of electrons in the conduction band of the oxide,

$$Fe_2O_3 = 3/2\ O_2(g) + 2Fe^{+++}\bullet + 6e \text{ (conduction band)} \qquad \textbf{(19)}$$

($Fe^{+++}\bullet$ = interstitial cation).

Since the transfer of electrons to the "n" semiconductor is not a very probable mechanism of catalysis, it is more likely that the rate controlling mechanism in this case will be associated with the transfer of electrons to the chlorate.

These ideas concerning the relationship between electrical properties and catalytic activity are further supported by experiments in which impurity defects are in the oxide. Table 7 shows that doping with 1/2 mole percent of Li^+ decreases the magnetic moment of Fe_2O_3, while doping with 1/2 mole percent of Zr^{++++} has the opposite effect. Correspondingly, the electrical conductivity of the Li^+ ion doped oxide is lower at the temperature of $KClO_3$ decomposition, but that of the Zr^{++++} doped sample is higher than the electrical conductivity of the undoped oxides. (Figure 30). This indicates that the n-character of the oxide decreases upon doping with the lower valent cation as would be expected if fewer electrons are in the conduction band than in the case of the Fe_2O_3 doped with the higher valent cations. For the Fe_2O_3 catalyst it was found that the catalytic activity decreased with a decrease in the n-character of the oxide as a result of doping. For example: Fe_2O_3 doped with Li^+ ion, which has a lower electrical conductivity at decomposition temperature of $KClO_3$ than the undoped oxide, has the lowest catalytic activity. The Zr^{++++} ion doped Fe_2O_3, which has the highest electrical conductivity at the temperature of catalyzed decomposition of $KClO_3$, was found to be the most active catalyst. (Figure 18). Interestingly the Be^{++} ion doped Fe_2O_3 showed an increase in catalytic activity which seems to be in agreement with the general trend observed with respect to magnetic suscptibility. The magnetic susceptibility of the Be^{++} doped sample is higher than the undoped Fe_2O_3. Since the doping with cations of higher valency than that of the host lattice should increase the concentration of conduction electrons or add electrons to holes in the "d" bands, it may be expected that the magnetic susceptibility would be higher the higher the valency of the dopant cation. This was observed to be true and correlates with the changes in electrical conductivity. Gamma-ray irradiation of Fe_2O_3 seems to create similar defects as in the case of the argon heat treated samples due to slight decomposition. This is reflected in the increased catalytic activity of irradiated Fe_2O_3 (Figure 16) with respect to $KClO_3$ decomposition. Slight decomposition on the surface of the oxide may be expressed by the following equation.

$$1/2\ Fe_2O_3 \rightarrow Fe^{+++}\bullet + 3/4\ O_2 + 3e \qquad (19a)$$

where $Fe^{+++}\bullet$ = interstitial Fe^{+3}, and e additional electrons available in the conduction band.

These ideas find their confirmation in the tentative results of the contact potential differences between irradiated and unirradiated Fe_2O_3 samples. It appears that irradiation lowers the work-function of the oxide which means in essence that the surface barrier for an electron transfer is lowered.

Considering the discussion pertaining to the n-type character of Fe_2O_3 it is not surprising that MgO as a typical p-type conductor responds in the opposite direction towards heat treatment and γ-irradiation. The catalytic activity of the oxide is increased, if it is pretreated in oxygen, and is decreased, if pretreatment is done in argon. (Figure 15) Correspondingly, the overall electrical conductivity is larger in the oxygen heat treated sample than in the argon treated MgO. (Figure 29) This indicates that the p-type character of MgO decreases in argon.

γ-irradiation has a similar effect as the argon treatment. (Figure 17) The catalytic activity of the irradiated MgO is lower than that of unirradiated MgO. Unfortunately, the correlation between catalytic activity, and electrical conductivity of irradiated and unirradiated MgO pellets is not as clear cut as in case of the MgO single crystal which was used in the heat treatment experiments, since large experimental errors are apparently introduced as a consequence of poor oxide electrode contacts. If, however, the conductivities are plotted according to Arrhenius law, consistent slopes are obtained of unirradiated samples on the one hand, and of irradiated sample on the other.

According to the Nernst- Einstein equation, electrical conductivity may be related to the diffusion coefficient, D, of charge carriers by:

$$\sigma = DN\rho^2/kT \qquad (20)$$

on the other hand, the diffusion coefficient may be expressed within the framework of absolute reaction[25] rate theory by

$$D = \lambda^2 kT/h \cdot \exp\ (\Delta S^{\ddagger}/RT) \qquad (21)$$

Thus,

$$\sigma = \frac{N\lambda^2\rho^2}{h}\ \exp\ (\Delta S^{\ddagger}/R)\ \exp.\ (-E^{\ddagger}/RT) \qquad (22)$$

where

N = number of charge carriers

ρ = carrier charge

λ = distance between jump sites

D = Planck's constant

k = Boltzmann's constant

$\Delta S^{\ddagger}$ = entropy of activation, and

$E^{\ddagger}$ = energy of activation.

Thus from the slope of logarithm of conduction vs the inverse temperature one may evaluate and compare activation energies which are a measure of the relative height of the activation barrier encountered by the charge carriers when leaving the surface of the oxide. The average activation energy calculated for the irradiated MgO is with 34.5 kcal/mole much higher than that of unirradiation MgO with 14.8 kcal/mole. This is consistent with their catalytic behavior. Irradiated MgO is less catalytic active than unirradiated MgO, because the energy barrier for charge transfer is enhance.

Based on the above interpretations and evidence, it appears that electron transfer between oxide catalyst and $KClO_3$ is the rate determining factor in the decomposition of the oxidant. The degree of n-type and/or p-type semiconductive character appears to determine the extent of catalytic activity of a given metal oxide. Insulators should, therefore, have the least catalytic effect on the decomposition of $KClO_3$.

C. Apparent Catalytic Effects of Chromium Oxides

During the DTA/TGA runs it was found that Cr(III) and Cr(VI) oxides were apparently the most reactive catalysts for the decomposition of potassium chlorate. There were, however, indications that these oxides also underwent irreversible reactions. The yellow color of the reaction products and discrepancies in overall weight loss of the mixtures suggested the hypothesis that potassium chromates or dichromates were formed during the decomposition of $KClO_3$. (See Figures 11, 12,and 20.

In order to obtain more information on the possible mechanism of this reaction, TGA was performed at several temperatures, and x-ray analyses were carried out on the reaction products. Table 13. In the case of CrO_3 there is apparently no evidence of formation of Cr_2O_3. If the sample is heated above 270°C, lines appear in the x-ray spectrum which indicate the formation of potassium dichromate, $K_2Cr_2O_7$. Table 13 shows that the ratio of $K_2Cr_2O_7/Cr_2O_3$ approaches infinity at around 360°C which means essentially that the first step in the decomposition of the $KClO_3/Cr_2O_3$ mixture is at least in part due to the reaction:

$$Cr_2O_3 + 2\ KClO_3 \quad K_2Cr_2O_7 + ClO_2 + 1/2\ Cl_2 \qquad (23)$$

the fact that bichromate is formed during reaction is only consistent with the formation of chlorine and/or chlorine oxides. This was confirmed by visual observation and mass spectrometric analysis.

It was observed in the reaction of chromium oxides with potassium chlorate that a yellow-greenish gas was liberated on heating indicating the probable release of chlorine and/or chlorine oxides. To verify this, a systematic mass spectrometric analysis of the gaseous decomposition products was conducted as a function of temperature. The preliminary data indicated that chlorine and chlorine oxides were formed during the reaction. See Figure 37. The mass spectrometric analysis shows the formation of Cl_2, ClO_2 and traces of ClO and ClO_3. The formation of the trace gases may be due to fragmentation and recombination from ClO_2 and with Cl, and/or O-radicals, within the mass spectrometer. More quantitative studies proved that formation of ClO_2 prevails at lower temperatures as is seen in Figure 38. With increasing temperatures, however, formation of ClO_2 decreases, while chlorine, Cl_2 and oxygen begin to predominate. These results give direct evidence that the decomposition of $KClO_3$ with chromium oxides follows a completely different reaction path than $KClO_3$ per se or in mixtures with other oxides which are catalysts in the true sense. Where CrO_3 is the catalyst, Cl_2 is principally formed during the decomposition of $KClO_3$; ClO_2 is present only in trace quantities. (Figure 37). There are however, indications that a new phase is formed which does not correspond to KCl, $KClO_3$, CrO_3, $K_2Cr_2O_7$ or the Cr_2O_3 phases.

D. Reaction Between Sulfur and Potassium Chlorate

A series of experiments was conducted to determine the reactivity of sulfur vapor with solid potassium chlorate with and without catalysis. Figure 21 shows the results of these experiments for the various fuel-oxidant-catalyst combinations. It is interesting to see that reaction between sulfur vapor and potassium chlorate occurs at relatively low temperatures just above 200°C indicating that a vapor phase reaction can be important. This effect, of course, would be more pronounced in an intimate mixture between sulfur and potassium chlorate since hot spots would develop during the preignition process. Another interesting observation is that in the presence of the iron oxide catalyst the exotherm is considerably enhanced. The temperatures of the exotherms apparently do not change appreciably in the presence of the oxide catalysts.

It appears that ignition occurs with sulfur vapor in the pressure range of 0.1 to 1 mm Hg. This is equivalent to a concentration of sulfur of about 10^{15} to 10^{16} molecules/cm^3. Sulfur vapor is known to consist of polyatomic molecules ranging from S_2 dimers to S_8 rings.[22] These polyatomic molecules are in thermodynamic equilibrium with each other and their concentration depends on the temperatures. At higher temperatures S_2 molecules prevail, while at lower temperature equilibrium is shifted toward the aggregated molecules.

In any case, however, the sulfur molecules will be very active in the vapor phase. Their strong electronegativity is possibly the reason for adsorption on the solid $KClO_3$ surfaces, where partial or complete electron transfer might take place. The mechanism may be considered analogous to the reaction of oxygen on the surface of semiconducting oxides, such as zinc oxide. Hypothetical steps in the mechanism of reaction between sulfur and potassium chlorate may be as follows:

1. Electrons are transferred from the valence band of $KClO_3$ to adsorbed S_2 or higher polyatomic sulfur molecules

$$S_2 + e \rightarrow S_2^- \text{ (ads)} + (e^+) \qquad (24)$$

e = electrons in the valence band of $KClO_3$

S_2^-(ads) = sulfur ion adsorbed on the surface of $KClO_3$

(e^+) = positive hole

2. The electron provided by the valence band of $KClO_3$ can only go into anti-bonding orbitals in the sulfur molecule. Consequently the bond energy between sulfur atoms if reduced, and the adsorbed sulfur ion-molecule may dissociate into atomic and ionic sulfur. These sulfur species can then pick up additional electrons from the valence band of the chlorate leaving positive holes, and thus creating an electric potential between the surface and the Bulk ions.

$$S_2^- \text{ (ads)} + 3e \rightarrow 2S^{2-} \text{ (ads)} + 3\,(e^+) \qquad (24)$$

3. The electrical potential will then be the driving force for K^+ ion migration to the surface, where K_2S is formed, leaving behind a cation vacancy in the bulk lattice. This behavior is analogous to V center formation in halides exposed to halogen gas.[1] The positive holes associated with the cation vacancy, comprises the color center.

$2K^{+\bullet} + S^{2-}\ (ads) \rightarrow K_2S$

$K^+\ (lattice) \rightarrow (K^+)\ + K^{+\bullet}$

$K^{+\bullet}$ = interstitial K^+ ion

(K^+) = K^+ - vacancy

4. Positive holes (as $ClO_3^{\cdot}$ radicals) may react with K_2S and form KCl and SO_2. The reaction should proceed spontaneously.

$2ClO_3^{\cdot} + K_2S \rightarrow 2KCl + 3SO_2$

From thermodynamic considerations can be estimated that the free energy change for the last reaction is -390kcal/mole.

The hypothesis of sulfur $KClO_3$ reaction is very tentative and should be verified by further experiments and theoretical studies.

CONCLUSIONS

1. The decomposition of potassium chlorate appears to be non-reversing with respect to molecular oxygen.

2. Potassium chloride appears to inhibit the disproportionation of potassium chlorate below 550°C. Above 550°C the chloride appears to accelerate the decomposition of $KClO_3$.

3. The activation energy for the decomposition of potassium chlorate was determined to be 51 kcal/mole.

4. The effects of creating electronic defect structure by doping with altervalent cationic impurities, by exposure to gamma ray radiation and heat treatment was investigated in relationship to catalytic activity. The results are consistent with a rate controlling electron transfer mechanism.

5. The higher the "p" or "n" semiconducting character of the metal oxides the higher appears to be the catalytic activity.

RECOMMENDATIONS

1. The effects of potassium perchlorate on thermal decomposition of potassium chlorate should be determined.

2. Thermal decomposition studies on potassium chlorate should be conducted at temperatures below 550°C in the presence and absence of varying concentrations of KCl.

3. A mechanism of decomposition should be more definitely established by kinetic studies at low temperatures.

4. Studies to more completely characterize the defect structure of the oxides and to determine the valence states of the dopant ions and changes in valence state that may occur on exposure to radiation and heat treatment should be conducted. This is necessary for an interpretation of the relationships between the defect structure and the electronic changes which were observed.

5. The effects of the substitution of the catalysts for the usual kaolin or oxide coolants on the performance of pyrotechnics should be investigated. This may lead to improved compositions for more rapid dissemination of agents.

6. The possible inhibition effects that chloride dopants may have with respect to decreasing the sensitivity of compositions should be investigated.

References

1. Garner, "Chemistry of the Solid State" Butterworth Scientific Publication, London (1955).

2. Rudloff, W. K., and Freeman, E. S., General Session No. 13 of the Division of Physical Chemistry at the ACS Meeting, Atlantic City, September 1965.

3. Otto, C. E., and Fry, H., J. Am. Chem. Soc., 45, 1134,(1923).

4. Galwey, A. K., and Jacobs, P. W. M., Trans. Far. Soc.,55, 1165, (1959).

5. Hermoni (Makovky) A., and Salmon, A., Bull. Res. Counc. Isreal, 9A, 206, (1960).

6. Solymosi, F., and Krix, E., J. Cat. 1, 468, (1962).

7. Solymosi, F., and Krix, N., ACTA Chim. Acad. Scient. Hung., 34, 241, (1962).

8. Solymosi, F., and Révész, L., Kin. i. Kat., 4, 88, (1963).

9. Gaidis, J. M., and Rochow, E. G., J. Chem. Ed. 40, 78, (1963).

10. Markowitz, M. M., Boryta, D. A. and Stewart, H. Jr., J. Phys. Chem. 68, 2282, (1964).

11. Shchidlovskii, A. A., Shmagin, L. V., and Bulandva, V. V., Izv. Vis. Uchebn, Zav. SSSR, Khim. i Khim. Tekch. 7, 862, (1964).

12. Shchidlovskii, A. A., Shmagin, L. V., and Bulanova, V. V., Ibid., 8, 553, (1965).

13. Solymosi, F., Comb. Flame 9, 141, (1965).

14. Markowitz, M. M., and Boryta, D. A., J. Phys. Chem. 69, 1114, (1965).

15. Vol'kenstein, F. F., "The Electronic Theory of Catalysis on Semiconductors", The Macmillan Company, New York, (1963), pp. 105.

16. Glasner A., and Weidenfeld, L., J. Am. Chem. Soc. 74, 2464, (1952).

17. Stern, K., and Bufalini, M., J. Phys. Chem. 64, 1781, (1960).

18. Freeman, E. S., and Carroll, B., J. Phys. Chem. 62, 394, (1958).

19. Dravnieks, A., "Contact Potentials in the Detection of Airborne Vapors", Chapter 6, p. 103 in "Conference on Surface Effects in Detection," ed. by J. I. Bregman and A. Dravnieks, IITRI, Spartan Books, Inc., Macmillan & Co., Ltd., Washington, D.C., London, (1965).

20. Mueller, G. O., "Praktikum der Quantitativen Analyse," 2nd Ed., S. Hirzel Verlag, Leipzig, (1952), p. 299.

21. Garner, Gray and Stone, Proc. Roy. Soc. A, 197, 294 (1949).

22. Holleman, A. F., and Wiegert, E., "Lehrbuch der Anorganischen Chemie, W. De Gruyter and Co., Berlin (1953). P. 491.

23. Anderson, D. A., and Freeman, E. S., Nature 195, 1297, (1962).

24. Freeman, E. S., and Campbell, C., Trans. Far. Soc., 59, 165, (1963).

25. Glasstone, S., Eyring, H. and Laidler, K. J., "The Theory of Rate Processes," McGraw-Hill, New York, (1941), P. 516.

UNCLASSIFIED

DOCUMENT CONTROL DATA - R&D

(Security classification of title, body of abstract and indexing annotation must be entered when the overall report is classified)

1. ORIGINATING ACTIVITY *(Corporate author)* IIT Research Institute 10 West 35th St. Chicago, Illinois 60616	2a. REPORT SECURITY CLASSIFICATION UNCLASSIFIED 2b. GROUP N/A

3. REPORT TITLE

THE CATALYTIC ACTIVITY OF METAL OXIDES ON THERMAL DECOMPOSITION REACTIONS

4. DESCRIPTIVE NOTES *(Type of report and inclusive dates)*

Final Technical Report - 22 March, 1965 - 30 September, 1966

5. AUTHOR(S) *(Last name, first name, initial)*

Freeman, Eli S., and Rudloff, Winfried

6. REPORT DATE March 1967	7a. TOTAL NO. OF PAGES 142	7b. NO. OF REFS 25

8a. CONTRACT OR GRANT NO. DA-18-035-AMC-341(A) b. PROJECT NO. 1C522301A60 c. d.	9a. ORIGINATOR'S REPORT NUMBER(S) IITRI-U6017-6 9b. OTHER REPORT NO(S) *(Any other numbers that may be assigned this report)* Final Technical Report

10. AVAILABILITY/LIMITATION NOTICES

Each transmittal of this document outside the Department of Defense must have prior approval of CO, ATTN: SMUEA-TSTI-T, US Army Edgewood Arsenal, Edgewood Arsenal, Maryland 21010

11. SUPPLEMENTARY NOTES Chemical Agents	12. SPONSORING MILITARY ACTIVITY Chemical Research Laboratory RESEARCH LABORATORIES

13. ABSTRACT

The effects of a selected series of solid metal oxides on the catalysis of the thermal decomposition of potassium chlorate and potassium perchlorate were investigated. The kinetics and rate parameters of the catalyzed decomposition reactions were studied and compared to the rate parameters observed in the absence of the solid oxides. Two oxides were selected for more precisely correlating the relationships between the electronic defect structure of the oxides and their catalytic behavior. The oxides investigated from this point of view were: ferric oxide and magnesium oxide. These oxides were doped with selected altervalent cation impurities, and heat treated at temperatures ranging from 700 to 1000 degrees C in oxygen and inert gas environment in order to introduce electronic defects. In addition, changes in catalytic activity in relationship to electronic changes as a result of exposure to Cobalt (60) gamma rays were investigated. The changes in semiconducting properties were studied and the results correlated with the changes in catalytic activity. A mechanism of decomposition of potassium chlorate is discussed as well as a proposed mechanism for the interaction of sulfur and potassium chlorate.

DD FORM 1 JAN 64 1473

UNCLASSIFIED

Keywords

Activation energy
Catalytic activity
Chlorine
Chlorine oxides
Chromium (III) oxide
Chromium (VI) oxide
Conduction band
Differential thermal analysis
Doping with altervalent cations
Electrical conductivity
Electronic defect structure
Freeman-Carroll equation
Gamma rays
Iron (III) oxide
Irradiation
Isothermal decomposition
Kinetics of $KClO_3$ decomposition
Magnesium oxide
Mass spectrometric analysis
n-semiconductor
Potassium chlorate
Potassium chloride
Potassium perchlorate
p-semiconductor
Sulfur
Thermogravimetric analysis
Valence band
x-ray analysis